Effects of metformin on human monocytic THP-1 cells – Implications for type 2 diabetes mellitus

by

An-Chi Tsuei

A thesis submitted in partial fulfillment

of the requirements for the degree

of

Master of Science in Biological Sciences

at

The University of Waikato

THE UNIVERSITY OF
WAIKATO
Te Whare Wānanga o Waikato

2010

Abstract

Metformin is an anti-hyperglycaemic agent widely prescribed for type 2 diabetes (T2D). Despite decades of clinical use, its exact pharmacological mechanism(s) is yet to be definitively determined. Accumulative data have shown its mild inhibitory effect on the complex 1 of the mitochondrial respiratory chain, which is thought to contribute to its anti-hyperglycaemic effect. Metformin is also thought to have a protective effect on cardiovascular disease (CVD), the most common complication in T2D. It is widely accepted that T2D is an inflammatory state thus it is not surprising that T2D patients have 2-4 times higher risk in developing CVD. Furthermore, the pathology of T2D has been proposed to involve dysfunctioning mitochondria, the organelle of energy sensing and production. The use of metformin, a mitochondria inhibitor, in cells under mitochondrial stress led us to speculate the physiological responses that ensue.

To understand metformin's mode of action and its involvement in inflammation processes the human monocytic leukemia THP-1 cells were used in this study. Since studies of metformin on this cell type is scarce if not non-existence the first task was to determine its cytoxicity in this cell line. Next the mRNA and protein expressions of heat shock protein 60 (Hsp60), a mitochondrial stress marker, was determined in metformin-treated THP-1 cells. Further, various cell types have shown surface expressed Hsp60 under stress conditions. Thus the study here attempted to optimise the detection of surface Hsp60 in THP-1 cells, as human Hsp60 has been shown to induce innate immune response. Localisation of Hsp60 on the cell surface in metformin-treated cells may exacerbate the already-inflammed state of T2D. Lastly, metformin's effect on PMA-stimulated monocyte differentiation was determined by the mRNA expression of CD14, a surface receptor on macrophages.

The results here agreed with published data that metformin at therapeutic concentrations are not cytotoxic and is a mild inhibitor of mitochondrial respiration. We also provide evidence that metformin up-regulated the mitochondria stress protein, Hsp60, in a time- and dose-dependent manner. In addition, live cell Hsp60 immunocytochemistry proved to be a promising method for surface Hsp60 detection in THP-1 cells. Finally, at the therapeutic concentration metformin caused a significant up-regulation in *cd14* expression, which contradicts with much acclaimed protective effect of metformin in the literature.

Acknowledgements

First and foremost, I would like to thank my master's supervisor, Dr. Ryan Martinus, for all your guidance and encouragement throughout the past two years. You have taught me to push myself further and to grab opportunities that may broaden my horizon. Also, thanks for the time you spent going through the drafts of this thesis in the last few months.

I would also like to thank the University of Waikato for awarding me scholarships throughout my study. With the financial assistance I could focus on my project while pursuing my interests outside of my study.

To everyone that I have worked with in the Cellular and Molecular Biology Laboratory, thanks for your friendship and encouragement. Special thanks to Julie Goldsbury for all your support, it has been a real pleasure working with you.

Big thanks to the people in the Molecular Genetics Laboratory for sharing the equipment and for treating me as a part of your group at the QMB meetings. To Dr. Gregory Jacobson, thanks very much for reviewing my thesis draft.

My gratitude also goes to Dr. Barry O'Brien for training me to use the confocal microscope. It has been great fun working with you and I really appreciate your assistance and guidance with my project.

I would like to acknowledge my friends, especially Ryland and Niharika, for going through the ups and downs with me during this two year journey. I am truly blessed to have you along the way.

Most importantly, I would like to thank my loving and supportive family, especially Mom and Dad. You have provided me more than any daughter could ask for and so this thesis is dedicated to you guys with lots and lots of love.

Table of Contents

Abstract…….. i

Acknowledgement……. iii

Table of Contents……... iv

List of Figures……..... vii

List of Tables……. ix

List of Equations…… x

List of Abbreviations……..... xi

1 LITERATURE REVIEW AND RESEARCH AIMS 1

1.1 Type 2 Diabetes Mellitus 1

1.1.1 Statistics 1

1.1.2 Definitions of Diabetes 2

1.1.3 Pathogenesis of T2D 2

1.1.4 Diabetes and Complications 4

1.2 Metformin 7

1.2.1 Chemistry and History 7

1.2.2 Cytotoxicity of Metformin 8

1.2.3 Metformin as an Anti-Hyperglycemic Agent 9

1.2.4 Molecular Mechanism of Metformin 11

1.2.5 Metformin, Oxidative Stress & More 16

1.2.6 Metformin & Vascular Disease 17

1.3 Heat Shock Proteins 24

1.3.1 Heat Shock Proteins in the HSP60 Family 25

1.3.2 Regulation of HSPs 27

1.3.3 Hsp60 “New” Locations 29

1.3.4 Hsp60 “New” Function 31

1.3.5 Receptor and Signaling Pathway for Hsp60 37

1.3.6 Hsp60 and Diseases 39

1.4 Aims and objectives 43

2 MATERIALS AND METHODS 44
2.1 Cell culture and Cytoxicity Assays 44
2.1.1 LDH Assay 44
2.1.2 MTT Assay 46
2.2 Quantification of Hsp60 Expression 48
2.2.1 Hsp60 mRNA Expression 48
2.2.2 Hsp60 Protein Expression 51
2.3 Differentiating THP-1 Cells 55
2.3.1 Cell Culture 55
2.3.2 CD14 mRNA Expression 55
2.4 Surface Expression of Hsp60 57
2.4.1 Cell Preparation 57
2.4.2 Cell Fixation 57
2.4.3 Hsp60 Immunocytochemistry 58
2.4.4 MitoSOX Red Staining 59
2.5 Media, Reagents & Common Solutions Preparation 60
2.6 Statistical Analysis 63
3 EFFECTS OF METFORMIN ON THP-1 CELL CULTURE 64
3.1 Introduction 64
3.2 Methods 65
3.2.1 Cell Culture 65
3.2.2 LDH Assay 65
3.2.3 MTT Assay 66
3.3 Results 67
3.3.1 Cell Growth 67
3.3.2 LDH Assay 70
3.3.3 MTT Assay 71
3.4 Discussion 74

4 EFFECTS OF METFORMIN ON MITOCHONDRIA AS INDICATED BY MODULATION OF HSP60 77

4.1 Introduction 77

4.2 Methods 78

4.2.1 Cell Culture 78

4.2.2 Hsp60 mRNA Quantification 78

4.2.3 Protein Extraction 78

4.3 Results 79

4.3.1 mRNA levels 79

4.3.2 Protein levels 81

4.4 Discussion 83

5 EFFECTS OF METFORMIN ON DIFFERENTIATION OF THP-1 CELLS 87

5.1 Introduction 87

5.2 Methods 88

5.2.1 Cell Culture 88

5.2.2 CD14 and Hsp60 mRNA Quantification 88

5.3 Results 89

5.4 Discussion 91

6 OPTIMISATION OF SURFACE HSP60 DETECTION 94

6.1 Introduction 94

6.2 Methods 95

6.3 Results and Discussion 96

6.3.1 Cytospin 96

6.3.2 Fixatives 96

6.3.3 Confocal Microscopy and Hsp60 ICC 100

7 FINAL SUMMARY AND FUTURE DIRECTIONS 105

8 REFERENCES 108

List of Figures

Chapter 1

Figure 1.1 – Recruitment of monocyte to nascent atherosclerotic plaque 5

Figure 1.2 – Chemical structures of phenformin and metformin 7

Figure 1.3 – van der Waals space filling models of the GroEL-GroES-$(ADP)_7$ complex 26

Chapter 2

Figure 2.1 – The assembly of a semi-dry transfer sandwich. 53

Chapter 3

Figure 3.1 – Cell growth in metformin 68

Figure 3.2 – Rate of cell death in metformin relatively to Ctrl. 69

Figure 3.3 – Percentage of lysed cells in the presence of metformin..... 70

Figure 3.4 – Standard curve for MTT assay..... 72

Figure 3.5 – Mitochondrial dehydrogenase activity in the presence of metformin 72

Figure 3.6 – Blue formazan deposits intracellularly after 30 min incubation..... 73

Chapter 4

Figure 4.1 –Hsp60 mRNA and protein expression in response to metformin 80

Figure 4.2 – Western blots of Hsp60 at 3, 7 and 14 days..... 81

Chapter 5

Figure 5.1 – THP-1 monocytes and THP-1-derived macrophages 90

Figure 5.2 – Expression of *cd14* and *hsp60* in metformin-treated THP-1-derived

macrophages..... 90

Chapter 6

Figure 6.1 – Trypan blue staining of cells after cytospin 96

Figure 6.2 – THP-1 cells stained with PI after fixation with different agents..... 97

Figure 6.3 – Co-localisation of PI and trypan blue staining..... 99

Figure 6.4 – Hsp60 expression in MIN6 cells..... 100

Figure 6.5 – Confocal microscopy of ICC 103

List of Tables

Chapter 1

Table 1.1 – Definitions of type 2 diabetes 2

Table 1.2 – IC_{50} values (μM) of metformin and phenformin in three cell models. 9

Table 1.3 – Favourable and adverse effects of metformin.....11

Table 1.4 – CVD outcome by anti-hyperglycaemic agents in trials. 20

Table 1.5 – Major mammalian HSP families..... 25

Table 1.6 – Activation of innate immune cells by microbial heat shock proteins 32

Chapter 2

Table 2.1 – Thermocycling conditions for *hsp60* and *gapdh* PCR..... 50

Table 2.2 – Primer sequences for *hsp60* and *gapdh* PCR..... 51

Table 2.3 – Thermocycling conditions for *cd14* and *gapdh* PCR..... 56

Table 2.4 – Primer sequences for *cd14* PCR. 56

Table 2.5 – Fixatives trialed for surface preservation. 58

List of Equations

Equation 2.1 – Calculating relative cytoxicity. 45

Equation 2.2 – Calculating corrected MTT absorbance. 46

Equation 2.3 – Calculating mitochondrial dehydrogenase activity. 47

Equation 2.4 – Calculating standard error of the mean in Excel. 63

List of Abbreviations

˚C, degree Celsius; abs, absorbance; ACC, acetyl-CoA carboxylase; ADP, adenosine diphosphate; AGE, advanced glycation endproduct; AICAR, aminoimidazole carboxamide ribonucleotide; AMP, adenosine monophosphate; AMPK, AMP-activated protein kinase; APC, antigen presenting cell; ATP, adenosine triphosphate; BAEC, bovine aortic endothelial cell; BSA, bovine serum albumin; CAT, chloramphenicol acetyl transferase; cDNA, complimentary deoxyribonucleic acid; CHO, Chinese hamster ovary; CLSM, confocal laser scanning microscopy; CRP, C-reactive protein; CSF, colony stimulating factor; CTL, cytotoxic T lymphocytes; Ctrl, control; CVD, cardiovascular disease; DC, dendritic cell; DMSO, dimethyl sulfoxide; EC, endothelial cell; ELISA, enzyme-linked immunosorbant assay; ER, endoplasmic reticulum; EtBr, ethidium bromide; ETS, electron transport system; FBS, foetal bovine serum; FITC, fluorescein isothiocyanate; GAPDH (G3PDH), glyceraldehyde 3-phosphate dehydrogenase; GLUT, glucose transporter; GSH, glutathione; h, hour; HbA1c, glycated haemoglobin; HDF, human diploid fibroblast; HDL, high density lipoprotein; HMEC, human microvascular endothelial cell; HSBP, heat shock binding protein; HSE, heat shock element; HSF, heat shock factor; HSP, heat shock protein; HUVEC, human umbilical venous endothelial cell; ICAM-1, intercellular adhesion molecule-1; ICC, immunocytochemistry; IFG, impaired fasting glucose; IFN, interferon; IGT, impaired glucose tolerance; IKK, I-κB kinase; IL, interleukin; IR, insulin resistance; JNK, c-Jun N-terminal kinases; KDa, Kilo Dalton; LAL, limulus amebocyte lysate; LDH, lactate dehydrogenase; LDL, low density lipoprotein; LPS, lipopolysaccharide; LUC, luciferase; MAPK, mitogen-activated protein kinase; MCP-1, monocyte chemoattractant protein-1; MeOH, methanol; MHC, major histocompatibility class; MI, myocardial

infarction; min, minute; MMP, matrix metalloproteinases; mRNA, messenger ribonucleic acid; MTT, 3-(4,5)-dimethylthiazol-2-yl)-2,5-diphenyl tetrazolium bromide; NADH, nicotinamide adenine dinucleotide; NF-κB, nuclear factor-κB; NOS, nitric oxide synthase; PAI-1, plasminogen activator inhibitor-1; OCT, organic cation transporter; OD, optical density; PAMP, pathogen-associated molecular pattern; PBMC, peripheral blood mononuclear cell; PBS, phosphate buffered saline; PCR, polymerase chain reaction; PFA, paraformaldehyde; PI, propidium iodide; PI3K, phosphoinositide 3-kinase; PMA, phorbol 12-myristate 13-acetate; PRR, pattern recognition receptor; PTP, permeability transition pore; R, rescue; rcf, relative centrifuge force; RNS, reactive nitrogen species; ROS, reactive oxygen species; rRNA, ribosomal ribonucleic acid; RT, room temperature; SA-β-gal, senescence-associated β-galactosidase; S.E.M., standard error of the mean; SMP, submitochondrial particles; SNS, self non-self; SOD, superoxide dismutase; SU, sulfonylurea; T2D, type 2 diabetes; t-BH, t-butyl hydroperoxide; TBS, tris buffered saline; Thr, threonine; TL, transmitted light; TLR, toll-like receptor; TNFα, tumor necrosis factor α; TZD, thiazolidinedione; VCAM-1, vascular cell adhesion molecule-1; WHO, World Health Organization; WR, working reagent; UCP-2, uncoupling protein-2; UV, ultraviolet

1 Literature Review and Research Aims

This chapter reviews the current literature on the pharmacology of an anti-diabetic agent, metformin. A review on the role of heat shock protein 60 (Hsp60) is also provided and focuses particularly in the context of type 2 diabetes and cardiovascular disease. Finally, the proposed hypothesis will be explained and presented at the end of the chapter.

1.1 Type 2 Diabetes Mellitus

1.1.1 Statistics

Type 2 Diabetes (T2D) is the most common metabolic disease in the world. Not only it reduces the quality of life for patients and their family, the cost of health care exceeds $130 billion dollars per year in the United States alone (Petersen 2003). Since December 2000, diabetes has been identified as a priority health objective and ‘improving diabetes services’ has been listed as one of 10 targets for the New Zealand health sector (Ministry of Health 2007). Here, 5,000 adults were newly diagnosed and approximately 81,000 people were known to have diabetes in the year 1996 (Ministry of Health 2002). Furthermore, people with Māori and Pacific origins have three times higher incident rates than Europeans, and are more than five times more likely to die from diabetes (Ministry of Health 2002). In addition, not only do patients with T2D have an increased risk of cardiovascular disease (CVD), but it is also the leading cause of death among these patients, accounting for 40% - 56% of all deaths, as documented by several studies (de Marco *et al*. 1999; Roper *et al*. 2002). The common association of T2D with CVD will be reviewed in Chapter 1.1.4.

1.1.2 Definitions of Diabetes

The World Health Organization (WHO) (World Health Organization 2006) recommended definition of diabetes and intermediate hyperglycaemia states are summarized in **Table 1.1**. Impaired fasting glucose (IFG) and impaired glucose tolerance (IGT) are stages in the development of diabetes and is listed in the order of severity of disease. There have been recommendations that glycated haemoglobin (HbA1c) should be included in diagnosis and risk categories for diabetes and the WHO is currently undergoing review.

Table 1.1 – Definitions of type 2 diabetes

Condition	**Fasting plasma glucose** mmol/l (mg/dl)	**2-h plasma glucose*** mmole/l (mg/dl)
Normal	< 6.1 (110)	< 7.8 (140)
Impaired fasting glucose (IFG)	6.1 to 6.9 (110 to 125)	< 7.8 (140)
Impaired glucose tolerance (IGT)	< 7.0 (126)	≥ 7.8 (140) and <11.1 (200)
Diabetes	≥ 7.0 (126)	≥ 11.1 (200)

*Venous plasma glucose 2 hours after 75 g of glucose ingested.

1.1.3 Pathogenesis of T2D

It is now clear that disease progression of T2D involves insulin resistance (IR) in the early stages and eventually defects in insulin secretion by pancreatic β cells lead to the onset of hyperglycemia. There is accumulation evidence suggesting that these features of T2D are attributable to defects in mitochondria, the organelles that govern energy production in the cell (Lowell & Shulmanz 2005; Mulder & Ling 2009).

In order to utilize blood glucose, β cells of the pancreatic islets of Langerhans must act as sensors to vary insulin output to the prevailing blood glucose level. Insulin is crucial for promoting glucose storage and the prevention of glycogen

breakdown. Glucose sensing by β cells is therefore essential for maintaining glucose homeostasis. The chain of events followed by glucose sensing include: oxidative mitochondrial metabolism leading to an increased ATP:ADP ratio, inhibition of an ATP:ADP-regulated potassium channel, plasma membrane depolarisation, calcium influx, and, finally insulin secretion. Insulin resistance is a condition where skeletal muscle and liver, the two key insulin-responsive organs, require higher levels of insulin for glucose sensing. Unable to uptake glucose by peripheral tissues, failure to synthesize glycogen and suppress glucose production in the liver all contribute to hyperglycaemia.

Several lines of evidence support T2D pathogenesis by mitochondrial dysfunction. First, accumulating intracellular fatty acids (fatty acyl CoAs, diacylglycerol) have been shown to cause IR by the suppression of insulin signaling, which can be attributable to defects in mitochondrial fatty acid oxidation. Second, IR individuals were found to have a lower ratio of type 1 to type 2 muscle fibers, where the former contain more mitochondria than the latter. It was thought that peroxisome proliferator-activated receptory coactivator 1α, one of the genes that regulate mitochondrial biogenesis, is down-regulated in these individuals. Third, it was found that in T2D β cell mass is reduced relatively to matched individuals (with similar degrees of IR). The cause of this is unknown, but a mitochondrial regulated apoptosis mechanism has been suggested. In addition, an inner mitochondrial membrane protein called uncoupling protein-2 (UCP-2) has been shown to negatively regulate glucose-stimulated insulin secretion. UCP-2 is an integral membrane protein that can leak protons across the membrane when activated, leading to decreased ATP production. The expression of UCP-2 was shown to be stimulated by hyperglycaemia and hyperlipidaemia both *in vivo* and *in vitro*, suggesting a pathogenic role. It was also found that superoxide, a

byproduct of the electron transport chain, stimulates the activity of UCP-2 when added exogenously to isolated mitochondria, ultimately resulting in β cell dysfunction. All of the above defects might be secondary to chronic increased exposure to both glucose and fatty acids, a situation usually associated with obesity.

1.1.4 Diabetes and Complications

Diabetes is a 'metabolic syndrome' where it is associated with pathophysiological conditions such as hyperglycaemia, hyperinsulinaemia, dyslipidaemia, abdominal obesity, raised blood pressure, pro-inflammatory state and atherosclerosis (Bailey 2008). Individuals with T2D have a two- to fourfold increase in CVD incidence than non-diabetic individuals (Zarich 2009). Chronic hyperglycaemia and insulin resistance both have important roles in the pathogenesis of CVD. Cardiovascular disease is a collective term for microvascular and macrovascular diseases. The former refers to blindness, end-stage renal disease and a variety of debilitating neuropathies whereas the latter refers to atherosclerotic events such as myocardial infarction (MI, heart attack), stroke and limb amputation (Brownlee 2001).

Monocyte recruitment and subsequent differentiation into macrophage is an important step in early atherosclerosis development (Libby 2002; Ludewig & Laman 2004). **Figure 1.1** depicts an atherosclerotic event where circulating monocytes attach to the subendothelial space by interacting with adhesions molecules such as vascular cell adhesion molecule-1 (VCAM-1). The following migration into the intima is driven by a gradient of chemoattractants. A dominant chemokine, monocyte chemoattractant protein-1 (MCP-1), participates in this process by interacting with its receptor CCR2. The monocytes being retained in

the intima eventually become macrophages, expressing scavenger receptors such as CD36 that bind modified forms of low density lipoprotein (LDL) (oxidized or glycated). Such macrophages are termed foam cells, named after their foamy appearance under the microscope. Foam cells then amplify inflammation at the lesion through the production of cytokines, reactive oxygen species (ROS), and tissue-damaging compounds such as matrix metalloproteinases (MMP). The accumulation of foam cell along with T helper cells results in the progression of the atherosclerotic lesion which can ultimately lead to a thrombotic event and the rupture of an endstage plaque (Ludewig & Laman 2004).

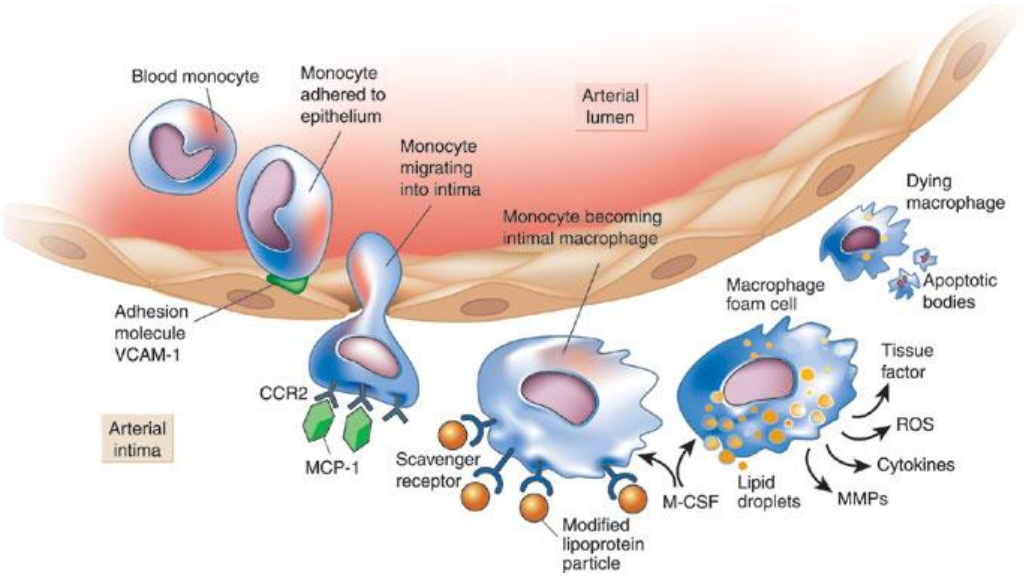

Figure 1.1 – Recruitment of monocyte to nascent atherosclerotic plaque. (Adapted from Libby (2002))

A closer look at monocytes reveals that CD14 is a specific marker for human monocytes (Passlick et al. 1989). CD14 functions as a receptor on the cell membrane for lipopolysaccharide (LPS)-binding protein/LPS complex recognition. In a study by Fogelstrand (2004), elevated circulating CD14+ monocyte, C-reactive protein (CRP), interleukin (IL)-6, and adhesion molecules intercellular endothelial cell (ICAM-1) and VCAM-1 were measured in diabetic women aged 64. The IGT group had values between the diabetic and normal group. Another study by Cipolletta (2005) further showed that poorly controlled diabetic monocytes are functionally activated as indicated by CD36 and CD68 expression. These two scavenger receptors are associated with the maturation of monocytes toward macrophages (Tsukamoto *et al.* 2002). In agreement with the atherosclerotic model above, increase in CD36 surface expression was paralleled by an increase in oxLDL uptake (Cipolletta *et al.* 2005). Furthermore, monocytes from a poor glucose control group had significantly increased ability to attach to endothelial cells.

In summary, T2D is a metabolic syndrome and mitochondrial dysfunction is thought to play a role in disease onset. Meanwhile, metabolic imbalance is commonly associated with imbalanced immune responses (Wellen & Hotamisligil 2005), in the case of T2D, a chronic low-grade inflammation is associated with the disease. Elevated cytokines and activated monocytes present in diabetic circulation are also seen in circulation of vascular inflammation. Not surprisingly, CVD is the most common complication in T2D and diabetes is considered a "CVD risk equivalent" (Zarich 2009).

1.2 Metformin

There are nine classes of approved drugs to treat T2D: insulin, sulphonylureas (SU), glinides, biguanides, α-glucosidase inhibitors, thiazolidinediones, glucagon-like peptide 1 mimics, amylin mimetic and dipeptidyl peptidase 4 inhibitors, either as monotherapy or in combination. The current recommendation by two major international diabetes associations is to initiate metformin therapy at diagnosis concurrently with lifestyle intervention (Nathan *et al*. 2009).

1.2.1 Chemistry and History

The biguanide family of anti-hyperglycaemic agents includes phenformin and metformin (**Figure 1.2**). They are the active glucose-lowering compound of French lilac (*Gallega officinalis*), of which the use can be traced back to the medieval times (Witters 2001). Although successful in the treatment of T2D, phenformin was withdrawn in the 1970s due to its association with lactic acidosis (Williams & Palmer 1975), leaving metformin as the only biguanide available today.

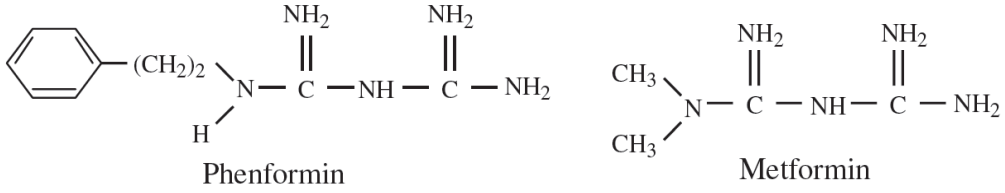

Figure 1.2 – Chemical structures of phenformin and metformin. (Adapted from Goodarzi & Bryer-Ash, 2005).

Metformin, chemical name N-1,1-dimethylbiguanide, is a white crystalline powder and is freely soluble in water. It is a weak base exhibiting a cationic charge at physiological pH (Wiernsperger 1999). Without the phenyl-ethyl ring that the phenformin possess, metformin is more polar and hence less lipid soluble.

Commercial name of metformin as monotherapy include Fortamet®, Glucophage®, Glucophage® XR, Glumetza®, and Riomet® (MedlinePlus 2008).

Contra-indications include renal and hepatic disease; cardiac or respiratory insufficiency; any hypoxic condition; severe infection; alcohol abuse; history of lactic acidosis; pregnancy and lactation (Bailey 2008).

In humans, metformin disposition is apparently unaffected by the presence of diabetes and the therapeutic levels range from 0.5 – 2.0 mg/L (around 3 – 15 μM) (Scheen 1996). Similarly, in normal and diabetic mice, the fasting plasma level of metformin is close to 10 μM and it hardly exceeds 100 μM after oral tablet intake (Wilcock & Bailey 1994). In the intestine the concentration can reach 10 mM and in the liver it is slightly higher than plasma levels. However, the concentrations in peripheral tissues such as skeletal muscle or fat are not much different from plasma levels (Wilcock & Bailey 1994; Wiernsperger 1999). It is therefore important to work within clinically relevant ranges of metformin concentration in this project.

1.2.2 Cytotoxicity of Metformin

The cytotoxicity effect of metformin has been analysed in detail by Dykens *et al* (2008). The IC_{50} values of phenformin and metformin on primary human hepatocyte, and HepG2 cells grown in either galactose or glucose are shown in **Table 1.2**. HepG2 cells grown solely on galactose were shown to be more reliant

on oxidative phosphorylation, thereby rendering the cells more susceptible to mitochondrial impairment (Marroquin *et al*. 2007; Dykens *et al*. 2008).

Table 1.2 – IC_{50} values (μM) of metformin and phenformin in three cell models.

Biguanide	Primary human hepatocytes	HepG2 in galactose	HepG2 in glucose
Metformin	657	1430	>2000
Phenformin	11.7	12.9	>500

The group then found that in primary human hepatocytes exposed to metformin concentration at 1 mM for 24h began to show dissipated membrane potential (ΔΨ) and induced ROS and at 2 mM there was a depletion of reduced glutathione (GSH, another measure of oxidative stress). At concentrations below 500 μM there was no detectable effect on these indices. However, 12.5 μM phenformin caused all of the above deleterious effects. It was also noted that cell numbers did not decrease at 24 h, indicating these concentrations were not immediately lethal.

Together these data confirm phenformin is much more potent than metformin and that metformin range below 500 μM had no detectable deleterious effects on these hepatic cell types.

1.2.3 Metformin as an Anti-Hyperglycemic Agent

It is well documented that metformin's major action is to reduce hepatic glucose production, which is increased at least twofold in T2D patients (reviewed by (Kirpichnikov *et al*. 2002). Metformin treatment was shown to decrease fasting plasma glucose by 25 – 30% in various studies and this was attributable to a reduction in the rate of gluconeogenesis (Kirpichnikov *et al*. 2002).

The second most important effect of metformin is the increase in insulin-stimulated glucose uptake in peripheral tissues (mainly skeletal muscle) (Kirpichnikov *et al*. 2002). Enhanced muscle uptake of insulin, increased insulin receptor tyrosine kinase activity, increased glucose transporter-4 (GLUT4) translocation and transport have been reported as a response to metformin therapy (reviewed by Goodarzi & Bryer-Ash 2005).

Other beneficial effects include reduction of triglycerides, total cholesterol, LDL cholesterol levels, and an increase in HDL cholesterol. Futhermore, in contrast with many other anti-hyperglycaemic medications, metformin is known to maintain or reduce the weight of patients. However, it may induce adverse gastrointestinal effects, interfere with vitamin B_{12} absorption and in rare cases, induce lactic acidosis. See **Table 1.3** for summarized effects of metformin.

Recently, there are data from trials and *in vitro* experiments suggesting that metformin has a vascular protective effect. This aspect will be discussed in detail in Chapter 1.2.6.

Table 1.3 – Favourable and adverse effects of metformin. (Adapted from Goodzari & Bryer-Ash 2005)

	Favourable effects	**Adverse effects**
Generally accepted	Improved glycaemic control (fasting plasma glucose by 3-4 mmol/l and HbA1c by 1.5-2%) Reduced triglycerides Reduced total cholesterol Reduced LDL-cholesterol Weight stability/reduction Stabilise/reduce serum insulin level	Gastrointestinal (diarrhea, abdominal discomfort) Lactic acidosis Metallic taste Reduced serum B_{12} levels
Some evidence	Blood pressure reduction Increased HDL-cholesterol Increased fibrinolytic activity (PAI-1 levels reduced) Reduced platelet aggregation Reduced fibrinogen levels Improved vascular relaxation Reduced CRP	

1.2.4 Molecular Mechanism of Metformin

Despite decades of clinical use, the exact mechanism of metformin action is yet to be definitively determined. A variety of possible mechanisms has been demonstrated to explain its hepatic effect, including phosphorylation of insulin receptor and insulin receptor substrate-2, inhibiting key enzymes in the gluconeogenic pathway, activation of pyruvate kinase, inhibition of hepatic glucagon effects and reduction in hepatic uptake of glucogenic substrates (lactate, alanine) (reviewed by Goodarzi & Bryer-Ash 2005). Alternatively, Wiernsperger (1999) proposed that metformin exerts its effects through physically normalising the membrane fluidity in the diabetic state, therefore restoring protein-protein or

protein-lipid interactions required for proper functioning of the processes regulating glucose transport/metabolism. However, two mechanisms dominate the literature, which propose that metformin functions through (1) inhibition of the mitochondrial respiratory chain and (2) activation of the AMPK pathway.

1.2.4.1 Metformin inhibits complex 1

Accumulating data support that the metformin's primary site of action to be the complex I of the mitochondrial respiratory chain (Owen *et al*. 2000; Brunmair *et al*. 2004; Guigas *et al*. 2004).

Owen *et al*. (2000) demonstrated that there is a time- and dose-dependent inhibition of respiration in metformin-treated rat hepatoma cells. Metformin (50 μM) caused 12.6 ± 4.3 and 29.4 ± 7.7 % inhibition after 24 and 60 h, respectively; whereas 100 μM metformin caused 25.8 ± 3.4 and 37.1 ± 10.0 % inhibition, respectively, when glutamate+malate was used as substrate. There was no inhibition on succinate oxidation, indicating that metformin does not affect complex 3 of the respiratory chain. The group then used isolated mitochondria to show that inhibition of respiration increased with increasing metformin concentrations. Concurrent results were also seen in submitochondrial particles (SMPs), confirming that metformin targets at the complex 1 of the respiratory chain and not at the dehydrogenases producing NADH. Liver mitochondria isolated from rats treated with 50 mg metformin daily for 5 days showed approximately 10% in glutamate+malate oxidation compared with control. The authors explained that little inhibition *in vivo* was due to a lost in accumulated metformin during mitochondria isolation however changes in liver metabolite concentrations are characteristic of complex 1 inhibition.

Similarly, inhibition of complex 1 by metformin was seen in intact KB cells, an oral squamous carcinoma cell line (Guigas *et al*. 2004). After 30 min incubation of 10 mM metformin with permeabilised KB cells, oxygen consumption was reduced by 33% ($p < 0.01$) when glutamate and malate was used as substrate. This reduction in oxygen consumption was comparable to that when CCCP (inhibitor of oxidative phosphorylation that abolishes the mitochondrial membrane proton gradient) was added, but not in seen when succinate and malate was used as substrates. To further confirm this, NADH decylubiquinone reductase activity was measured in permeabilised KB cells pre-incubated with or without 10 mM or 100 μM metformin. Complex 1 activity was measured after hypo-osmotic shock-induced mitochondrial membrane rupture, and NADH oxidation monitored before and after the addition of 6 μM rotenone. Rotenone-sensitive activity of complex 1 was reduced by 34% ($P < 0.01$) and 24% ($P < 0.05$) in 10 mM and 100 μM metformin, respectively. As a control, citrate synthase activity was not altered.

Interestingly, thiazolidinediones (TZDs), another class of anti-diabetic drug that predominantly increases insulin-stimulated glucose uptake in skeletal muscle, was also shown to inhibit complex 1 of the respiratory chain (Brunmair *et al*. 2004). The effects of TZDs and metformin to some extent resemble those of exercise and AICAR (5-aminoimidazole-4-carboxamide- 1-β-D-ribofuranoside). TZDs and metformin both reduce the ratios of ATP to AMP, ATP to ADP, and phosphocreatine to creatine *in vitro* (reviewed by Brunmair *et al.* 2004). AICAR, a mimic of AMP, is known to activate the enzyme AMP-activated protein kinase, which promotes catabolic pathways while suppress anabolic ones and causes insulin sensitisation in the long term (Hardie *et al*. 2006). This finding supports the hypothesis that changes in the cellular energy status could have a role in the pharmacological and physiological modulation of insulin activity (Brunmair *et al*.

2004).

1.2.4.2 Metformin activates the AMP-activated protein kinase

The AMP-activated protein kinase (AMPK) is a phylogenetically conserved heterotrimer protein that functions as a metabolic sensor. It is activated by stimuli that either inhibit ATP production (e.g. hypoxia, hyperglycaemia) or that accelerate ATP consumption (e.g. exercise) which lead to an increase in AMP:ATP ratio. AMPK activation requires the phosphorylation of Thr172 on the α subunit in a highly sensitive manner. The downstream targets of AMPK include several biosynthetic enzymes such as acetyl-CoA carboxylase (ACC), hydroxymethylglutaryl-CoA reductase, glucagon synthase, and endothelial nitric oxide synthase (eNOS) (Hardie *et al*. 2006).

Several studies have shown that AMPK is a target of metformin. Zou *et al* (2004) demonstrated a dose-dependent AMPK activation in bovine aortic endothelial cells (BAEC) by metformin (100-500 μM), and this activation is mediated by mitochondrial generated reactive nitrogen species (RNS). The authors deduced that the product of complex 1 inhibition, $O_2^{\cdot -}$, reacts with NO to form $ONOO^-$, which is required in AMPK activation. This was derived from (1) BAECs depleted of functional mitochondria (ρ°-BAECs) did not activate AMPK by metformin, and (2) over-expression of superoxide dismutase (SOD) or inhibition of NOS blocked metformin-induced AMPK activation. Zou *et al* (2004) also showed activation of PI3K by metformin or $ONOO^-$ increased association of LKB1 with AMPK, thereby enhancing AMPK activity. LKB1 is one of the upstream kinases that can phosphorylate Thr172 and its expression appears to be constitutive (Hardie *et al*. 2006) and this is consistent in this experiment.

The same group furthered discovered that AMPK activation by metformin led to the phosphorylation of eNOS in BAECs and its association with heat shock protein 90 (Hsp90), resulting in increased activation of eNOS and NO bioactivity (Davis *et al*. 2006). The association of Hsp90 with eNOS is considered an important step in controlling eNOS activity (Davis *et al*. 2006) and NO is known to improve vasorelaxation. In high glucose-induced cells, metformin relieved inhibited AMPK and eNOS activity and further decreased the expression of adhesion molecules and endothelial apoptosis.

Hattori and collegues (2006) demonstrated that metformin dose-dependently inhibited tumor necrosis factor α- (TNFα)-induced nuclear factor-κB (NF-κB) activation and TNFα-induced IκB kinase activity in human umbilical vein endothelial cells (HUVECs). The outcome is attenuated expression of various pro-inflammatory cytokines and cell adhesion molecules, such as VCAM-1, E-selectin, intercellular adhesion molecule-1 (ICAM-1), and monocyte chemoattractant protein-1 (MCP-1).

The data from Davis *et al* (2006) and Hattori *et al*. (2006) suggest that metformin improves endothelial functions and may reduce cardiovascular events in patients with T2D. Activation of AMPK is the common pathway in these two studies and, not surprisingly it has been reviewed whether new therapeutic agents should target AMPK to control metabolic disease and vascular disease (Wong *et al*. 2009).

A centrally important question is: which is the primary target of metformin? There has been no report of metformin binding to complex 1 or AMPK, although there is evidence that the biguanide family is a substrate of the organic cation transporter (OCT)-1 (Wang *et al*. 2003; Sogame *et al*. 2009). Regardless of the uptake

mechanism, the site of action that results in metformin's anti-hyperglycaemic effects seems to be complex 1 of the mitochondrial respiratory chain. Activation of AMPK could be the secondary effect due to an increase in AMP:ATP ratio caused by inhibited oxidative phosphorylation. If AMPK represents the primary target, it is possible that one of the proteins in the cascade of phosphorylation events can locate on the outer mitochondrial membrane, thereby indirectly affect complex 1 (Guigas *et al*. 2004).

1.2.5 Metformin, Oxidative Stress & More

It is generally recognized that hyperglycaemia contributes to vascular complications by mitochondria-generated oxidative stress (Nishikawa *et al*. 2000) (Brownlee 2001). Complex 1 and 3 are two main sites of superoxide generation in the inner mitochondrial membrane (Kwong & Sohal 1998).

Indeed, metformin, being an inhibitor of the complex 1, has been shown to reduce ROS production in rat liver mitochondria via the reverse electron flux through the complex 1 while forward flux-related ROS production was unaltered (Batandier *et al*. 2006).

In intact KB cells metformin completely prevented cell death induced by an exogenous glutathione-oxidizing agent, t-butyl hydroperoxide (t-BH), independent of the concentration used (100 μM or 10 mM). This was confirmed by determining the release of cytochrome *c* from the mitochondrial intermembrane space to the cytoplasm, a pro-apoptotic event in the commitment to cell death (Guigas *et al*. 2004). The mechanism by which metformin prevented cell death involved the modulation of mitochondrial permeability transition pore (PTP) opening, which was exclusive to complex 1 inhibitors (Guigas *et al*. 2004).

Similarly, metformin prevented high glucose-induced cell death in a human dermal microvascular endothelial cell line, HMEC-1 (Detaille *et al*. 2005). It was deduced that metformin also prevented PTP opening in HMEC-1 cells under glucose-induced oxidative stress. The calcium retention capacity is related to potency of inhibition on complex 1 as shown by studies using rotenone.

In contrast, a study by Carvalho and colleagues (2008) reported that metformin treatment resulted in a slight, although not significant, increase in H_2O_2 production in rat liver mitochondria. A short term trial involving fifteen T2D patients treated with metformin also showed an elevation in oxidative stress as measured by malidialdehyde levels (Skrha *et al*. 2007). This is also consistent with the fact that induction of $ONOO^-$ was required for the activation of AMPK as mentioned above (Zou *et al*. 2004).

Further, metformin exacerbated Ca^{2+}-induced mitochondrial PTP opening in a concentration-dependent manner. Similarly, metformin in cultured glioma cells caused mitochondrial depolarization- and oxidative stress-dependent apoptosis (Isakovic *et al*. 2007).

The conflicting result reflects the central role that mitochondria play in cell viability, as well as the complexity of the many metabolic and oxidative equilibria and pathways that converge at the level of mitochondrial integrity (Dykens *et al*. 2008).

1.2.6 Metformin & Vascular Disease

Adding to the effect of metformin on lowering blood glucose, several trials indicate that metformin has protective effects on CVD compared with other treatments. Metformin has also shown to reduced development of atherosclerotic

lesions in animal models. Other modest favourable effects include reduced dyslipidaemia, reduced pro-inflammatory cytokines and adhesion molecules, improved glycation status, and anti-thrombotic effects. It should be noted that these beneficial effects could be secondary effects due to reduced weight/blood glucose/insulin rather than attributed to direct properties of metformin.

1.2.6.1 Evidence from trials

A summary of vascular outcome by metformin treatment in various trials is listed in **Table 1.4**.

In a sub-study of the United Kingdom Prospective Diabetes Study (UKPDS) it was found that early and intensive glycaemic control with metformin reduced the risk of MI and diabetes-related death by 39% and 42%, respectively, compared with the conventional (diet) treated group in overweight T2D patients. Since SU/insulin had similar glucose-lowering efficacy as metformin but did not reduce myocardial infarction significantly, the vasoprotective by metformin was thought to be independent of the level of HbA1c (Turner *et al.* 1998). Although UKPDS did not provide evidence on CVD risks in non-obese T2D patients, recent short trials have demonstrated metformin reduced biomarkers for CVD risk compared with repaglinide, an insulin secretagogue (Lund *et al*. 2008).

In contrast to the above, the 'A Diabetes Outcome Progression Trial' (ADOPT), which followed 4360 newly diagnosed T2D patients allocated to rosiglitazone (glitazone), glyburide (SU), or metformin, revealed that there were fewer CVD events in the glyburide group than the others (Kahn *et al*. 2006).

Further, in the DIGAMI-2 trial, T2D patients followed after a myocardial infarction showed there were no differences in CVD mortality between the

intervention groups with insulin, SU or metformin. While insulin therapy increased the risk of a new MI, metformin had a protective effect (Mellbin *et al*. 2008).

A relative small 'Hyperinsulinemia: the Outcome of its Metabolic Effects' (HOME) trial allocated 390 patients to either placebo or metformin as an add-on to ongoing insulin therapy. There was no significant decrease for the risk of primary outcome, which is an aggregate of microvascular disease, CVD and mortality. In addition, although secondary microvascular disease outcome was not significant, metformin significantly reduced the risk of secondary CVD outcomes such as myocardial infarction, stroke, and peripheral arterial reconstruction by 39%. The hypoglycaemic efficacies were comparable in both groups however changes in body weight in the metformin/insulin group partly explained the difference in CVD (Wulffele *et al*. 2002).

In a three months trial, metformin reduced carotid intima-media thickness as measured by ultrasound (Bailey 2008). In several animal trials, metformin was shown to reduce plaque formation. In one experiment, metformin reduced aortic plaque formation even without significantly affecting blood lipids in rabbits fed a high cholesterol diet (Bailey 2008).

Table 1.4 – CVD outcome by anti-hyperglycaemic agents in trials.

Trial	Sample size	Specifications	Treatment groups	Follow up period	Major findings relating to vascular outcome
UKPDS (United Kingdom Prospective Diabetes Study)	753	Overweight T2D patients	Conventional (diet) or intensive glycaemic control with MET or SU/insulin	Average of 10 years	• MET significantly reduced risk of MI (39%), diabetes-related death (42%), and all-cause mortality (36%). • MET significantly reduced the incidence of CVD compared with SU/insulin. • MET did not reduce the number of patients with microvascular outcome measures. • The study did not separate non-obese patients thus there is lack of data for CVD risk in these patients.
ADOPT (A Diabetes Outcome Progression Trial)	4360	Newly diagnosed T2D patients	Rosiglitazone, glyburide, or MET	4 years	• Not statistically powerful enough to detect differences in CVD risk, only that there were fewer CVD events in the glyburide group than the other two.
DIGAMI-2	1181	T2D patients after MI	Insulin, SU, or MET	2 years	• MET had a protective effect on the development of a new MI.
HOME (Hyperinsulineamia: the Outcome of its Metabolic Effects)	390	T2D	Placebo or MET in addition to ongoing insulin	4.3 years	• No significant decrease for risk of primary outcome – aggregate microvascular disease • MET significantly reduced the risk of secondary CVD outcome by 39% but not significant in microvascular outcome. • Changes in body weight partly explained the difference in CVD risks.

Abbreviations: CVD, cardiovascular disease; MET, metformin; MI, myocardial infarction; SU, sulphonylureas; T2D, type 2 diabetes.

1.2.6.2 Potential mechanism

Cell culture and animal studies have shown a possible association between insulin resistance, compensatory hyperinsulinaemia and the development of atherosclerosis (reviewed by Hemmingson *et al.* 2009). Hyperglycaemia, on the other hand, is also a risk factor for CVD. It is possible the anti-atherogenic effects exerted by anti-hyperglycaemic agents are attributable to their improvement on insulin sensitivity, thereby reduce CVD risks. Similarly, lowering blood glucose could account for the beneficial effects on CVD development. Metformin seems to have additional protective effect independent of these mechanisms by improving several aspects of cardio-metabolic dysfunction that commonly occur in T2D based on various in vitro experiments. The following is an overview of the effects of metformin on the main recognized pathophysiological parameters associated with CVD (modified from Bailey 2008):

(1) Blood pressure – There is no measurable changes in blood pressure by metformin.

(2) Lipids – In diabetes, increased free fatty acids contributes to secretion of vLDL, which when modified have high affinity for scavenger receptors on macrophages. Lipid laden macrophages, namely foam cells, participate in early plaque formation. Metformin improves dyslipidaemia in diabetic patients, decreases oxidative stress and reduces lipid oxidation by lowering blood glucose.

(3) Endothelial function – Metformin was shown to increase endothelium-dependent vasodilation in a three month trial (Mather *et al.* 2001) possibly by inducing eNOS activation and improving NO bioactivity (Davis *et al*. 2006). Metformin was also shown to reduce monocyte adhesion to human

ECs by decreased expression of VCAM-1, ICAM-1 and E-selectin in endothelial cells (ECs). The effect of lowered advanced glycation endproducts (AGEs) could also contribute to the reduced expression of adhesion molecules. Metformin also reduced differentiation of cultured human monocytes into macrophages and foam cells (Mamputu *et al.* 2002).

(4) Inflammation – Metformin has been shown to reduce CRP concentrations in T2D independently of glycaemic control. Metformin also reduced TNFα-induced of NF-κB activation in HUVECs (Hattori *et al*. 2006).

(5) Glycation and oxidative stress – Hyperglycaemia-induced AGEs can activate AGE receptors on ECs and macrophages, leading to production of cytokines and ROS. Metformin was shown to reduce the formation of AGEs (Beisswenger *et al.* 1999). Several studies have shown metformin reduced production of ROS in cell cultures (Ouslimani *et al.* 2005) and partially reverse the reduced antioxidant defenses in T2D (Libby 2002)

(6) Anti-thrombotic effects – Metformin has been shown to reduce hypercoagulation and increase fibrinolysis by decreasing the levels of plasminogen activator inhibitor (PAI)-1 and increasing tissue plasminogen activator activity (Grant 1996). Furthermore, metformin decreased platelet aggregation in T2D patients. These anti-thrombotic actions seem to be independent of the anti-hyperglycaemic effect (Grant 2003).

Overall, these effects might contribute to the beneficial effects of metformin on the risk of CVD in T2D. However, what still remain unclear is (1) whether there is a direct causal relationship between lowering blood glucose and the risk of developing CVD, and (2) it has still not been clarified which anti-diabetic interventions prevent CVD to the greatest extent in patients with T2D, despite much research. Metformin (and glitazones) may have a beneficial effect on CVD risk but conclusive documentation is yet unavailable.

1.3 Heat Shock Proteins

Heat shock proteins (HSPs) are a group of highly phylogenetically conserved proteins present in all prokaryotes and eukaryotes. First discovered in temperature shocked *Drosophila* in 1962, then it was recognised that heavy metals, metabolic poisons, hypoxia, and free radicals also led to the production of these stress proteins (Shamaei-Tousi *et al*. 2007a). In actual fact, HSPs are constitutively expressed and they serve as molecular chaperones where they bind to nascent polypeptide chains and partially folded proteins to prevent their aggregation and misfolding. HSPs are also involved in the degradation of aged or damaged proteins. Under cellular stress, however, the expression of these stress proteins can be induced to prevent cellular damage.

HSPs can be classified into six families, the small HSPs (sHSP), HSP40, 60, 70 90, and HSP110, based on their molecular mass. A summary of mammalian HSP families is listed in **Table 1.5**.

Recently HSPs have been detected on the cell surface and the extracellular milieu (see Chapter 1.3.3) and their immunoregulatory role has been established. Members in the HSP60 and HSP70 families have been widely studied for their ability to stimulate innate and adaptive immunity as well as their abundance in cancer cells. The occurrence of these proteins is particularly important in diseases such as diabetes and CVD as (1) diabetes is associated with a low level chronic inflammation, (2) cells in the diabetic state are in stress due to hyperglycaemia, and (3) (endothelial) inflammation is involved in the pathogenesis CVD, a major complication in T2D. In later chapters the association of Hsp60 with T2D and CVD will be reviewed.

Table 1.5 – Major mammalian HSP families. (Adapted from Habich and Burkart 2007)

Families	Size (KDa)	Prominent members	Localisation
Small HSPs	12 – 43	B-crystallin	Cytoplasm
		Hsp27	Cytoplasm, nucleus
HSP40	~40	Hsp40	Cytoplasm, nucleus
Hsp60	~60	Hsp60	Mitochondria
		TCP1	Cytoplasm
HSP70	~70	Hsp70	Cytoplasm
		Hsc70	Nucleus
		Grp78/BiP	Cytoplasm, ER
HSP90	~90	Hsp90 (α and β)	Cytoplasm
		Gp96	ER
HSP110	~110	Hsp110	Cytoplasm

1.3.1 Heat Shock Proteins in the HSP60 Family

Proteins in the HSP60 family have a size of around 60 KDa and they have a high sequence homology between species. Hsp60 of bacterial origin have homology higher than 97% at their protein levels, while prokaryotic and human Hsp60 show over 70% homology at most conserved regions.

The *E. coli* GroEL is a well-studied member of the HSP60, known for its role in assisting protein folding alongside its cofactor GroES (Hsp10) in an ATP-dependent manner. Crystal structure of GroEL showed that it exists as two identical heptameric rings stacked back to back to form a central cavity (**Figure 1.3**) (Chen & Sigler 1999). In the presence of adenine nucleotides the GroES binds to the apical domain of the GroEL complex acting like a cap. The apical domain also serves as binding site for unfolded protein substrate (Levy-Rimler *et al*. 2002).

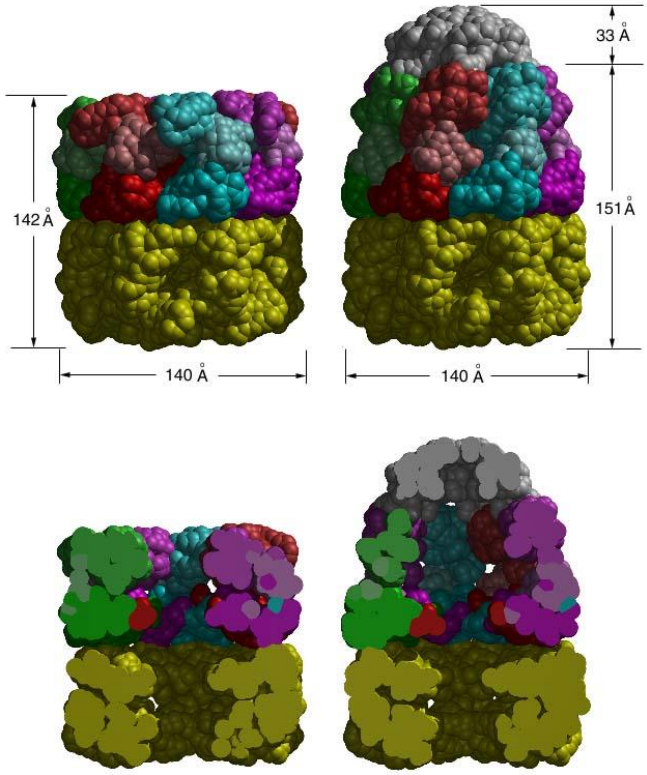

Figure 1.3 – van der Waals space filling models of the GroEL-GroES-$(ADP)_7$ complex. Image adapted from Sigler *et al*. (1998). The overall structure and dimensions of GroEL (left) and GroEL-GroES-$(ADP)_7$ (right) are shown. The upper panels show the outer views while the lower panels show the cavity of the models cut in half through the vertical plane.

In eukaryotes, Hsp60 can be found in the chloroplast of plants and mitochondrion and cytosol (T-complex polypeptide-1) of mammalian species. While the yeast and chloroplast Hsp60 exist and function as tetradecamers, mitochondrial Hsp60 can exist in solution in a dynamic equilibrium between monomers, heptamers and tetradecamers (Levy-Rimler *et al*. 2002). Mitochondrial Hsp60 forms tetradecamers in the presence of ATP while it dissociates into monomers at very low concentrations (Levy-Rimler *et al*. 2001). The cytosolic Hsp60 Hsp60 forms heterooligomeric ring structures and assists folding of cytoskeletal proteins such

as actin and tubulin (Llorca *et al.* 2000).

Hsp60, like most mitochondrial proteins, is a nuclear-encoded protein that carries an N-terminal presequence that, upon translocation into the organelle, is cleaved off (Wiedemann *et al*. 2004).

Recently, the occurrence of extra-mitochondrial Hsp60 has been documented. Hsp60 has been found on the cell surface and extracellularly such as human circulation (Chapter 1.3.3). Hsp60 in such a localisation has an immunoregulatory property and the possibility of cross-reactivity to microbial Hsp60 has been implied (Chapter 1.3.4). The localization and function of extra-mitochondrial Hsp60 will be discussed in detail in later sections. Because Hsp60 has different functions depending on its localization, it is known as a moonlighting protein (Shamaei-Tousi *et al*. 2007a).

1.3.2 Regulation of HSPs

Heat shock proteins can make up to 5-10% of the total protein content in healthy growing conditions, but the synthesis of these proteins can be induced up to 15% of total protein content by stresses that induce protein unfolding, misfolding, aggregation, or a flux of newly synthesized non-native proteins (Pockley 2003).

The inducible HSP is regulated by heat shock factors (HSFs), which are transcription factors that are normally negatively regulated but activate upon stress. In contrast to yeast and fruit fly where only one HSF was identified, several members of the HSF family exist for vertebrates and plants, suggesting diversification and specialization of these HSFs.

Although sharing 40% structural homology, HSF 1 functions in response to stress stimuli whereas HSF2 activates under early embryonic development,

differentiation and is activated by inhibition of ubiquitin-dependent proteasome (Pirkkala *et al*. 2001). Activation of HSF1 begins from oligomerisation from the inert monomer to an active trimer, which regains DNA binding activity and undergoes stress-induced serine phosphorylation and nuclear localization. Subsequently, HSF1 binds to the heat shock element (HSE) located upstream of heat shock responsive genes which results in HSP gene transcription. Several HSF1-binding proteins have been implied in HSF1 inactivation. For example, Hsp70 has been shown to play a role in HSF1 deactivation in several experiments, whereas the formation of a heterocomplex involving Hsp90 was shown to modulate different steps of the HSF1 activation-deactivation pathway. In addition, an 8.5 kDa nuclear protein termed heat shock factor binding protein 1 (HSBP1) was also found to hinder oligomerisation of HSF1. The mechanisms to repress DNA binding by HSF1 suggest the cell's need for tight transcription regulation and thereby maintaining protein homeostasis.

HSF3 is an avian-specific HSF and, like HSF1, it is a stress-responsive transcription factor, namely heat response. Activation of HSF3 requires the oligomerisation from dimeric to nuclear trimeric structure that acts as a transactivator (Pirkkala *et al*. 2001).

HSF4 is the most recently discovered mammalian HSF which is restricted to certain tissues. HSF4 was shown to have properties of a transcription repressor but it is still unclear whether it is a stress-responsive factor.

Even though HSFs demonstrate differentiated functions, as supported by the fact that neither HSF2 nor any other HSF is able to functionally substitute for HSF1, HSFs have been proposed to have overlapping roles depending on different stimuli. Furthermore, there also exists the possibility that HSFs could cooperate in order to regulate expression of their target genes, as shown by the maximal heat

protection by avian HSF1 and 3.

1.3.3 Hsp60 “New” Locations

In addition to its mitochondrial location, increasing reports suggest the existence of Hsp60 on the cell membrane and the extracellular space. This is consistent across prokaryotic and eukaryotic cells, and under both normal and stress conditions.

1.3.3.1 Surface Hsp60 Expression

Using immunogold cryothin-section EM and immunofluorescence, it was found that 16% of the labeled GroEL proteins in the *E. coli* cell were located in the membrane fraction under normal conditions. Furthermore, the density of gold-bound GroEL was higher in the membrane region than in the cytosol (Newman & Crooke 2000). Other membrane associated Hsp60 in prokaryotic cells have been documented and reviewed by Horvath *et al*. (2008).

In a study by Solty and Gupta (1996) using immunogold electron microscopy on various mammalian cell lines, 80 - 85% of the Hsp60 was localised in the mitochondrial matrix whereas the remainder was seen at extramitochondrial sites. These sites included the foci of the endoplasmic reticulum, on the cell membrane and other unidentified vesicles. The group further confirmed the cell membrane localisation by biotin labeling of the plasma membrane proteins and followed by immunoprecipitation and Western blots.

A more recent work by Pfister *et al*. (2005) also detected the occurrence of surface Hsp60 in HUVECs. Confocal laser scanning microscopy (CLSM) revealed that

there was no production of Hsp60 on the surface of unstressed cells but after 42°C treatment for 30 min (and recovered for 6 h) a significant portion (10.9 ± 3.6%) of cells had exposed Hsp60 on the surface, comparable to the 9.5% detected by flow cytometry. The number of cells that had surface expressed Hsp60 also increased from 1.1% to 9.5% followed by heat stress.

1.3.3.2 Extracellular Hsp60 Expression

It has been established in recent years that Hsp60 can be found in extracellular space and in the circulatory system. Hsp60 has also been detected in the culture media followed by stress as measured by enzyme-linked immunosorbant assay (ELISA) (Liao *et al.* 2000). Circulating HSP levels are decreased in aging and increased in a number of pathological conditions such as hypertension, atherosclerosis and post-trauma or surgery (reviewed by Tsan & Gao 2004; Bangen et al. 2007).

For example, in a study on plasma levels of Hsp60 involving 860 healthy men (457) and women (304), 46.9% of the subjects had Hsp60 levels below 1 ng/mL (detection limit of ELISA), 26.5% were between 1 and 1,000 ng/mL, and 26.6% were above 1,000 ng/mL. Molecular analyses showed that the circulating Hsp60 was the full-length protein lacking the N-terminal presequence, indicating that the circulating Hsp60 originated in the mitochondria of unknown cell types (Shamaei-Tousi *et al*. 2007b).

1.3.3.3 Secretion Pathway

There is evidence suggesting the involvement of exosomes and/or lipid raft in the release of Hsp60 (Gupta & Knowlton 2006), however, regardless of the

mechanism, it is believed that Hsp60 is actively secreted rather than by necrosis.

1.3.4 Hsp60 “New” Function

In addition to their intracellular chaperone roles, HSPs serve as regulators of the immune system when expressed on the surface or secreted into the circulation. Several studies have shown effects of Hsp60 on the innate and adaptive immune systems. Microbial heat shock proteins are known activators of the innate immune response (see **Table 1.6**) and have been shown to elicit potent antigen-specific immunity (adaptive immune response).

Earlier studies revealed that recombinant human HSPs can elicit several immune responses through the conserved toll-like receptor (TLR) family. The resulting activation of downstream signaling pathway (Toll/IL-1 receptor pathway led to activation of NF-κB) and cytokine release patterns shared striking similarity with that of bacterial LPS and therefore it was determined that these data were due to endotoxin contamination. To overcome this problem, HSPs were purified from eukaryotic hosts and several control measures were introduced, such as limulus amebocyte lysate (LAL) assay to measure endotoxin levels, treating of HSP with polymyxin B which binds LPS, heat denaturation of HSP, and mice defective for the recognition of LPS.

Table 1.6 – Activation of innate immune cells by microbial heat shock proteins. Adapted from Wallin *et al* (2002).

Heat shock protein	Cell type	Effect
M. leprae Hsp65	Monocytes (THP-1)	Production of TNF-α, IL-6 and IL-8
M. tuberculosis Hsp60	Monocytes (THP-1)	CD14-dependent production of TNF-α and IL-1β
M. bovi Hsp65	Monocyte-derived macrophages	Production of TNF-α and IL-1β
L. pneumophila Hsp60, *E. coli* GroEL, *M. Leprae* Hsp65, and *M. bovis* Hsp65	Peritoneal macrophages	Induction of transcription of TNF-α, IL-1α, IL-1β, IL-6 and GM-CSF mRNA, and increase in supernatant IL-1 bioactivity
Mycobacterial Hsp65	Peritoneal macrophages	Production of TNF-α, IL-6 and reactive nitrogen intermediates
L. pneumophila Hsp60	Macrophages	PKC- and cell-surface-receptor-dependent production of IL-1
L. pnemophila Hsp60 and *M. bovis* Hsp65	Macrophages	Production of IL-12
Recombinant *M. bovis* Hsp65	HUVECs	Increased adhesiveness to monocytes and granulocytes, and up-regulation of E-selectin, VCAM-1 and ICAM-1 expression
E. coli GroES, GroEL and DNAk	Monocytes HUVECs	Production of TNF-α, IL-6 and GM-CSF Production of IL-6 and GM-CSF, and up-regulation of E-selectin, ICAM-1 and VCAM-1 expression
Recombinant chlamydial Hsp60	Vascular endothelium and macrophages	Up-regulation of expression of adhesion molecules, production of IL-6 and activation of NF-κB
Recombinant chlamydial Hsp60	Macrophages and dendritic cells	Activation of the Toll/IL-1 signaling pathway

Abbreviations (in alphabetical order): GM-CSF, granulocyte-macrophage colony-stimulating factor; ICAM-1, intracellular adhesion molecule 1; IL, interleukin; *L. pneumophila*, *Legionella pneumophila*; M. bovis, Mycobacterium bovis; M. leprae, Mycobacterium leprae; M. tuberculosis, Mycobacterium tuberculosis; NF-κB, nuclear factor κB; TNF-α, tumor necrosis factor α; VCAM-1, vascular cell adhesion molecule 1.

Later studies using endotoxin-free HSPs have demonstrated their immune stimulatory and modulatory roles in three ways: (1) HSPs bind antigenic peptides and mediate major histocompatibility class (MHC) I presentation, (2) they act as endogenous danger signals under cell stress and tissue damage, and (3) HSPs bind to pathogen-associated molecular pattern (PAMP) molecules and induce signaling through pattern recognition receptors (PRR) (Osterloh & Breloer 2008).

1.3.4.1 HSPs are Carriers of Antigenic Peptides

Cytosolic HSPs such as Hsp70, Hsp90 and gp96 play important roles in antigen presentation, cross-presentation, and tumor immunity (reviewed in Tsan & Gao 2004). The HSP/peptide complex is internalized by antigen presenting cells (APCs) via CD91-mediated endocytosis, leading to MHC I presentation and the induction of cytotoxic T lymphocytes (CTL). This has significant implications in development of vaccines and therapeutics for cancer and infectious diseases. However, Hsp60 has not been implicated in binding antigenic peptides and therefore will not be discussed in this review.

1.3.4.2 Hsp60 as an Danger Signal

Two theories have been proposed relating to immune regulation – the Expanded Self-Nonself (SNS) theory and the Danger model. The former was proposed by Janeway which states that immune response depends on the discrimination between “infectious nonself” and “noninfectious self” by APCs (Janeway 1992). Antigen presenting cells possess an array of PRRs specific for conserved molecules on pathogens (e.g. bacteria), also known as PAMP. Upon PAMP/PRR association, APCs become activated by producing costimulatory signals and

present foreign antigens to T cells. Toll like receptors are known PRRs and the family consists of 10 members (TLR1-10) (Takeda & Akira 2004). This theory falls short, however, in describing events such as transplantation, tumors and autoimmunity, as Matzinger pointed out (1998).

The Danger model states that regardless of the 'foreign-ness' of a substance, what really matters in the end is whether it causes damage or not (Matzinger 1998). If there is no damage done, the cells and their environment continue to function well despite the presence of the substance. However, if the cell dies of necrosis or becomes stressed or damaged, an immune response is initiated. Namely, the Danger model responds to endogenous signals that originate from stressed or injured cells. Such signals can be classified into two categories: pre-packaged and inducible.

Heat shock proteins are good candidate as inducible danger signals as they are up-regulated by several stressful conditions and, as discussed in Chapter 1.3.3, can be expressed on the cell surface or actively secreted. HSPs such as Hsp60, Hsp70, Hsp90 and gp96 from a variety of preparations have been shown to be potent activator of the innate immune system, inducing the production of cytokines such as TNFα, IL-1, IL-6, IL-12 and the release of NO by monocytes, macrophages, and APCs (reviewed by Tsan & Gao 2004). They have also been shown to induce the maturation of APCs as demonstrated by the up-regulation of MHC class I and II molecules.

Although it is still under debate whether human Hsp60 is still able to induce the above responses without presence of endotoxin co-stimulation, there is evidence of a role for Hsp60 in modulating the innate immune response. Osterloh and collegues (2004; 2007) demonstrated the ability of Hsp60 to modulate immune cell functions by using transgenic cell lines expressing Hsp60 on the cell surface.

Surface Hsp60 was shown to induce the maturation of murine APCs and the expression of interferon α (IFNα) in these cells. This signaling pathway was found to be important for enhanced T cell activation and is distinct to those induced by LPS (Osterloh *et al*. 2007). As Tsan and Gao (2004) pointed out, these cytokine-like effects of HSP differ from their molecular chaperone function in that they require no peptide binding, no ATP hydrolysis, no cofactors, and no protein complex assembly.

1.3.4.3 Modulation of PAMP-Signaling by Hsp60

Accumulating evidence points to that HSPs are able to bind PAMP molecules and in turn modulate PAMP-induced stimulation. Human and murine Hsp60 expressed on the cell surface of eukaryotic cells were shown to bind ^{3}H-labeled LPS. This binding was not only specific, saturable, but also able to be competed by unlabeled LPS (Habich *et al*. 2005). The identification of a LPS binding region on the Hsp60 further support a role of Hsp60 as LPS-binding protein (Habich *et al*. 2005).

What happens when Hsp60 binds to LPS? Indeed, HSPs have been shown to associate with PRR. Extracellular Hsp60 was shown to bind to macrophages and dendritic cells (DCs) in distinct areas that colocalises with CD14 (Osterloh *et al*. 2007).

While it is clear now that highly purified Hsp60 and Hsp70 do not induce the release of pro-inflammatory cytokines such as TNFα (Bausinger *et al*. 2002; Gao & Tsan 2003), heat shock protein binding to PAMP was shown to have a synergistic effect on inflammatory stimulation. The addition of recombinant Hsp60 and Hsp70 was shown to enhance LPS-induced TNFα release in

macrophages (Zheng *et al*. 2004). Similar data were seen by Bangen *et al*. (2007) where pre-incubation of LPS with Hsp60 and Hsp70 caused a dose-dependent increase in TNFα secretion by peripheral blood-derived mononuclear cells (PBMC). After pre-incubation with LPS, murine cell surface Hsp60 enhanced LPS-induced IL-12p40 production in peritoneal macrophages and IFNγ release T cells in a synergistic manner (Osterloh *et al*. 2007).

Together these data indicate Hsp60's role as a multifaceted modulator of the innate immune system and have potential influences on the adaptive immune responses. Heat shock protein 60 not only acts as an intercellular danger signal but also serves as sensors for hazardous signals, providing effective recognition of PAMPs such as LPS and increase the efficiency of immune responses. Furthermore, HSPs' cytokine effects have been proposed to contribute to the pathogenesis of autoimmune diseases and chronic inflammation (Tsan & Gao 2004).

1.3.5 Receptor and Signaling Pathway for Hsp60

The search for the Hsp60 receptors continues to be a controversial topic due to (1) possibility of endotoxin contamination even after several control method, and (2) the LPS-binding nature of Hsp60. The heated debate centered on whether it shared the same receptors for LPS, namely CD14 and TLR4. Heat shock protein 70 have been shown to bind to various receptors such as CD14, TLR4, LOX-1, CD40 and CCR5 (Binder *et al*. 2004), it was proposed that either Hsp60 may also be promiscuous in receptor binding or that some of these receptors were mistakenly identified (Henderson & Mesher 2007). Nevertheless, some evidence of Hsp60 receptors and signaling are presented here.

The binding of Hsp60 to different cell types such as macrophage and EC have been shown. Using flow cytometry, Alexa Fluor 488 labelled human Hsp60 was shown to bind to macrophages in a specific ligand-receptor manner at submicromolar concentrations (Habich *et al*. 2002). This binding was saturable and could be competed only with unlabelled Hsp60, not with unrelated control proteins. The binding was further confirmed with confocal microscopy and with EC and DC (Habich *et al*. 2002). Furthermore, the binding of human Hsp60 to macrophages could not be competed by Hsp60 of hamster or bacterial origins, suggesting heterogeneity of receptors for Hsp60 (Habich *et al*. 2003).

Using human CD14-transfected astrocytoma cells (which normally lacks response to LPS) and Chinese hamster overy (CHO) cells, Kol and colleagues (2000) discovered that CD14 was necessary but not sufficient for responsiveness to human Hsp60. TLRs have been described as components of the CD14 signaling complex and TLR4, in particular, has been described as a co-receptor for LPS (Triantafilou & Triantafilou 2002). The group also showed that Hsp60, like LPS, induced activation of p38 mitogen-activated protein kinase (MAPK) in PBMC,

which resulted in activation of NF-κB leading to the release of IL-6. Limulus amebocyte lysate assay and heat sensitivity of Hsp60 were used as control.

In a study by Vabulas *et al* (2001), chlamydial and human Hsp60 were shown to induce the stress-activated protein kinases c-Jun N-terminal kinases 1/2 (JNK1/2) and p38, the MAPK ERK1/2 and the I-κB kinase (IKK) in murine macrophages. This activation was mediated by TLR2 and TLR4 as cells defective of these receptors displayed impaired responses. In addition, activation of the pathway was compromised when cells were treated with an inhibitor known to disrupt endocytosis. The preparations of chlamydial and human Hsp60 contained less than 0.1 pg/μg protein as determined by LAL assay.

More recently experiments using genetically engineered eukaryotic cells expressing Hsp60 on the cell membrane revealed that the signaling is independent of TLR4 and that previous data were due to PAMP-associated TLR signaling (Osterloh *et al*. 2008). In the endotoxin-free environment Hsp60 did not result in expression of cytokines such as IL-6, IL-12 and TNFα, but up-regulated IFNα expression in APC, which was required for T cell activation. Membrane-associated Hsp60 also enhanced IFNγ release in TLR4-mutant APC in T cell co-stimulation and this effect was not seen after LPS administration.

Using a completely different approach in a search for Hsp60 receptors, Henderson and Mesher (2007) ran murine whole cell lysate through a column immobilized with Mycobacterium tuberculosis Cpn60.1 and the bound fraction was analysed by peptide mass fingerprinting. BiP, an Hsp70 in the endoplasmic reticulum lumen, VCAM-1 precursor, and polycomb protein Suz 12 were the three best-matched candidate for Cpn60.1. Interestingly, the hypothesized receptors, CD14 or TLR4, were not identified in this study, possibly due to a detection limit of the method or it could indicate previously described receptors were faulty.

Hsp70 has been proposed to act synergistically with Hsp60 (Alard *et al*. 2009), making it a likely candidate receptor.

1.3.6 Hsp60 and Diseases

1.3.6.1 Hsp60 in T2D

In a study by Aguilar-Zavala and colleagues (2008) TNFα, Hsp60 and other markers for chronic disease were measured in patients (n = 151) who < 1 year and > 5 years since T2D diagnosis. It was found that Hsp60 associated negatively with years since diagnosis and positively with glucose levels. Elevated Hsp60 may be a result of psychological and physical damage caused by T2D. This indicates Hsp60 may be a marker of pathological disorder at the early phase of T2D, similarly to the finding that Hsp60 also is associated with early CVD (Pockley *et al*. 2000). The induction of auto-antibodies might explain the decline of Hsp60 in later phases (Hoppichler *et al*. 1996). Elevated Hsp60 may also arise from hyperglycaemia-induced tissue damage as indicated by its positive correlation with glucose levels.

Plasma Hsp60 was also measured in 855 T1D and T2D patients by Shamaei-Tousi and colleagues (2006). There was a significantly higher proportion of patients with CVD and MI had detectable circulating Hsp60 compared with those without. This result was in agreement with the proposal that release of Hsp60 into circulation is an early risk factor in atherosclerosis (Pockley *et al*. 2000; Xu *et al*. 2000).

1.3.6.2 Hsp60 and atherosclerosis

Since T2D is regarded a CVD risk equivalent, this section will look at how Hsp60 is associated with the pathogenesis and progression of CVD.

Several studies have shown that Hsp60 is a powerful immunogen and immunomodulator in experimental models of arthritis, diabetes (type 1) and atheroscelerosis (Shamaei-Tousi *et al*. 2007a). With respect to atherogenesis, Wick *et al*. (2004) have generated experimental data to support the hypothesis that it is driven by cross-reactive immunity to bacterial Hsp60 proteins. In addition, there is increasing data supporting that members of HSP60 are inducers and mediators of vascular disease. First, Hsp60 is present in the serum of normal individuals (Pockley *et al*. 1999) and serum Hsp60 levels correlate with the presence of early atherosclerosis (Pockley *et al*. 2000; Xu *et al*. 2000). Several atherosclerosis risk factors (hyperlipidemia, diabetes, smoking, and hypertension) have been identified to cause induction of Hsp expression in vascular smooth muscle cells (Liao *et al.* 2000). Shear stress, such as during raised blood pressure, has been shown to induce Hsp60 expression in cultured human endothelial cells (Hochleitner *et al.* 2000). Another major contributor to the atherosclerotic plaque is foam cells which have accumulated oxidized LDL. Given that *in vitro* exposure to oxidized LDL induces Hsp60 expression by monocytic cell lines, it is likely that foam cells in the early atherosclerotic lesion express Hsps (reviewed by Pockley 2002).

During early vascular inflammation, enhanced expression of cytokines such as IL-6, VCAM-1 and MCP-1 are often observed. Therefore, alternatively, heat shock protein expression may be secondary to the oxidative stress induced by the resulting infiltrating leukocytes (Pockley 2002).

Once expressed extracellularly, Hsps have the potential to induce the nonspecific innate immune system and promote the adaptive immune system (Chapter 1.3.4). Indeed, raised levels of anti-HSP antibodies have also been associated with the presence and progression of vascular disease. Levels of antibodies to human Hsp60 are increased in peripheral vascular disease (Wright *et al.* 2000) and elevated levels of mycobacterial Hsp65 are also documented in various CVDs. The existence of such antibodies sparked arguments in relation to vascular injury and the pathogenesis of atherosclerosis. Some suggest that self-HSP antibodies have direct pro-inflammatory role in autoimmune disease while others have shown the presence of immunoregulatory T cells that can differentiate self and non-self Hsp60s and exert different outcomes (reviewed by Pockley 2002).

Since microbial Hsp60s are known potent immunogens involved in the pathogenesis of infectious diseases, it is plausible that they were present concomitantly under atherosclerotic-driving conditions. Chlamydial Hsp60 frequently colocalises with human Hsp60 in macrophages of atherosclerotic plaques (reviewed by Pockley 2002; Tsan & Gao 2004). Given the Th1 pro-inflammatory properties of bacterial Hsp60, the coexisting Hsp60 might be driving regulatory T cells to produce antibodies and shifts to a Th2-type cytokine response (Pockley 2002).

In summary, intracellular Hsp60 can be induced under cellular stresses to fulfill cytoprotective functions. The discovery of surface-expressed and circulating Hsp60 opened up a new field of research detailing their immune-regulatory roles. Human Hsp60 was shown to modulate APC function in a way distinct to LPS induction. Furthermore, Hsp60 has the ability to bind to LPS and enhance its signals. The immune-stimulatory effects of Hsp60, possibly due to cross-reactivity

to microbial Hsp, have been implicated in the development of atherosclerosis. T2D is a high risk factor for CVDs and therefore the presence of Hsp60 in T2D patients not only is a marker for psychological and physiological stresses but also a marker for early atherosclerosis.

1.4 Aims and objectives

Many studies have focused on the effects of metformin on cells of hepatic origin but data on monocytic cells are lacking. Circulatory monocytes are key players in innate immunity and aberrant expression of surface proteins on monocytes have been observed in T2D patients. Further, metformin has been shown to inhibit complex 1 of the mitochondrial respiratory chain. We therefore propose that metformin may cause a mitochondrial specific stress response through the modulation of Hsp60 expression. If Hsp60 was expressed on the surface of the stressed monocytic cells it may have immunoregulatory importance.

In this study, the cytoxicity of metformin will first be investigated in the human acute monocytic leukemia THP-1 cell line using different assays. The mRNA and protein expression of Hsp60 in metformin-treated THP-1 cells will next be determined. Surface expression of Hsp60 has been detected in various cell lines previously and here we will investigate whether metformin treatment will result in the same.

Lastly, metformin has been said to have protective effects on CVD risks in T2D patients. Since monocyte attachment to ECs and subsequent differentiation into macrophages are critical steps in developing atherosclerosis, the effect of metformin on PMA-stimulated macrophage formation *in vitro* will be studied here.

Overall this study aims to gain better understanding of metformin's pharmaceutical effects on monocytic cells through the studies of (1) its cytotoxic effects, (2) mitochondrial stress protein expression, and (3) monocyte-macrophage differentiation marker expression.

2 Materials and Methods

2.1 Cell culture and Cytoxicity Assays

The human acute monocytic leukemia THP-1 cell line was purchased from the American Tissue Culture Collection (No. TIB-202). The cells were grown in THP-1 media containing RPMI Media 1640 (Gibco) supplemented with 10% fetal bovine serum (FBS), 1 mM pyruvate and 1X penicillin/streptomycin. Cells were grown at 37°C, 5% CO_2 in a humidified incubator (standard incubation conditions). Cells were passage every 7 days by centrifugation (Megafuge 1.0) at 400 rcf approximately and re-suspended with pre-warmed fresh THP-1 media. All experiments were carried out using near-confluent cells which have been passaged 2 days prior to the experiments.

2.1.1 LDH Assay

Lactate dehydrogenase (LDH) is a cytosolic enzyme which is only released into the media by necrotic cells. The Promega CytoTox96 NonRadioactive Cytotoxicity Assay kit was used to determine LDH content. Following the manufacturer's methods, each duplicated sample were treated identically until the end of cell culture where one was spun at 400 rcf for 5 min at RT to collect supernatant and the other one used as the maximum control. A correct volume of 10X lysis solution was added to the maximum control and the cells returned to standard incubation conditions for 30 min. The cell lysate were centrifuged at 2,000 rcf for 5 min at 4°C to pellet cell debris. The supernatant of both samples were stored in -20°C until further analysis.

To reconstitute assay substrate, the substrate vial and buffer were warmed to RT and 12 mL of buffer was added to dissolve the substrate. The reconstituted substrate was kept at RT until time of assay. On the day of the assay, a positive sample was prepared by diluting the LDH Positive 1:1000 in PBS. In a 96-well plate, 50 µL of reconstituted substrate was added to 50 µL of positive sample, media blank, and sample supernatant in triplicates and incubated at RT for 30 min in the dark. The assay was ended by the addition of 100 µL Stop Solution and air bubbles removed before measuring the absorbance at 490 nm using a Model 680 Microplate Reader (Bio-Rad).

To obtain the percentage of LDH content relative to the maximum control, the data was first averaged and then subtracted with the media blank reading. Maximum control was multiplied by 1.1 to account for the diluting factor and then the sample was normalised to the maximum control (**Equation 2.1**). The final data was presented as a percentage and can be interpreted as the percentage of dead cells present in the original cell culture, assuming that each dead cell released an equal amount of LDH content.

$$\% \text{ Cytoxicity} = \frac{\text{Experimental LDH release (OD490)}}{\text{Maximum LDH release (OD490)}}$$

Equation 2.1 – Calculating relative cytoxicity.

2.1.2 MTT Assay

MTT [3-(4,5-dimethylthiazol-2-yl)-2,5-diphenyl tetrazolium bromide] is a tetrazolium dye which, when reduced by cellular dehydrogenases, forms blue crystals intracellularly. The crystals can then be dissolved and quantitated using a spectrophotometer. The Sigma MTT Based *In vitro* Toxicology Assay Kit was used with a few adaptations from the manufacturer's manual. MTT was dissolved in THP-1 media and pre-warmed to 37˚C. A standard curve with varying cell density was first carried out to determine cell density to be used. On a 96-well plate, 100 µL of THP-1 cells at 10^5 cells/mL were serially diluted and seeded in quadruplicate. A triplicate of blank media was also plated. Followed by an overnight rest, one set of serially diluted cells were taken to assess cell density by trypan blue (Sigma) exclusion. Ten microlitre of MTT was then added to each well and incubated at standard incubation conditions for 1-2 h or until blue crystals can be seen under the microscope. Solubilisation solution (100 µL) was added to each well and trituration done to help dissolve the crystals. The absorbance was read at 570 nm and the background read at 655 nm. After subtracting 655 nm readings from 570 nm, blank was subtracted to construct a standard curve. The region of cell density with linear increase of absorbance was determined for experimental cells.

Absorbance (corrected) = (Sample OD570 – 655 nm) – (Blank OD570 – 655 nm)

Equation 2.2 – Calculating corrected MTT absorbance.

Experimental samples were assayed the same way, with 10 µL of MTT per 100 µL cell suspension, followed by the addition of 100 µL Solubilization Solution. After reading absorbance at 570 and 655 nm the data were calculated as **Equation 2.2**. Experimental values were then normalized to Ctrl and number of cells and expressed as a percentage of mitochondrial dehydrogenase activity (**Equation 2.3**), since dehydrogenases are mainly localized in the mitochondria.

$$\text{Mito. dehydrogenase activity (\%)} = \frac{\text{Experimental sample absorbance (corrected)}}{\text{Ctrl sample absorbance (corrected)}} \div \text{no. of cells} \times 100\%$$

Equation 2.3 – Calculating mitochondrial dehydrogenase activity.

2.2 Quantification of Hsp60 Expression

2.2.1 Hsp60 mRNA Expression

To quantify the Hsp60 mRNA expression in the THP-1 cells, total RNA was extracted and reverse transcribed into cDNA. Any DNA contaminant was removed by DNase I treatment and semi-quantitative PCR was carried out. These methods are described below.

2.2.1.1 RNA extraction

Total RNA was extracted using TRIzol (Invitrogen) according to the manufacturer's protocol. Cells were pelleted at 400 rcf for 5 min and supernatant discarded. 500 µL TRIzol was used to lyse cells and incubated at RT for 15 min or alternatively stored at -80°C. Chloroform (100 µL) was then added to each tube and tubes shaken vigorously for 10-15 sec. The mixture was incubated at RT for 3 min before centrifugation at 12,000 rcf for 15 min at 4°C. The aqueous layer was carefully transferred to a new tube and mixed with an equal volume of isopropanol. Next, the mixture was incubated at RT for 10 min and centrifuged at 12,000 rcf for 10 min at 4°C. The supernatant was discarded and the RNA pellet washed with 500 µL 75% ethanol in DEPC water. After another centrifugation at 7,500 rcf for 5 min at 4°C to pellet RNA, the supernatant again discarded and the ethanol allowed to completely evaporate. The RNA pellet was re-suspended in 30 µL TE buffer (Promega) and kept on ice. Quantification of RNA was done with a Nanodrop ND-1000 spectrophotometer (Nanodrop). Samples with a 260 to 280 nm ratio of 1.8-2.1 were considered having good RNA purity. RNA integrity was assessed by running the samples on a non-denaturing 1% agarose gel in TBE

buffer. Briefly, 1 µg RNA was heated in 65°C for 10 min and immediately placed on ice before loading on to the gel. Samples showing discernable 28s and 18s rRNA bands in a ratio of 2:1 were considered as having good integrity.

2.2.1.2 DNase I Treatment

RNA samples were treated with amplification grade DNase I (Roche) before cDNA synthesis to remove any contaminating genomic DNA. RNA (1 µg) was made up to 8 µL with PCR water and was then mixed with 1 µL 10X reaction buffer and 1 µL DNase I. The mixture was incubated at RT for 15 min before the addition of 1 µL 25 mM EDTA. Next, a 10 min incubation at 65°C was carried out to inactivate the DNase I enzyme, the samples were cooled on ice for at least 1 min before proceeding to cDNA synthesis.

2.2.1.3 cDNA Synthesis

cDNA template was synthesized using the Roche Two-Step RT-PCR kit following the manufacturer's protocol. One microlitre of oligo dT_{12-18} primer was added to the DNase I-treated RNA samples and was incubated at 65°C for 10 min to remove secondary structures. A reaction mixture containing 1X RT buffer, 1 U RNase inhibitor, 1 mM dNTP, and 1 U reverse transcriptase per reaction was made up to a volume of 20 µL with PCR water and mixed gently. The samples were incubated at 55°C for 30 min and the reaction terminated at 85°C for 5 min. cDNA samples were stored at -20°C.

2.2.1.4 Semi-Quantitative PCR

PCR amplification was carried out using Fast Start Taq Polymerase (Roche). Each PCR reaction contained 1 µL cDNA, 1X PCR buffer ($MgCl_2$), 0.2 mM dNTP, 0.1 µM forward and reverse primers (Invitrogen) (sequences in **Table 2.2**), 0.2 µL Fast Start Taq Polymerase and the volume was made up to 25 µL with PCR water. Each PCR run included a negative control containing 1 µL PCR water instead of cDNA. The thermocycling conditions for *hsp60* and *gapdh* (the house keeping gene) are described in **Table 2.1** below.

Table 2.1. Thermocycling conditions for *hsp60* and *gapdh* PCR.

Product		**Denaturation**	**Annealing**	**Extention**	
hsp60	Initial denaturation at 95°C for 4 min	95°C 1 min	55°C 1 min	72°C 1 min	Final extension at 72°C for 10 min
gapdh		95°C 1 min	60°C 1 min	72°C 1 min	

The number of cycles that lied within the linear amplification range was used to quantitate the gene of interest by normalising to *gapdh* expression levels. The PCR products were run, along with a DNA ladder, on a 1% agarose gel stained with EtBr and buffered in 1X TAE. The gels were run at 80 V for approximately 40 min and visualised by exposing to UV light and an image acquired by a MiniBIS Pro Illuminator controlled by GelCapture software (both by DNR Bio-Imaging Systems). The intensity of the bands was analysed using the Gel Quant software (DNR Bio-Imaging Systems).

Table 2.2 – Primer sequences for *hsp60* and *gapdh* PCR.

Product	Sequences	Product size
hsp60	Forward: TTC GAT GCA TTC CAG CTT G Reverse: TTG GGC TTC CTG TCA CAG TT	439 bp
gapdh	Forward: ACC ACA GTC CAT GCC ATC AC Reverse: TCC ACC ACC CTG TTG CTG TA	451 bp

2.2.2 Hsp60 Protein Expression

2.2.2.1 Protein Extraction

Total protein was isolated using the TENT buffer containing 50 mM Tris (pH 7.5), 250 mM NaCl, 5 mM EDTA (pH 8.0), 1% Triton X-100 and freshly supplemented with 0.4 mM phenylmethylsulfonyl fluoride as protease inhibitor.

THP-1 cells treatment with metformin (0 – 500 µM) were pelleted at 400 rcf for 5 min and ruptured with 100 µL TENT buffer by vortexing. Followed by 30 min incubation at 4°C, samples were spun at 10,000 rcf for 5 min at 4°C to pellet cell debris. The supernatant was transferred to a new tube and stored at -20°C until further analysis.

2.2.2.2 Protein Estimation

Protein concentration was estimated using the BCA Protein Assay Kit (Pierce) following the manufacturer's protocol. A working reagent (WR) was made up containing 50 parts of reagent A with 1 part reagent B prior to the assay. A standard curve comprised of known concentrations of serially diluted bovine serum albumin (BSA) (Pierce) in phosphate buffered saline (PBS) was assayed along with samples with unknown concentrations. Twenty-five microlitre of each

standard and unknown was transferred onto a 96-well plate in duplicates followed by the addition of 200 µL WR to each well. The content was mixed briefly on a plate shaker before incubating at 37°C for 30 min. The plate was read at 560 nm using the Microplate Reader and the concentration of samples calculated from the standard curve.

2.2.2.3 Protein Separation and Transfer

Gel Preparation

Total protein was separated on a discontinuous gel (0.76mm). The 10 % separating polyacrylamide gel was prepared by mixing the following reagents: 4.1 mL distilled water, 2.5 mL 1.5 M Tris (pH 8.8), 100 µL 10% SDS, 3.3 mL acylamide-bis stock (Bio-Rad). Immediately before casting, 50 µL 10 % ammonium persulphate (APS, prepared fresh) (Bio-Rad) and 10 µL TEMED (Bio-Rad) were added in a fume hood and the mixture applied between the plates. A layer of 70 % ethanol was immediately overlaid gently. The separating gel was allowed to polymerise for 1 h.

The stacking gel was prepared by adding 6.1 mL distilled water, 2.5 mL 0.5 M Tris (pH 6.8), 100 µL 10 % SDS, 1.3 mL acylamide-bis stock (4%), 50 µL 10 % APS and 10 µL TEMED. Once the separating gel was set, the ethanol was poured off and was washed with the stacking gel mixture. The stacking gel was casted on top of the separating gel and the comb gently inserted and allow to it to polymerise for 45 min. The gel was assembled in a Mini-Protean 3 Cell gel tank (Bio-Rad) buffered with 1X electrode buffer.

Sample Preparation

Each sample containing 15 µg total protein was made up to a volume of 20 µL with protein loading buffer. The samples were denatured in boiling water bath for 5 min before loaded in the wells. Five microlitre of protein Kaleidoscope ladder (Bio-Rad) and a Hsp60 standard (250 ng) were also loaded alongside the samples. The gel was electrophoresed at 200V for 40 min or until the dye front reached the bottom.

Semi-Dry Transfer

Semi-dry transfer was carried out using a 3-buffer system containing a cathode buffer and anode I & II buffers (see Common solutions in Chapter 2.5). The gel was removed from the glass plates and trimmed to the relevant area and equilibrated in cathode buffer for 15 min. In parallel, a sheet of 0.45 µm nitrocellulose membrane (Bio-Rad) was cut to the same size of the gel and gently placed in anode buffer II to equilibrate for 5 min. Six pieces of extra thick filter paper (Bio-Rad) was cut slightly bigger than the membrane; three of which soaked in cathode buffer, two in anode buffer I and one piece in anode buffer II. The transfer sandwich was assembled as in **Figure 2.1** and air bubbles removed by rolling action over the top of the stack. Once the cathode plate was pressed down, the transfer cell (Bio-Rad) was run at 15V for 90 min.

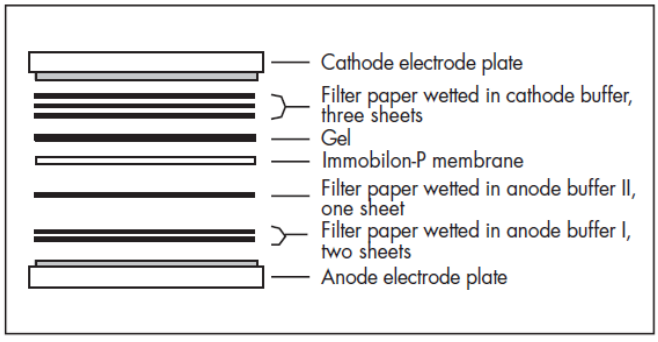

Figure 2.1 – The assembly of a semi-dry transfer sandwich. (Image adapted from Millipore Immobilon-P user guide)

After transfer, the membrane was rinsed in ddH_20 briefly before stained with Ponceau S for 1 min to assess loading consistency. The stain was then washed away with ddH_20 before western blotting.

2.2.2.4 Western Blotting

The membrane was blocked in 10 % skim milk in TBST overnight at 4°C. The following day, the membrane was incubated in polyclonal rabbit anti-Hsp60 (Stressgen SPA-805) 1:5,000 in 5 % skim milk in TBST for 1 h at RT on a rotary shaker. After 3 X 5 min washes in TBST, the membrane was then incubated in peroxidase conjugated goat anti-rabbit IgG (Sigma) 1:1,000 in 5 % skim milk in TBST for 1 h at RT. Another 3 X 5 min washes in TBST was carried out and the membrane transferred onto a glass plate. The membrane was incubated with SuperSignal West Pico Chemiluminescent Substrate (Pierce) for 5 min and covered with a piece of clear plastic sheet. The membrane was visualized by the LAS-1000 Plus Gel Documentation System (Fujifilm) and the intensity of the bands was analysed using the Gel Quant software.

2.3 Differentiating THP-1 Cells

2.3.1 Cell Culture

Phorbol 12-myristate 13-acetate (PMA) (Sigma) was used to stimulate differentiation of monocyte cells into macrophages. On a 24-well plate, near confluent THP-1 cells cultured in metformin-containing media (0, 100, 250, 500 µM) were treated with 50 nM PMA for 2-3 days or until cells show macrophage characteristics under the microscope.

2.3.2 CD14 mRNA Expression

Total RNA extraction and subsequent procedures were similar to Chapter 2.2.1 with a few changes, as described below.

2.3.2.1 RNA Extraction

Cells showing macrophage characteristics were harvested and total RNA extracted using TRIzol. This procedure differed slightly to Chapter 2.2.1.1 in that most cells were adherent. The media was transferred to eppendorf tubes and spun at 400 rcf for 5 min and the pellet containing suspended cells was lysed in 250 µL Trizol. Meanwhile, the attached macrophages were lysed using 250 µL Trizol. The two portions were combined and the RNA extraction carried out as described in Chapter 2.2.1.1. DNase I treatment and cDNA synthesis were carried out the same way as Chapter 2.2.1.3 and 2.2.1.4, respectively.

2.3.2.2 Semi-Quantitative PCR of CD14

The effect of metformin on the differentiation of THP-1 cells was determined by the expression of *cd14* mRNA in the extracted total RNA samples. DNase I treatment and cDNA synthesis were carried out as described in Chapter 2.2.1.2 and 2.2.1.3, respectively.

Semi-quantitative PCR was carried out as described in Chapter 2.2.1.4 and the thermocycling conditions and primer sequences for *cd14* PCR are indicated in **Table 2.3** and **2.4**, respectively.

Table 2.3 – Thermocycling conditions for *cd14* and *gapdh* PCR.

Product		**Denaturation**	**Annealing**	**Extention**	
cd14	Initial denaturation at 95°C for 4 min	95°C 1 min	52°C 30 sec	72°C 30 sec	Final extension at 72°C for 10 min
gapdh		95°C 1 min	60°C 1 min	72°C 1 min	

Table 2.4 – Primer sequences for *cd14* PCR.

Product	**Sequences**	**Product size**
cd14	Forward: CTG CAA CTT CTC CGA ACC TC Reverse: CCA GTA GCT GAG CAG GAA CC	215 bp

2.4 Surface Expression of Hsp60

2.4.1 Cell Preparation

For staining to be carried out on poly-L-lysine pre-coated microscopic slides, THP-1 cells were first pelleted at 400 rcf for 5 min and re-suspended in pre-warmed PBS to a cell density of 5 x 10^4 cells/mL. Next, 150 µL of cells was spun onto slides using a Shandon Cytospin 4 Cytocentrifuge (Thermo Scientific) at 600 rpm (41 rcf) for 3 min. This speed and time combination was optimised to maintain cell integrity during centrifugation (as tested by trypan blue staining) and to allow cells to remain adhered to the slides during the washing steps. The area of the monolayer of cells was marked using a Dako Pen (Dako) before placing the slide into the fixative. For live cell staining, cells were also spun onto the slides using the cytospin using the above settings at the end of the experiments.

2.4.2 Cell Fixation

After cells were spun onto slides using a cytospin, several fixatives were trialed (**Table 2.5**) to select the one which will not permeabilise the cells.

The cells were washed in 3 X 5 min PBS before staining with 500 nM propidium iodide (PI) (AppliChem) for 5 min in the dark. After another 3 X 5 min PBS wash the slides were air-dried briefly and fixed with Dako fluorescent mounting agent (Dako) and stored at 4°C wrapped in foil.

Table 2.5 – Fixatives trialed for surface preservation.

Fixative	Content	Conditions
Methanol:Acetone (1:1)	Freshly made HPLC grade methanol and acetone	RT for 15 min
Methanol, ice cold	Fresh HPLC grade methanol pre chilled at -20°C	-20°C for 10 min
4% Paraformaldehyde in PBS	In the fumehood, measure, dissolve 2 g of paraformaldehyde (PFA) powder in 40 mL PBS. Add 2 drops 10 M NaOH. Stir on 65°C plate until clear. Adjust pH to 7.4 and bring volume to 50 mL. Filter through a 0.2 µm filter. Store at 4°C.	RT for 10 min
1% Paraformaldehyde in PBS	Mix 1 part 4% PFA with 3 parts PBS.	RT for 10 min
4% Formaldehyde in PBS	Dilute 37% formaldehyde solution in PBS to 4% formaldehyde.	RT for 10 min
1% Formaldehyde in PBS	Mix 1 part 4% formaldehyde in 3 parts PBS.	RT for 10 min
2% Glutaraldehye	Dilute the 50% glutaraldehyde stock solution to 2% with PBS	RT for 10 min

2.4.3 Hsp60 Immunocytochemistry

In live cell immunocytochemistry (ICC), THP-1 cell media was replaced with pre-warming media containing rabbit anti-Hsp60 antibody (1:200) and incubated at 37˚C for 1 h. A negative control was included which did not have the anti-Hsp60 antibody. Following 3 X 5 min washes with pre-warmed PBS, cells were incubated in media containing FITC-conjugated anti-rabbit IgG (1:400) (Jackson ImmunoResearch) for 1 h. The cells were washed three times in PBS, stained with PI for 5 min and spun onto slides using a cytospin. The cells were washed in PBS for 3 times and then mounted with Dako mounting agent. Alternatively, cells were spun onto slides by a cytospin and then ICC was carried

out after the cells were fixed with 1% PFA.

2.4.4 MitoSOX Red Staining

MitoSOX Red (Invitrogen) specifically targets mitochondria in live cells where it gets oxidised by superoxide and exhibits its red fluorescence. Following the manufacturer's manual, MitoSOX Red was dissolved in DMSO to make a 1 mM stock and a 0.5 μM working solution was made in pre-warmed THP-1 media. Live THP-1 cells were gently smeared onto a slide and air dried for 5 min before a generous drop of MitoSOX working solution was applied over the cells and the slide was incubated at 37˚C for 30 min. After three 5 min washes in PBS the cells were fixed in 1% PFA at RT for 10 min. Another three 5 min washes were done and the cells were counterstained in 300 nM DAPI in PBS for 5 min. The slide was washed and mounted with the Dako mounting agent.

The microscopic slides in this section were viewed under a Nikon Eclipse TS100 inverted microscope with a UV block and appropriate filters. Images were taken with a Nikon CoolPix 4500 digital camera. Alternatively, an Olympus FV1000 laser scanning confocal microscope (LSCM) controlled by the Olympus FluoView software (ver1.6a) was used.

2.5 Media, Reagents & Common Solutions Preparation

Name	Composition
THP-1 media	1 mL 100 mM sodium pyruvate 1 mL 100X penicillin/streptomycin 10 mL FBS Bring volume to 100 mL with RPMI 1640 medium then filter through a 0.22 μm filter. Store at 4˚C.
Metformin (100 mM)	212 mg metformin (HCl) Dissolve in 10 mL ddH_2O and filter through a 0.22 μm filter. Store at 4˚C in 1 mL aliquots.
Metformin (25 mM)	Mix 1 part 100 mM metformin and 3 part sterile ddH_2O. Store at 4˚C in 1 mL aliquots.
0.1 % DEPC water	1 mL DEPC 1 L ddH_2O Stir over night and then autoclave.
0.5 M EDTA	14.61g EDTA Dissolve in 80 mL ddH_2O, adjust to pH 8 then bring to 100 mL.
10x TBE buffer	54g Tris 27.5 boric acid 20 mL 0.5M EDTA Dissolve in 900 mL ddH_2O then bring volume to 1L.
50x TAE buffer	141g Tris 28.55 mL glacial acetic acid 50 mL of 0.5 M EDTA Dissolve in 300 mL ddH_2O , pH should be 8.5 then bring volume to 500 mL.
Phosphate buffered saline (PBS)	8g NaCl (137 mM) 0.2g KCl (2.7 mM) 1.44g Na_2HPO_4 (4.0 mM) 0.24g KH_2PO_4 (1.7 mM)

	Dissolve in 800 mL ddH_2O and adjust to pH 7, bring to 1L.
1.5M Tris-HCl pH 8.8	90.83g Tris Dissolve in 400 mL ddH_2O, adjust to pH 8.8 and bring to 500 mL.
0.5M Tris-HCl pH 6.8	15.14g Tris Dissolve in 200 mL ddH_2O, adjust to pH 6.8 and bring to 250 mL.
10% SDS	25g SDS Make up to 250 mL with ddH_2O water.
5x Electrode buffer	15g Tris (124 mM) 72g glycine (959 mM) 50 mL of 10% SDS (0.5%) Made up to 1L with ddH_2O.
Protein loading buffer	3 mL 10% SDS 1 mL 1M Tris pH6.8 0.2 mL 2% bromophenol blue 4 mL glycerol 0.8 mL ddH_2O Mix well and store in 1 mL aliquots at -20˚C. Add β-mercaptoethanol (5%) fresh on the day.
Gel fixative/destain	400 mL methanol (40%) 100 mL acetic acid (10%) 500 mL of ddH_2O
Commassie Blue stain	0.5g Brilliant Blue R-250 (0.1%) Dissolve in 500 mL of fixative/destain and filter through #1 filter paper
Cathod buffer	0.303g Tris 0.3g glycine 10 mL methanol Dissolve in 80 mL ddH_2O, adjust to pH 9.4 and bring to 100 mL.

Anode buffer I	3.63g Tris 10 mL methanol Dissolve in 80 mL ddH_2O, adjust to pH 10.4 and bring to 100 mL.
Anode buffer II	0.303g Tris 10 mL methanol Dossolve in 80 mL ddH_2O, adjust to pH 10.4 and bring to 100 mL.
10x Tris buffered saline (TBS)	12.10g Tris (0.1M) 87.66g NaCl (1.5M) Dissolve in 800 mL ddH_2O, adjust to pH 7.7 and bring to 1 L.
Ponceau S	Add in the order: 10 mL MQ water 0.3 mL glacial acetic acid 33mg Ponceau S Bring to 30 mL with MQ water and store at RT.
TBS-Tween (TBST)	100 mL 10x TBS 0.5 mL Tween20 (0.05%) Make up to 1 L with ddH_2O.
TENT buffer	1.51g Tris (50 mM) 10.96g NaCl (150 mM) 0.37g EDTA (5 mM) 0.75 mL TritonX-100 (0.25%) Dissolve in 200 mL ddH_2O, adjust to pH 7.4 and bring to 250 mL. Supplement with 0.4 mM phenylmethylsulfonyl fluoride fresh.

2.6 Statistical Analysis

All statistical analysis in this study was carried out using Microsoft Excel. Data were averaged when appropriate and standard error of the mean (S.E.M.) was calculated using **Equation 2.4** in Excel.

```
STDEV (A1:A2) / SQRT (COUNT (A1:A2))
```

Equation 2.4 – Calculating standard error of the mean in Excel.

A two-tailed student's *t*-test was carried out to determine the significance of the data. The accepted level of significance was $p < 0.05$, which was denoted as "*", whereas $p < 0.01$ was denoted as "#" throughout this study.

3 Effects of Metformin on THP-1 Cell Culture

3.1 Introduction

T2D is associated with a chronic low-level state inflammation and therefore patients are at a high risk for developing CVD. Metformin is a widely prescribed anti-hyperglycaemic drug and it has been shown to inhibit the complex 1 of the mitochondrial respiratory chain (Chapter 1.2.4.1). Although its cytotoxicity has been characterized in hepatocytes and HepG2 cells (Dykens *et al*. 2008), there is a lack of such study on human monocytic cells, the cells that can elicit innate immune responses and play important roles in the pathogenesis of atherosclerosis (Chapter 1.1.4). Therefore, THP-1 human monocyte cells were chosen as an *in vitro* model to study the effects of metformin on the immune system.

The plasma concentration of metformin has been documented at 10 – 100 μM in humans and mice and it could reach 10 mM in the intestine (Wilcock & Bailey 1994). Various researchers have used metformin concentrations from the range of 10 μM to up to 30 mM in cell cultures but due to the differences in the cell type and nature of experiment, the first task of this project was to test the toxicity of metformin on intact THP-1 cells. A range of metformin concentration was chosen and (0, 10-500 μM, and 1, 10 mM) supplemented to cells growing at near confluent stage. First of all, cell growth was monitored every 48 h by Trypan blue exclusion assay, then LDH assay was used to measure the cytoxicity of metformin. Lastly, MTT assay was carried out to measure cell viability and indirectly measure mitochondrial dehydrogenase activity (Marshall *et al*. 1995).

3.2 Methods

3.2.1 Cell Culture

Metformin stock at 25 mM and 100 mM was prepared as in Chapter 2.5. A uridine stock at 20 mM was also prepared in the same way. THP-1 cells at the exponential growth phase were seeded at a density of 22,000 cells/mL onto a 24-well plate containing 1.5 mL media with 0, 10, 100, 250, 500 µM and 1 and 10 mM metformin in duplicates. Another 24-well plate contained the same metformin concentrations but the media was supplemented with 200 µM uridine. Uridine is required for cellular pyrimidine biosynthesis when the mitochondrial electron transport system is inactive (Martinus *et al*. 1993). The plates were then placed back in standard incubation conditions and the cell density estimated by the trypan blue exclusion method every 48 h.

3.2.2 LDH Assay

Lactose dehydrogenase is an intracellular enzyme which will only be released after cell death. The measure of LDH in the cell supernatant is therefore a way to assess cytoxicity.

Near confluent THP-1 cells treated with metformin (0 – 500 µM) were seeded onto a 24-well plate in 1 mL duplicates and incubated in standard incubation conditions. After 48 h, samples were prepared as described in Chapter 2.1.1. Briefly, one set of cells was pelleted to collect supernatant while the other set of cells (maximum control) was lysed with 100 µL Lysis Solution and supernatant collected. After the assay, Stop Solution was added and absorbance measured at

490 nm. The data were calculated according to **Equation 2.1** and presented as a percentage of the corresponding maximum control.

3.2.3 MTT Assay

MTT [3-(4,5-dimethylthiazol-2-yl)-2,5-diphenyl tetrazolium bromide] assay is commonly accepted as a measure of cell proliferation and/or viability and is based on the activity of intracellular oxidoreductase enzymes, where NADH is responsible for most MTT reduction (Berridge *et al*. 2005). Since most oxidoreductases are localized in the mitochondrial respiratory chain, the assay here is also an indirect measure of mitochondrial respiration. The assay was carried out following the supplier's manual and with the methods described in Chapter 2.1.2.

On a 96-well plate THP-1 cells at 12,000 cell/mL were serially diluted and plated to construct a standard curve for MTT assay. It was determined that cell density below 6,000 per well was suitable for the assay. Cells treated with metformin (0, 100, 250, 500 µM) was seeded at around 4,000 cells per well in quintuplicate and rest overnight. Duplicated wells of each treatment group were taken to assess cell density and 10 µL MTT added to the remaining triplicated wells. After 30 min incubation (or until blue crystals were seen) at 37°C, 100 µL Solubilization Solution was added and proceed as described above. The data was subtracted with 655 nm readings and corresponding blanks then normalised to the cell densities noted at the beginning of the assay.

3.3 Results

3.3.1 Cell Growth

As shown in **Figure 3.1**a, Control (Ctrl) cells containing no metformin had a doubling time of 48 hrs as usual and the 10 μM group had comparable if not faster doubling time. Cells treated with 100 and 250 μM metformin showed a slight reduced growth rate compared with Ctrl whereas the 500 μM and 1 mM groups had 73.73% and 48.12% of the Ctrl cell number, respectively, at the end of the culture period. 10 mM metformin was cytotoxic as cells were unable to multiply and were no longer viable after 2 days.

In parallel, cells were treated the same way except 5 mM pyruvate and 0.2 mM uridine (hereon abbreviated as “Rescue” or “R”) were added to the media as supplements for cells with compromised mitochondrial respiratory chain. The cells were treated for the same length of time and cell numbers noted (**Figure 3.1**b). With Rescue, Ctrl, 10, and 100 μM groups had similar doubling time whereas 250 and 500 μM showed concentration-dependent decrease in growth rate. The cytotoxic effect of 10 mM metformin was seen as early as 2 days and the effect was beginning to show at 96 h for the 1 mM group.

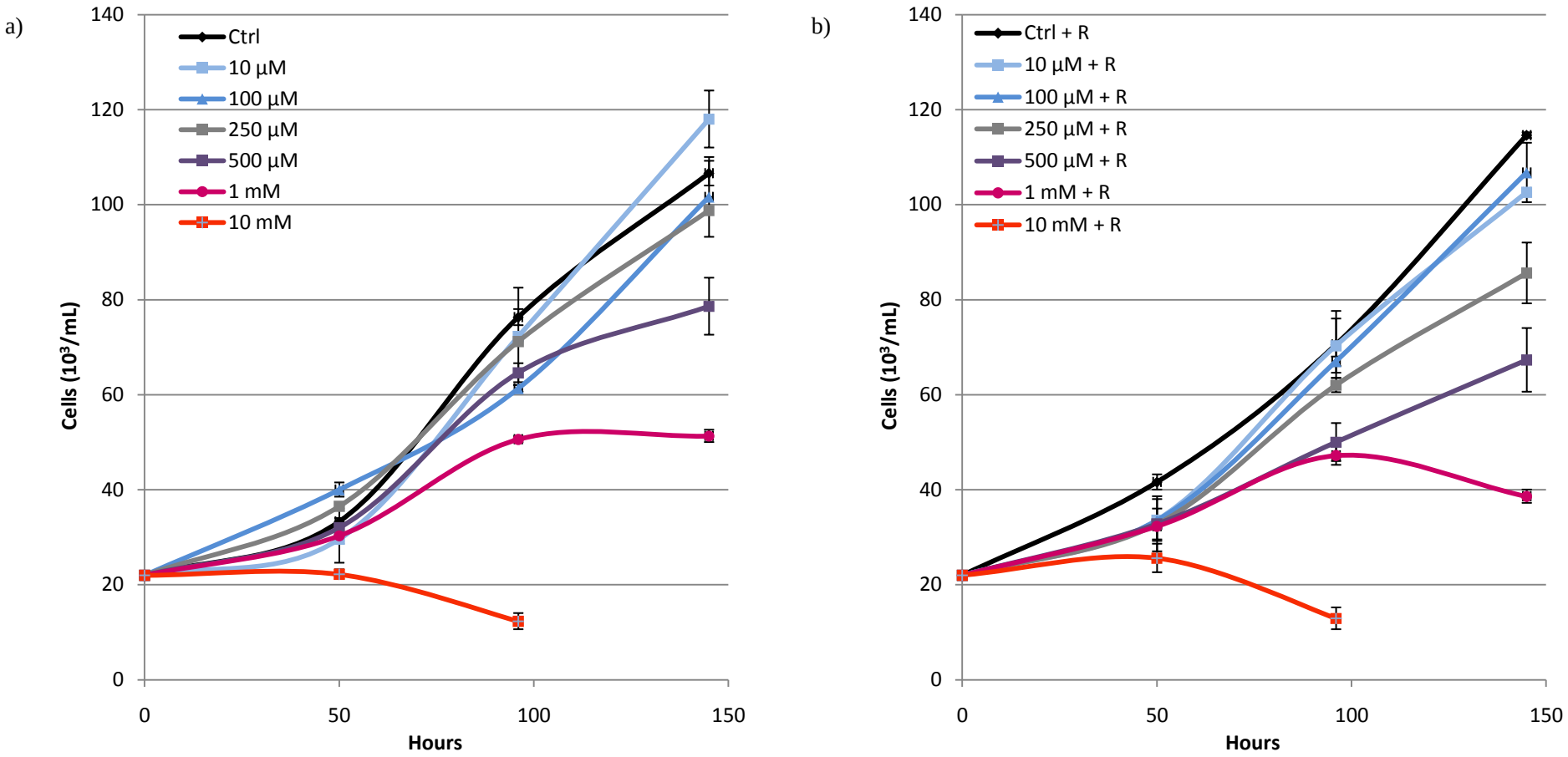

Figure 3.1 – Cell growth in metformin. a) Without Rescue. b) With Rescue (5 mM pyruvate + 0.2 mM uridine). Error bars showing S.E.M.

To compare cells in the absence and presence of Rescue, the number of cells at each time point was normalised to the number of Ctrl cells. The slopes were then taken from the graph plotting against the percentage of surviving cells versus time (not shown) and presented in **Figure 3.2**, which indicates the rate of growth inhibition for each treatment. 10 μM metformin appeared to increase cell proliferation or prevent cell death regardless of Rescue presence; 100 μM showed differentiated effects where the Rescue relieved the inhibition seen without Rescue. At metformin concentrations 250 μM and above, cells showed a dose-dependent increase in growth inhibition. **Figure 3.2** also indicates that, regardless of the presence of Rescue, 1 mM metformin had approximately 50% growth rate of Ctrl and that 10 mM metformin is highly toxic to cells.

Due to metformin's cytotoxic effect at 10 mM, this dose was excluded from experiments from here on.

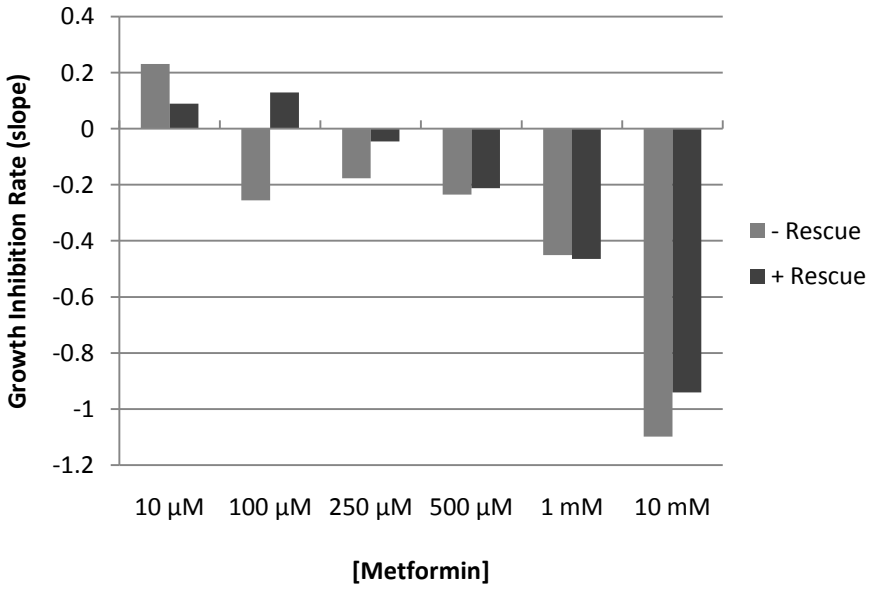

Figure 3.2 – Rate of cell death in metformin relatively to Ctrl.

3.3.2 LDH Assay

Lactate dehydrogenase is an intracellular enzyme that is only released into the media upon cell death, thus this assay was used to determine the cytoxicity of metformin on THP-1 cells.

After 72 h in culture, the percentage of LDH content relative to corresponding maximum control samples were calculated. Assuming that every death cell released equal amount of LDH, the percentage of LDH content was interpreted as the percentage of lysed cell as shown in **Figure 3.3**. The control sample had 45.04 ± 0.99% lysed cells, and was not significantly different to 100 and 250 µM groups, which had 43.97 ± 1.40% and 45.42 ± 0.46% lysed cells, respectively. Treatment of 500 µM and 1 mM metformin resulted in a significantly reduced ($p < 0.05$) percentage of lysed cells compared with Ctrl, giving 39.72 ± 0.44% and 33.60 ± 1.33% lysed cells, respectively.

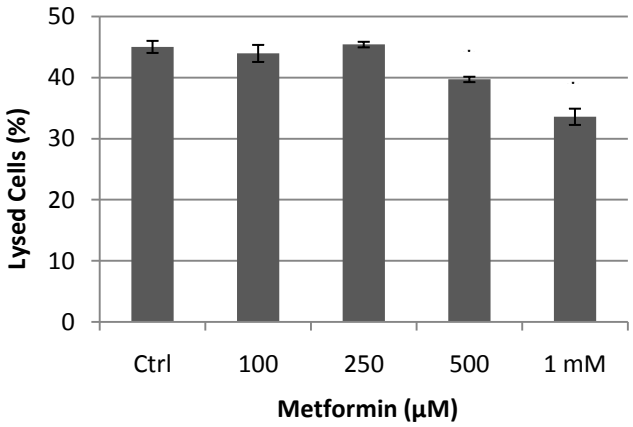

Figure 3.3 – Percentage of lysed cells in the presence of metformin. Bar graph showing means ± S.E.M. * = $p < 0.05$.

3.3.3 MTT Assay

A standard curve was constructed by serially diluted THP-1 cells and MTT assay was carried out to ensure MTT forzaman deposit is proportional to cell number. As **Figure 3.4** indicates, cell number beyond 6,000 per well began leveling off in crystal formation and therefore seeding culture for experimental assay were approximately 4,000 cells per well.

The indirect measurement of mitochondrial dehydrogenase activity in the presence of metformin showed that there is a slight increase at 100 μM (117.67%). At 250 and 500 μM there is a decreasing trend, 95.35 and 59.07%, respectively, indicating inhibited mitochondrial respiration (**Figure 3.5**). The difference in the amount of blue deposit between Control and 500 μM metformin can be seen through light microscopy in **Figure 3.6**d.

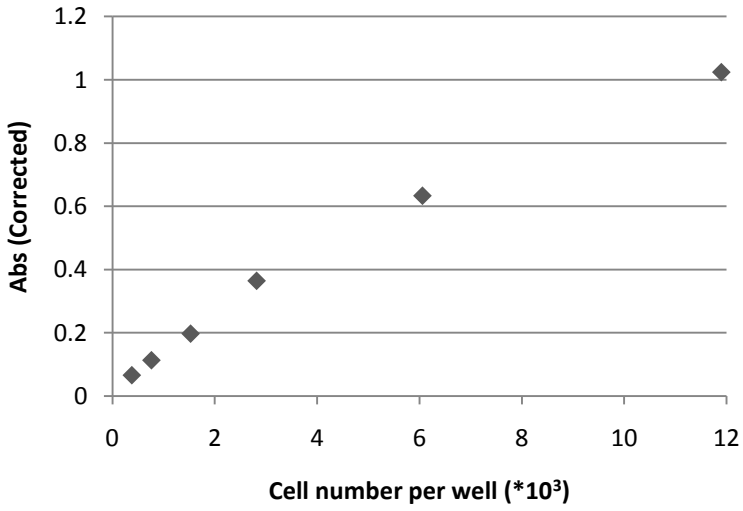

Figure 3.4 – Standard curve for MTT assay. Cell number up to around 4,000 per well showed linear increase in absorbance.

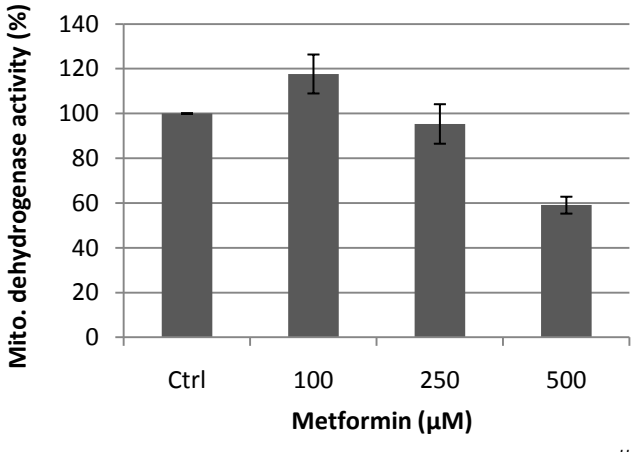

Figure 3.5 – Mitochondrial dehydrogenase activity in the presence of metformin. Bar graph showing the mean ± S.E.M of triplicated wells. # = $P < 0.01$.

a) b)

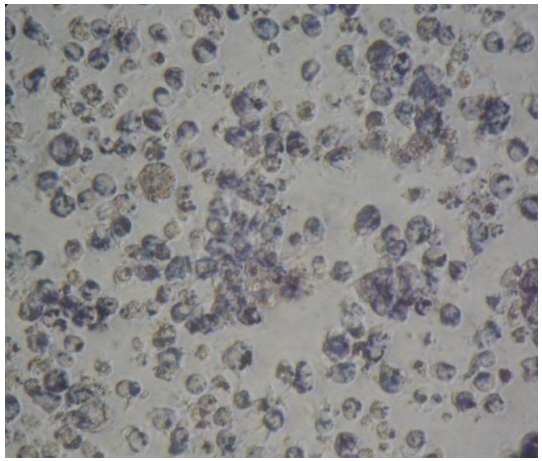

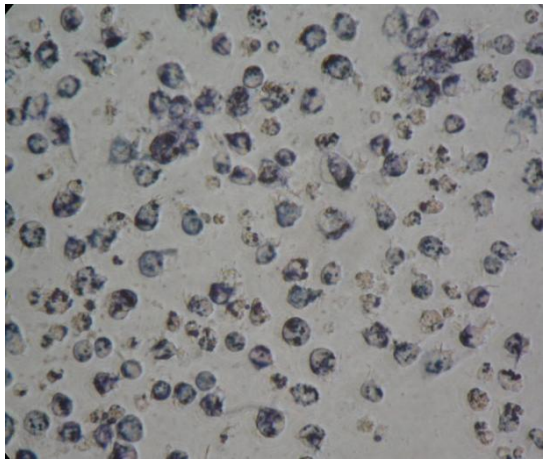

c) d)

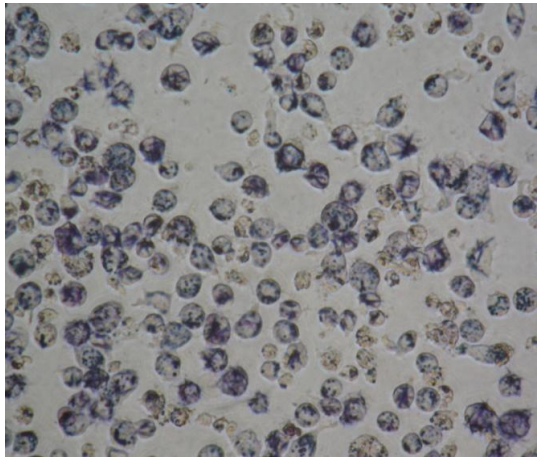

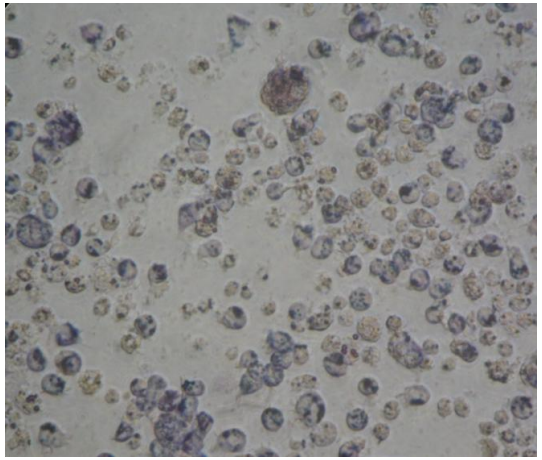

Figure 3.6 –Blue formazan deposits intracellularly after 30 min incubation. a-d) show crystal formation in Ctrl, 100, 250, and 500 µM groups, respectively.

3.4 Discussion

The objective of this study was to assess the cytotoxicity of metformin on THP-1 monocyte cells. Three methods were used: trypan blue exclusion, LDH assay and MTT assay. While all of these are measures of cell viability, MTT assay is commonly used as an indirect measurement of mitochondrial respiration (Marshall *et al*. 1995).

It was reviewed in Chapter 1.2.1 that plasma metformin levels ranges from 10 – 100 μM and in the intestine it could reach 10 mM in diabetic mouse (Wiernsperger 1999). In this experiment, THP-1 cells were incubated with a wide range of metformin concentrations and it was shown that within plasma levels of metformin, THP-1 cells grew similarly to the Ctrl. It was clear that 10 mM metformin was highly cytotoxic as THP-1 cells could not maintain viable for periods longer than 48 h (**Figure 3.1**a & b).

Knowing metformin is a complex 1 inhibitor, cells were supplemented with 5 mM pyruvate and 0.2 mM uridine ('Rescue' or R) in an effort to restore cell viability at high drug dosages. These two supplements have been shown to allow the growth of cells completely lacking the mitochondrial respiratory system (Martinus *et al*. 1993). The reduction of pyruvate to lactate provides a pathway for the re-oxidation of excess NADH generated during glycolysis, whereas uridine is required for cellular pyrimidine biosynthesis when the mitochondrial electron transport system (ETS) is inactive. This Rescue did not have significant effects on cell growth as shown in **Figure 3.2** probably because (1) lactate buildup reduces cell growth: under metformin inhibition, cells accelerate glycolysis to compensate for reduced ATP production via oxidative phosphorylation. The resulting lactate from glycolysis normally serves as substrate for gluconeogenesis in the liver and

therefore in this cell culture system lactate could not be completely oxidized, leading to a buildup in cell culture. (2) Accelerated glycolysis at high metformin concentrations could lead to fast turnover rate for glucose and therefore substrate depletion is another factor. This could explain the lack of influence of Rescue. (3) Metformin also affects other pathways involved in cell growth. For example, metformin is a known activator of AMPK, a cellular energy sensor. When activated, cells switch on catabolic pathways that generate ATP while switching off biosynthetic pathways and other processes that consume ATP, such as protein synthesis (Hardie *et al*. 2006).

The LDH assay showed that compared with Ctrl (45.0%), 500 μM and 1 mM groups had significantly reduced ($p < 0.05$) cell lysis, at 39.7% and 33.6%, respectively. This indicated that inhibited growth in 500 μM and 1 mM metformin was not to due to cell death but possibly due to metformin's inhibitory effects on mitochondrial respiration. The evidence for this will be discussed later. Interestingly, reduced cell death by metformin has been observed by other studies (Guigas *et al*. 2004). Metformin was shown to prevent cell death induced by a glutathione-oxidising agent (t-BH) through delaying the mitochondrial PTP opening, and therefore prevent cell death. The authors postulated that the ability of metformin to inhibit PTP opening may help prevent deleterious effects caused by hyperglycaemia, adding to metformin's favourable effects. Similarly, metformin also prevented high glucose-induced cell death in HMEC-1. The data here is consistent with metformin's cytoprotective effect.

In support of metformin being a mild complex 1 inhibitory, there were two observations documented in this study. Firstly, it was noted that after a few days the colour of media became yellow as metformin concentration increased, most

likely due to the buildup of lactic acid during glycolysis, as described above. The second evidence for complex 1 inhibition came from MTT assay as it indicated a significant 40.93% inhibition in mitochondrial dehydrogenases at 500 μM metformin. Although it has been argued that reduction of MTT can also occur in cellular compartments other than mitochondria such as on the plasma membrane or in the cytosol, it was suggested that the contribution of mitochondria to the reduction decreased over time (Bernas & Dobrucki 2002). Therefore the assay was stopped as soon as MTT deposit was clearly seen under the microscope to minimize extramitochondrial reduction. Previously, 100 μM metformin was shown to exhibit 12.6% of mitochondrial respiration using glutamate and malate as substrate in rat hepatoma cells at 24 h (Owen *et al*. 2000). Another experiment showed that 10 mM metformin inhibited 53% of respiration in KB (human carcinoma-derived) cells after 30 min (Guigas *et al*. 2004). The extent of mitochondrial inhibition was not as great as the above, possibly due to the difference in cell types and the assay used, as MTT assay is not a direct measurement of complex 1 activity. This probably explained the lack of inhibition of respiration at 100 μM metformin.

4 Effects of Metformin on Mitochondria as Indicated by Modulation of Hsp60

4.1 Introduction

It is now widely known that metformin is a mild but specific inhibitor for complex 1 of the mitochondrial respiratory chain (Chapter 1.2.4.1) and data presented in the previous chapter supports this concept. The aim of this chapter is to assess the stress level in metformin treated THP-1 cells by monitoring the expression of Hsp60, a mitochondrial stress protein. Accordingly, mRNA and intracellular levels of Hsp60 were determined by semi-quantitative PCR and Western blot, respectively.

4.2 Methods

4.2.1 Cell Culture

On two separate 6-well plates, near confluent THP-1 cells were seeded at a density of 71,000 cells/mL in 3 mL of media containing 0, 100, 250, and 500 μM metformin and kept at standard incubation conditions. At 72 h, approximately 1 mL (10^5 cells) of cells from each plate was removed for RNA and protein extraction. Pre-warmed media was then added to each well to bring volume back to 3 mL. The same process was repeated at 7 and 14 days.

4.2.2 Hsp60 mRNA Quantification

RNA extraction was carried out as described in Chapter 2.2.1.1 and this was followed by DNase I treatment (Chapter 2.2.1.2) and cDNA synthesis (Chapter 2.2.1.3). Finally, *hsp60* and *gapdh* PCR was carried out (Chapter 2.2.1.4) and the products ran on an agarose gel, visualised and quantitated. The cycle number that represented the linear increase region was used to calculate the relative *hsp60* expression and fold changes.

4.2.3 Protein Extraction

Protein extraction was carried out as described in Chapter 2.2.2. Briefly, protein extracted by TENT buffer was assayed to determine protein concentration (Chapter 2.2.2.2). Fifteen microgram of protein was then separated on a 10% SDS-PAGE and transferred to a nylon membrane (Chapter 2.2.2.3). Western blot was carried out to visualise and quantitate the Hsp60 bands (Chapter 2.2.2.4).

4.3 Results

4.3.1 mRNA levels

Hsp60 mRNA levels were determined by semi-quantitative PCR and normalised to GAPDH expression. After three days incubation of metformin with THP-1 cells, there was a statistically significant ($P < 0.05$) decrease (0.29 ± 0.17 of Ctrl) in *hsp60* expression at 250 µM. There was a 1.18 ± 0.11 and 3.02 ± 1.39-fold increase at 100 and 500 µM, respectively, but this was found to be not significant based on the Student's *t*-test (**Figure 4.1**a).

At seven days exposure to metformin, *hsp60* expression increased dramatically at all concentrations compared with Ctrl (**Figure 4.1**b). Hsp60 mRNA had a 7.27 ± 0.40, 6.67 ± 0.82, and 9.68 ± 0.23-fold increase in the 100, 250, and 500 µM groups, respectively.

At 14 days, the 500 µM group continued to show a significant increased *hsp60* level (2.66 ± 0.26-fold) (**Figure 4.1**c). In contrary, the other two groups showed decreased levels, at 0.58 ± 0.03 and 0.14 ± 0.00 ($p < 0.05$) of the Ctrl, respectively.

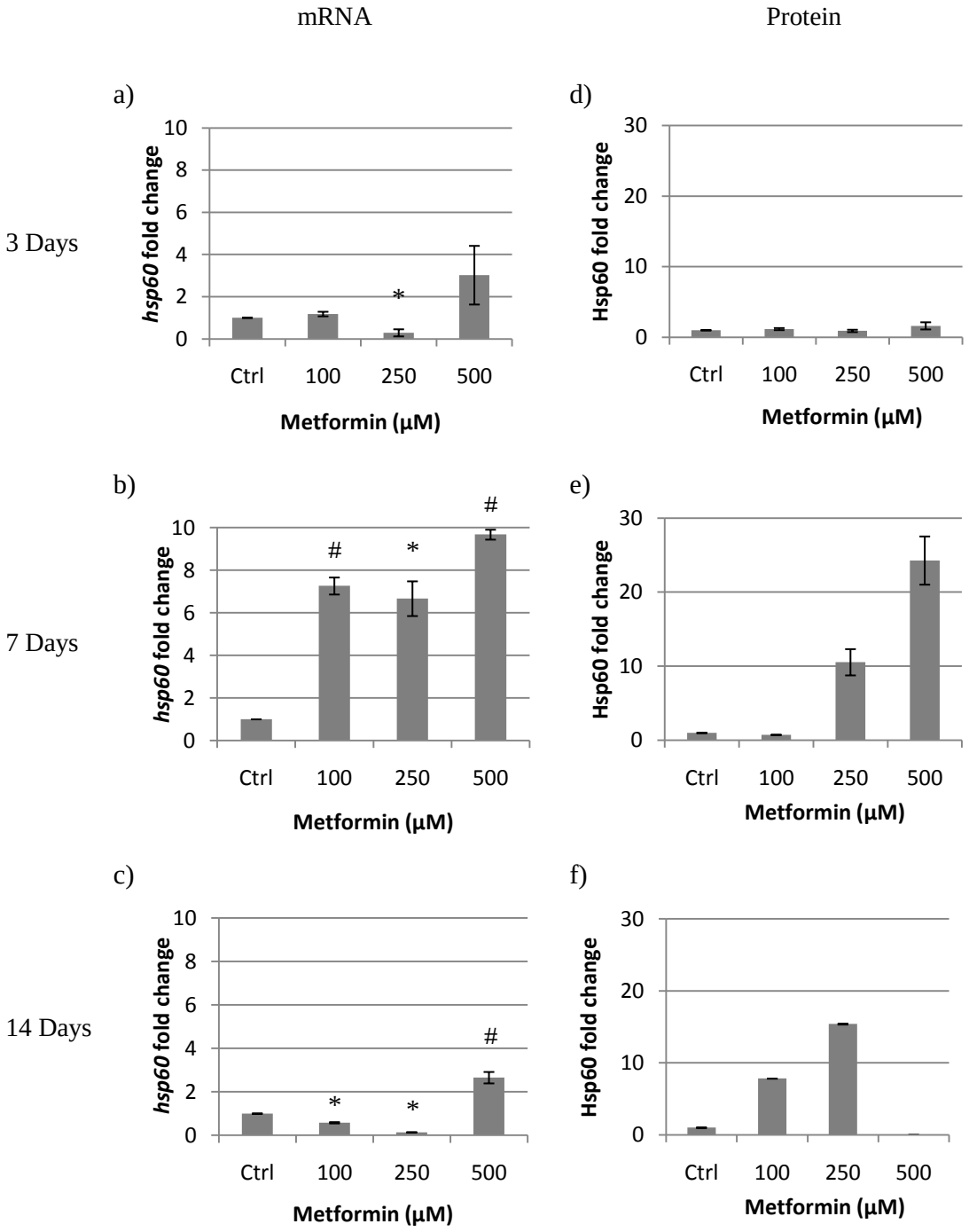

Figure 4.1 –Hsp60 mRNA and protein expression in response to metformin. Left panel shows the mRNA expression and right panel shows the protein expression. THP-1 cells were treated for 3 days (top), 7 days (middle), or 14 days (bottom). Bar graphs represent mean ± S.E.M. *= $p < 0.05$ and # = $p < 0.01$.

Overall, in response to 500 μM exposure *hsp60* remained elevated compared to Ctrl throughout the experiment with a peak expression at seven days. Significant increase in *hsp60* was only seen at seven days for 100 and 250 μM groups while other times it was mostly unchanged or decreased.

4.3.2 Protein levels

After total protein was separated on a polyacrylamide gel and transferred to a nylon membrane, Ponceau S staining showed the standard Hsp60 band to be at 60 kDa and that protein loading was even. After Western blot a single band for the each sample was seen and the bands appear to be same size as the standard Hsp60 protein band (data not shown). The bands were quantitated using the Gel Quant software and the relative expression to Ctrl was plotted (**Figure 4.1**d-f).

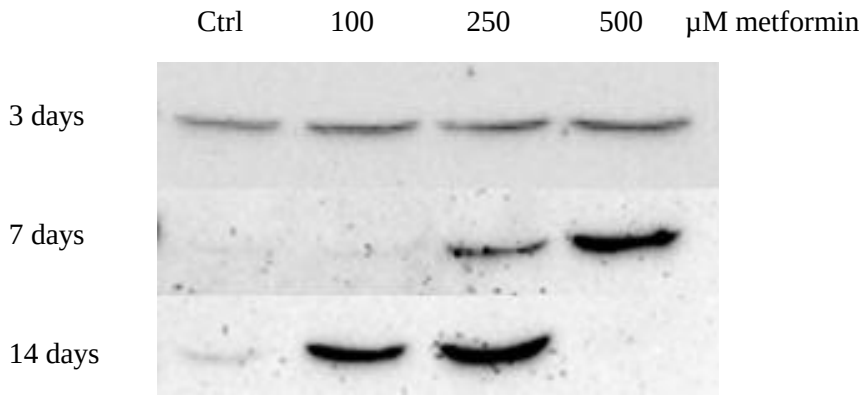

Figure 4.2 – Western blots of Hsp60 at 3, 7 and 14 days. Equal loading was confirmed by Ponceau S staining.

Hsp60 protein expression follows a similar, but somewhat delayed pattern to mRNA expression, with some exceptions. At three days, there was no significant change in comparison to Ctrl at all metformin concentrations although there was a slight (1.62-fold) increase in Hsp60 at 500 μM metformin.

At seven days, a dramatic increase was seen at 250 and 500 μM metformin resulting in 10.55 and 25.28-fold increase in Hsp60, respectively. In the two western blots carried out, the Ctrl band in one was not detectable and therefore student t-test could not be done. Nevertheless, the increase in Hsp60 expression was obvious as seen in **Figure 4.2**.

At 14 days, Hsp60 showed a dose-dependent increase in 100 and 250 μM compared with Ctrl, at 7.83- and 15.40-fold, respectively. Again, the Ctrl was not detectable in one blot thus statistical analysis was not possible. There was no band detected in the 500 μM group.

4.4 Discussion

Up-regulation of the mitochondrial Hsp60 has been used previously as a marker for stressors that target mitochondria specifically, such as in ρ° cells lacking mitochondrial DNA and in COS-7 cells expressing a mutant mitochondrial mutant protein (Martinus *et al*. 1996; Zhao *et al*. 2002). In this chapter, Hsp60 mRNA and protein expressions were measured in THP-1 cells were treated with metformin for 3, 7, or 14 days. This experiment is unique in that a monocytic cell line was used and the exposure to metformin is relative long term compared to other studies.

The nuclear-encoded Hsp60 transcript showed an up-regulation as early as three days at 500 μM and remained elevated throughout the experiment, however the 100 and 250 μM groups showed only a transient up-regulation which occurred at day seven. The up-regulation of *hsp60* suggests metformin treatment caused a mitochondrial stress response in THP-1 cells possibly due to inhibited oxidative respiration. To confirm this correlation, an experiment can be set up in a temporal way where mitochondria are isolated for the measurement of oxygen consumption and *hsp60* expression measured.

The protein levels of Hsp60 stayed mostly unchanged at day three then a corresponding increase in 250 and 500 μM groups was observed at day seven, although there was a lack of an increase in Hsp60 at 100 μM. While 100 and 250 μM groups showed a dose-dependent increase in mRNA levels at 14 days, the opposite trend was seen at the protein level. A few possible mechanisms exist for this transient mRNA response with marked protein increase: (1) the transcription of *hsp60* was attenuated by proteins that bind to HSF thereby repressing DNA binding. (2) A delayed protein expression is due to a lag in translation from

mRNA transcripts. (3) The cells have reduced ability to response to stress due to high passage number, which is reflected on *hsp60* expression. (4) An increase in Hsp60 protein levels does not necessarily require up-regulated transcription.

In Chapter 1.3.2 it was reviewed that HSFs, the transcription factors governing the transcription of HSPs, are normally inactivated by HSF binding proteins. Many of these HSF binding proteins are in fact HSPs so that a feedback regulation exists to maintain protein homeostasis. Therefore, although metformin-treated cells are constantly under mitochondrial stress, the expression of *hsp60* is fluctuating by a series of activation and deactivation. One way to confirm this is by promoter reporter assays. For example, Zhao *et al*. (2002) transfected COS-7 cells with a construct containing chloramphenicol acetyl transferase (CAT) and luciferase (LUC) downstream of *hsp10* and *hsp60* promoter, respectively, which allowed the detection if the promoter was activated.

It was shown in heat shocked monkey Stertoli cells that *hsp60* responded after 4 h however Hsp60 levels did not increase until 12 h after treatment (Chen *et al*. 2008). Similarly, the marked increase in *hsp60* at day seven would require time to allow for translation and translocation to the mitochondria. Thus, at the time of protein isolation, the proteome most likely represented the transcripts hours before this. This would probably explain the discrepancy in mRNA and protein levels in this experiment.

The lack of Hsp60 expression can also be explained by the senescence of cells. In human diploid fibroblasts (HDFs) it was shown that late passage cells were less sensitive to oxidative stress and therefore did not elicit Hsp60-mediated apoptosis as early passage cells did (Lee *et al*. 2008). The senescence-associated marker appeared at passage 30 (P30) in HDFs (Lee *et al*. 2008) and was seen at passage

P20 in another study (Ghneim *et al*. 2003). THP-1 cells used here were at P18-20 and could potentially be "aged" and had reduced stress response as implicated by *hsp60* expression. An assay measuring senescence biomarkers such as the senescence-associated β-galactosidase (SA-β-gal) can be done to determine this.

In a study on the role of Hsp60 in apoptosis, it was noted that an accumulation of Hsp60 in the cytosol without mitochondrial release and did not seem to result from increased mRNA levels in PC3 cells (Chandra *et al*. 2007). A similar scenario where Hsp60 increased without a corresponding mRNA increase was also observed in rat kidney cortex cells (Itoh *et al*. 2002) but the underlying mechanisms remain unclear. It is possible that the marked increase in Hsp60 seen here resulted in the same fashion as the above. Interestingly, the accumulation of Hsp60 without mitochondrial release was associated with an anti-apoptosis outcome (Chandra *et al*. 2007). Further, rotenone, a more potent version of metformin, caused cytosolic Hsp60 accumulation without mitochondrial release (Chandra *et al*. 2007). An interesting follow-up experiment would be the determination of Hsp60 in cytosolic and mitochondria fractions versus total protein to see whether a similar effect to rotenone can be seen. Since metformin has been shown to prevent cell death (Chapter 1.2.5 and also Chapter 3), it is possible the up-regulated Hsp60 expression plays an anti-apoptotic role.

It could not be determined from these results whether Hsp60 up-regulation was a mitochondrial specific response or a general cellular stress response. LDH assay indicated at day 3 the cells were healthy (Chapter 3) but the assay was not carried out day seven or 14. The lack of a Hsp60 band in **Figure 4.1** (f) was probably due to poor maintenance in long term treatment in high metformin causing cell death but LDH assay was needed to verify this. In addition, inducible HSPs such as

cytosolic Hsp70 and mtHsp70 should be included as indicators of general stress. Future work should also include LDH and MTT assays at each time point along with stress markers that are not specific to mitochondria. If metformin did induce a mitochondrial-specific stress it signifies that a mechanism exists in sensing the mitochondrial stress followed by mitochondria-nuclear communication which ultimately leads to the activation of target genes.

The increased levels of total Hsp60 protein in this chapter raised questions as to whether these proteins can be expressed on the cell surface, as has been shown previously. Surface exposed Hsp60 has important immunological roles (Chapter 1.3.4) when expressed on the circulatory monocytic cells especially in the diabetic context. The identification of surface Hsp60 in metformin-treated THP-1 cells will be described in Chapter 6.

5 Effects of Metformin on Differentiation of THP-1 Cells

5.1 Introduction

Type 2 diabetes is accompanied with various pathophysiological conditions that put patients at a 2-4 times higher chance of developing CVD (Chapter 1.1.4). Although still inconclusive, metformin may have protective effects against CVD based on trials, animal models and cell culture studies (Chapter 1.2.6).

Differentiated THP-1 macrophages have been widely used as an *in vitro* model of human macrophages to study their involvement in inflammation (Tuomisto *et al*. 2005; Kang *et al*. 2009). The aim of this chapter was to determine the response of metformin-treated THP-1 cells to PMA. The marker chosen for monocyte differentiation was CD14, a surface receptor present on macrophages (Tuomisto *et al*. 2005). The expression of CD14 and Hsp60 mRNA was determined by semi-quantitative RT-PCR.

5.2 Methods

5.2.1 Cell Culture

Near confluent THP-1 cells at 50,000 cells/mL were seeded onto a 24-well plate in media containing 0, 100, 250, or 500 μM metformin. The cells were returned to standard incubation conditions to rest overnight. The second day, a stock of 10 μM PMA was diluted in DMSO and added to each plate to make a final PMA concentration at 50 nM. After 48 h the cells were harvested as described in Chapter 2.2.6.

5.2.2 CD14 and Hsp60 mRNA Quantification

Total RNA was extracted in TRIzol as described in Chapter 2.3.2.1 which is slightly modified from Chapter 2.2.1.1 as cells were no longer in suspension. DNase I treatment, reverse transcription and semi-quantitative PCR were carried out as described in Chapter 2.2.1.3&4 and 2.3.2.2 and the primer sequences for *cd14* can be found in **Table 2.4**. CD14 was chosen as a marker as it is one of the ten highly up-regulated genes in PMA-stimulated THP-1 macrophages compared to undifferentiated THP-1 monocytes (Tuomisto *et al*. 2005) and its activation is commonly seen in T2D and may be associated with inflammation (Fogelstrand *et al*. 2004; Cipolletta *et al*. 2005).

5.3 Results

THP-1 cells treated with metformin were differentiated with PMA and the expression of a macrophage marker, *cd14*, was measured. Already at 19 h, THP-1 cells have shown characteristic morphology of macrophages such as adhesion and spreading (**Figure 5.1**). Cells were harvested at 48 h by TRIzol and adhesion was stable as cells could not be detached by washing.

At 48 h after PMA addition, cells treated with 100 μM metformin showed a significant 1.48-fold increase in *cd14* expression compared with Ctrl (**Figure 5.2**a). In contrary, the 500 μM group had significantly decreased *cd14* levels, at 0.23-fold of the Ctrl. The 250 μM group had comparable levels of *cd14* to Ctrl.

The levels of *hsp60* were also measured in THP-1 derived macrophages and showed significant increases in all metformin concentrations compared with Ctrl, at 2.74, 1.49 and 2.08-fold, respectively (**Figure 5.2**b, light shade). **Figure 4.1**a, the expression of *hsp60* in undifferentiated THP-1 cells, is also plotted in **Figure 5.2**b (dark shade). It shows that 100 and 250 μM groups had significant elevated *hsp60* levels after differentiation ($p < 0.05$ and $p < 0.01$, respectively). The levels of *hsp60* before and after differentiation had no significant changes.

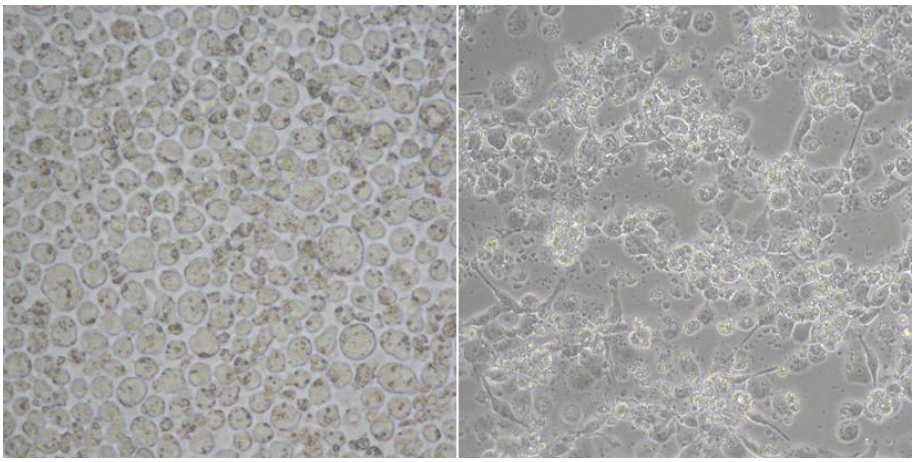

Figure 5.1 – THP-1 monocytes and THP-1-derived macrophages. Monocytes have round-shaped morphology (left) and macrophages adopt elongated morphology with clustering and spreading of the cells.

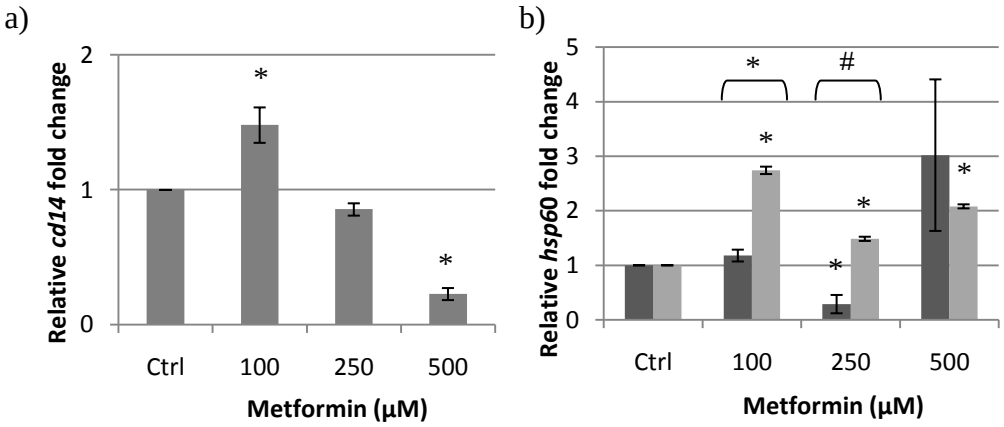

Figure 5.2 – Expression of *cd14* and *hsp60* in metformin-treated THP-1-derived macrophages. * = $p < 0.05$; # = $p < 0.01$.

5.4 Discussion

Monocyte activation and recruitment and subsequent differentiation into macrophages are crucial steps in the development of atherosclerosis as reviewed in Chapter 1.1.4. In this chapter, the ability of PMA-stimulated THP-1 differentiation in the presence of metformin was investigated. Using a specific surface receptor, CD14, as a gene marker for differentiation it was found that therapeutic concentration of metformin (100 μM) caused a significant 1.48-fold increase in *cd14* levels at 48 h (**Figure 5.2**a). At 500 μM metformin, however, *cd14* levels were significantly decreased and the 250 μM group had similar levels of *cd14* compared with Ctrl.

Binding of CD14 to LPS is known to initiate intracellular signals which ultimately lead to the secretion of pro-inflammatory cytokines. The binding of LPS also leads to clustering with other receptors that are involved in atherosclerosis such as CD11b, CD18, and scavenger receptor CD36 (Pfeiffer *et al*. 2001). Therefore the data here indicate that THP-1 monocyte cells exposed to metformin at the therapeutic range expressed higher levels of *cd14* than Ctrl cells, thereby may have high chance of promoting pro-inflammatory responses. Stimulation of THP-1-derived macrophages with LPS and subsequent measurement of TNFα levels in the culture media could be carried out to confirm this.

In Chapter 3 it was shown that 500 μM metformin markedly reduce cell growth rate by reduced respiration. The reduced ability for cells to differentiate, as indicated by *cd14* expression, likely reflects limited ability for cells to carry out energy costing activities. This is supported by the evidence that metformin activates the AMPK pathway, leading to inhibition of anabolic pathways (Chapter 1.2.4.2).

It was stated in a meeting abstract by Mamputu *et al*. (2002) that metformin was shown to reduce differentiation of culture human monocytes into macrophages and monocyte adhesion to endothelial cells and that foam cell formation was also reduced. Unfortunately the full article was not available so it is unclear which cell type, culture conditions and metformin concentration were used. Thus the data in this study could not be compared to our study.

In a trial involving 112 women aged 64 years with T2D, IGT or NGT it was shown that T2D group had higher levels of CD14+ monocytes as measured by flow cytometry than the latter two groups (Fogelstrand *et al*. 2004). Further, treatment with metformin had no influence on the results (Fogelstrand *et al*. 2004). The discrepancy could be a result of the malignant cell type used in this study and also an increase in mRNA expression does not necessary correlate with protein expression. The correlation coefficient between the expression of THP-1 derived macrophages and human peripheral blood mononuclear (HPBM)-derived macrophages range from 0.80 to 0.88 depending on the time-point and stimulation used (Tuomisto *et al*. 2005). The main difference lies in genes related to cell proliferation. In a comparison study on gene and protein expression in monocytes and monocyte-derived macrophages, it was found that expression changes in protein level were smaller than changes at the mRNA level, probably due to transcript variants and selective translation (Tuomisto *et al*. 2005). Therefore, future studies should include the measurement of surface CD14 in THP-1 cells (or HPBM cells) exposed to metformin using flow cytometry. Other molecules that could potentially be involved in development of atherosclerosis, such as Cdk-1 (transcription factor) and CD36 can also be determined, perhaps in a time-dependent manner.

In the current study, the expression of *hsp60* was also measured and found to be up-regulated after differentiation (**Figure 5.2**b). Transcriptional activation of several HSPs, namely the stress-inducible Hsp60, Hsp70, Hsp90 and the constitutive Hsc70, have been documented in peritoneal macrophages induced by colony stimulating factor (CSF) (Teshima *et al*. 1996). The transcription of these genes coincided with O^{2-} production by macrophages stimulated with PMA indicated that HSPs may play a protective role against harmful oxidative damage associated with the respiratory burst (Teshima *et al*. 1996). The maturation of macrophages involves up-regulation of several genes and subsequent protein synthesis and folding, which further justify the induction of molecular chaperones.

The up-regulation of *hsp60* in the 100 μM group observed in this study could be the result of the above reasons. However the elevated levels of *hsp60* cannot be explained the same way in 250 and 500 μM groups, as THP-1 cells appeared to have similar or less ability to differentiate. Whether this was due to elevated cellular stress is unclear as the expression of other HSPs was unavailable.

In summary, THP-1 monocytes treated with a therapeutic concentration of metformin had increased differentiation rate as measured by *cd14*. At high metformin (500 μM) cells showed significant reduced differentiation compared with Ctrl. Depending on the metformin concentration used, the elevated *hsp60* levels may be a result of (1) an influx of newly synthesized protein due to the transition from monocyte to macrophage; (2) increased requirement for cytoprotection due to oxidative damage associated with macrophage respiratory burst; and/or (3) a cellular stress condition caused by metformin treatment. The results here partly contradicted the much acclaimed beneficial effect of metformin on CVD however more conclusive data are required.

6 Optimisation of Surface Hsp60 Detection

6.1 Introduction

Surface expressed Hsp60 has been detected in stressed rat aortic endothelial cells and human umbilical venous endothelial cells (HUVECs) using immunocytochemistry (ICC) (Xu *et al*. 1994; Pfister *et al*. 2005). Surface Hsp60 has also been detected in other cell lines such as Chinese hamster ovary (CHO) (Soltys & Gupta 1996), human T-cell lines (Soltys & Gupta 1997) and human breast and lung carcinoma cells (Barazi *et al*. 2002). The aim of this chapter is to optimize a method for detection of surface expressed Hsp60 in human monocytic THP-1 cells. The expression of Hsp60 on the cell surface under cellular stress, in this case metformin, may have important physiological and pathological significance in the context of T2D.

The optimisation involved using different cytospin speeds, fixing with different agents, and ICC in live or fixed cells. The results will be discussed in the same section in this chapter.

6.2 Methods

To obtain intact cell membrane for surface Hsp60 staining, the cytospin settings were first optimised. Next, several fixatives were trialed without the permeabilisation step. Alternatively, ICC was carried out in live cells. The methods of cytospin, fixation and Hsp60 ICC are described in Chapter 2.4. The cells were viewed under an inverted microscope or a confocal microscope.

6.3 Results and Discussion

6.3.1 Cytospin

THP-1 cells in suspension were spun using a cytospin centrifuge at various speeds and duration. The mildest combination to spin cells onto a poly-L-lysine pre-coated slide was 600 rpm for 3 min. At a shorter time cells tend to wash off during washing steps in ICC. Immediately after cytospin the cells were stained with Trypan blue and **Figure 6.1** shows that cell viability was > 90%.

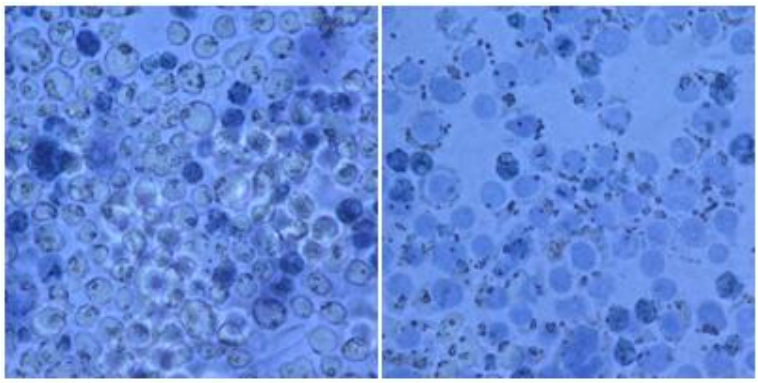

Figure 6.1 – Trypan blue staining of cells after cytospin. Cells that have taken up the dark blue dye indicates a loss of membrane integrity, hence are dead cells.

6.3.2 Fixatives

The staining of PI requires permeabilisation of cell membrane, thus skipping this step should theoretically allow the staining of only necrotic cells. However this was not the case, at least not in THP-1 cells.

a) 4% Formaldehyde

b) 1% Formaldehyde

c) MeOH/Acetone (1:1) RT

d) Ice cold MeOH

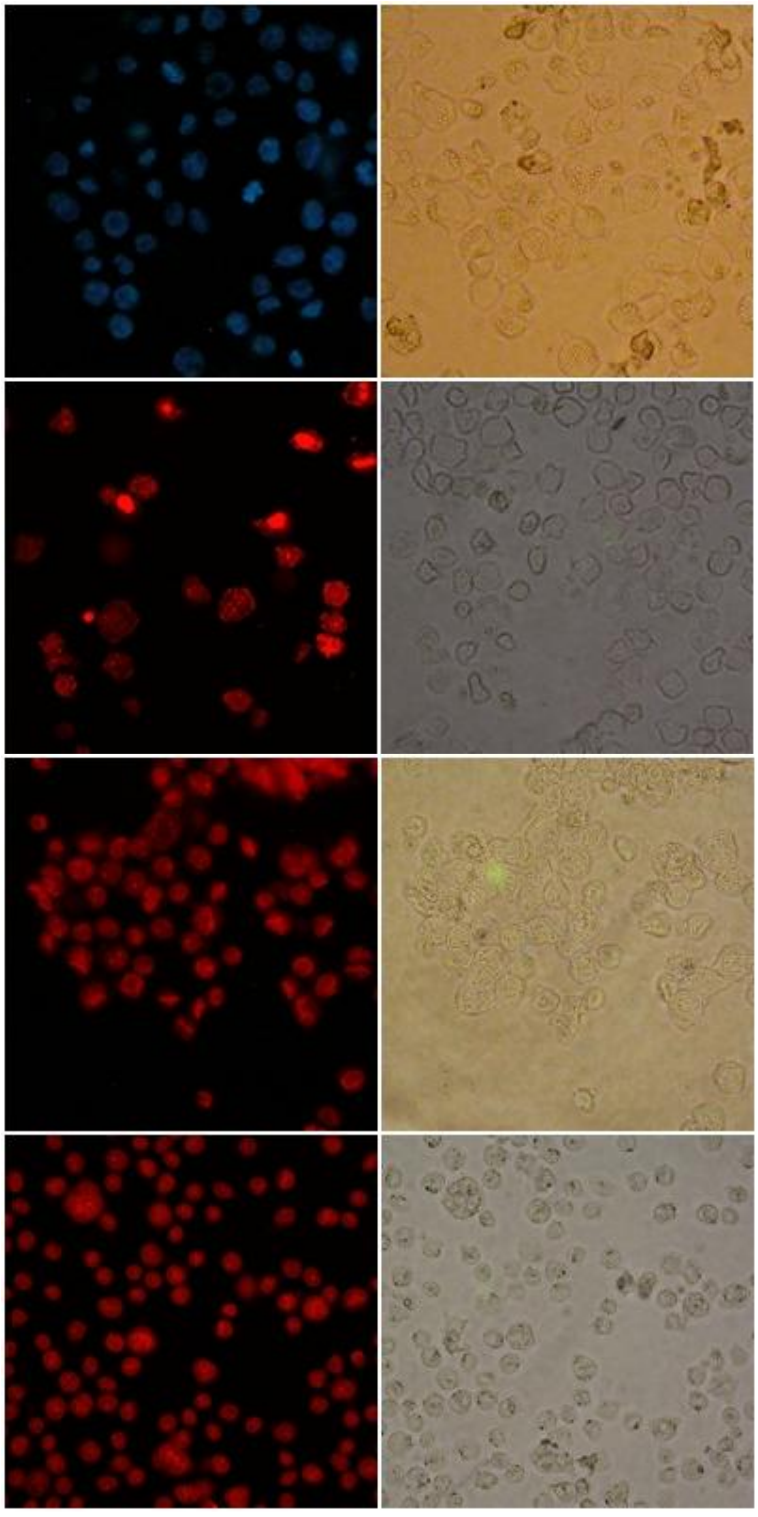

Figure 6.2 – THP-1 cells stained with PI after fixation with different agents.

e) 4% PFA

f) 1% PFA

g) 2% glutaraldehyde

h) 1% PFA permeabilised

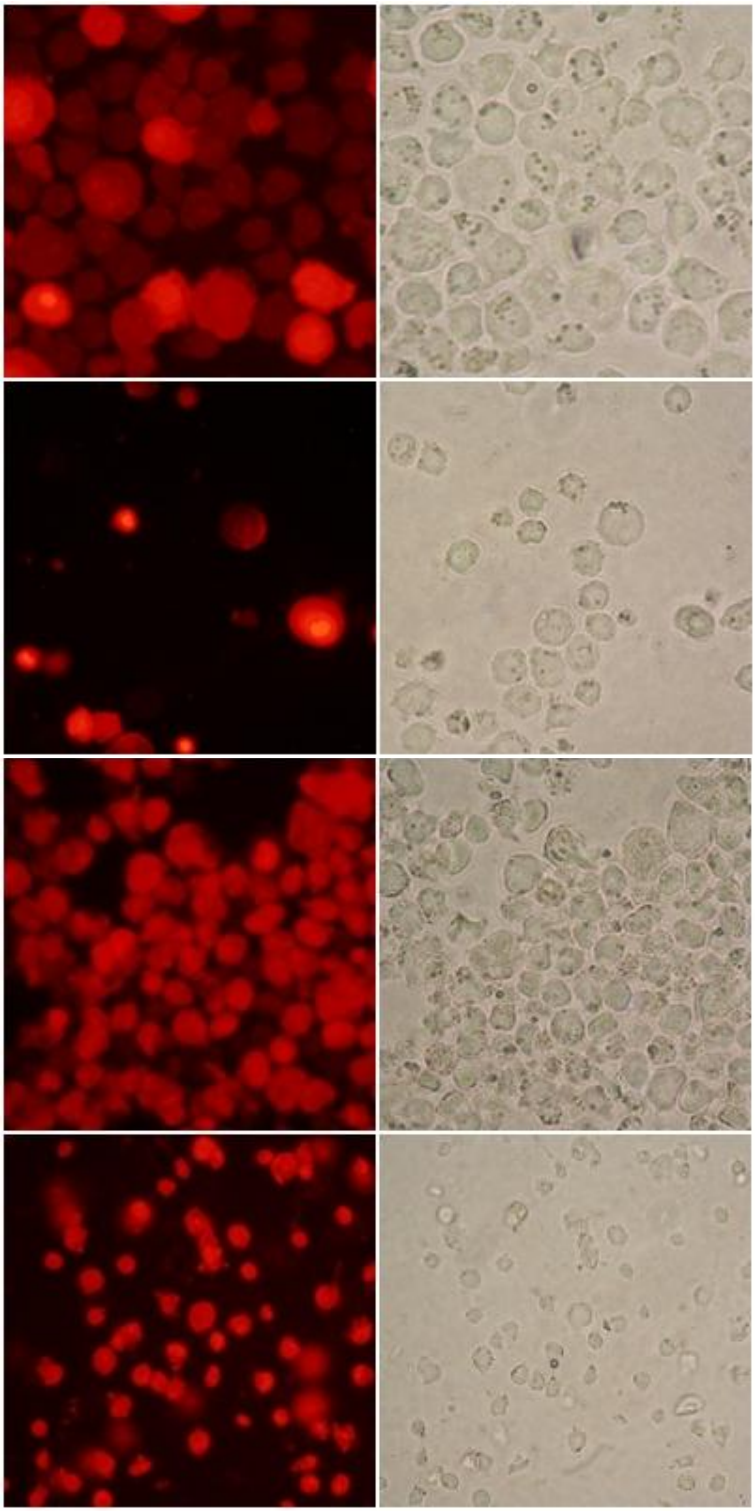

Figure 6.2 (continued) – THP-1 cells stained with PI after fixation with different agents.

Of the fixatives used, formaldehyde and PFA at 1% seemed to have allowed the least PI staining, indicating good fixing agents (**Figure 6.2**b,f). Using methanol/acetone (1:1), ice cold methanol, 4% aldehydes and 2% glutaraldehyde seemed to allow PI to penetrate the membrane and stain the nucleus of most cells (**Figure 6.2**a, c, d, e, g) comparable to permeabilised cells (**Figure 6.2**h).

Later it was found that if cells were stained with PI before cytospin and fixation, the PI-stained cells co-localised with the cells stained with trypan blue, indicating only dead cells took up the dyes (**Figure 6.3**). A few examples are indicated by the arrows below. Thus, Hsp60 ICC and PI were carried out under standard incubation conditions prior to fixation.

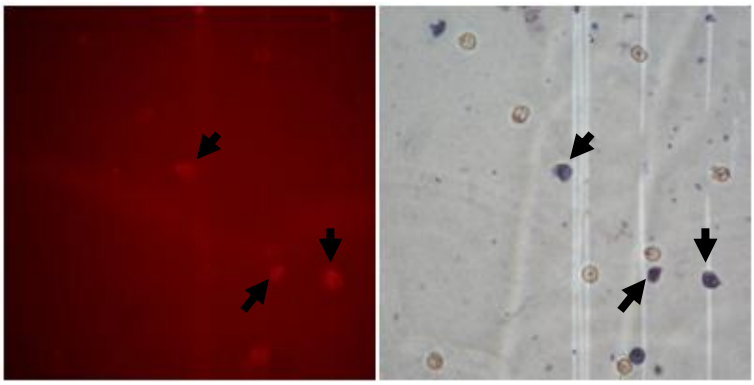

Figure 6.3 – Co-localisation of PI and trypan blue staining. The arrows indicate examples of dead cells stained by both trypan blue and PI.

6.3.3 Confocal Microscopy and Hsp60 ICC

The immunostaining with anti-Hsp60 antibody was carried out next and the slides were examined by CLSM to gain better resolution and reduce bleaching. The anti-Hsp60 antibody has previously been shown in MIN6 cells to co-localise with transfected GFP-Hsp60, see **Figure 6.4** (Martinus & Johnson unpublished data).

Figure 6.5 shows the cells stained with PI only, Hsp60 ICC negative (without primary antibody), Hsp60 ICC after cells were fixed, Hsp60 ICC in live cells, and cells stained with MitoSOX red. The nucleus was stained with either PI or DAPI in **Figure 6.5**. Using transmitted light (TL) all the cells could be seen and this gives an overview of cell morphology.

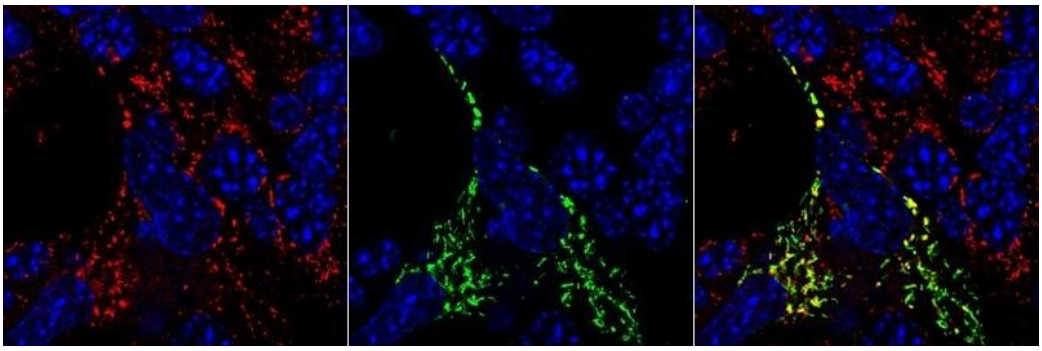

Figure 6.4 – Hsp60 expression in MIN6 cells. From left to right, anti-Hsp60 antibody, GFP-Hsp60 and the merger of the two.

Propidium iodide stained most of the cells as shown in **Figure 6.5**a. Some cells have a flattened appearance as shown by the TL image, probably an artifact due to centrifugation by cytospin. The intensity of the dye also varied between cells and this was commonly seen in all slides.

The Hsp60 ICC negative in **Figure 6.5**b shows there was non-specific binding of the FITC-conjugated secondary antibody. During ICC there was no additional

blocking agent (BSA) but FBS was present at all time in culture media. The use of detergent was also avoided in washing butter (PBS) as it is known to cause rupture of the cell membrane. The cells which have non-specific binding seem to be those that have not taken up PI, indicating that these cells were not necrotic. Interestingly, cells stained with PI seemed to have a flattened appearance as shown by the TL image, indicating they may have been ruptured or splattered during the cytospin procedure.

Hsp60 ICC was carried out either in live or fixed cells. The videos of the sequential z-stack images can be found in the complementary CD at the back cover (video 1-3). The collapsed z-stack images are shown in **Figure 6.5**c & d which show that ICC in live and fixed cells have very different staining patterns, indicating that the fixative (1% PFA) changed the structure of the antigen in some way. This is different to the study by Pfister *et al*. (2005) who showed that fixation (4% PFA or MeOH/acetone) of HUVECs did not alter the distribution of 'clustered' Hsp60 on the surface. In the current study, fixed cells had a uniform 'cloudy' FITC pattern and most cells (90%) have taken up PI (TL image not shown). Hsp60 ICC in live cells had distinct FITC 'speckles' in approximately 20% of the cells but most cells also had the 'cloudy' pattern. PI staining had varied intensities as mentioned earlier and around 10% of cells had high PI intensity. The cells with 'speckles' had medium PI intensity.

The 'speckles' in **Figure 6.5**d were possible surface expressed Hsp60 as these did not resemble the commonly described mitochondrial morphology such as 'bean-shaped', or network-like interconnected tubular structures (Karbowski & Youle 2003). Further, surface expressed Hsp60 had been described to have a spot- or string-shaped appearance in ECs (Xu *et al*. 1994), similar to the 'speckles' seen

here. To differentiate from mitochondrial Hsp60 staining, THP-1 cells were stained with a mitochondrial specific dye, MitoSOX red, which targets functional mitochondria that are producing superoxide. **Figure 6.5**e shows cells stained with MitoSOX red (coloured orange used to distinguish from PI) and counterstained with DAPI after cells were fixed. This is a collapsed image of the z-stack and the video can also be found in the complementary CD (video 4). Unlike **Figure 6.5**d, these cells had more areas in orange, indicating abundant mitochondria, more or less arranged around the nucleus. Some are 'bean-shaped' but most are also 'speckled' or spotty however a tubular network structure was not seen here.

Although **Figure 6.5**d & e (or videos 2 & 3) are different in the arrangement and the intensity of the FITC and MitoSOX staining, they still share a similar spotty pattern. Thus it cannot be ruled out that the 'speckles' in Hsp60 ICC are intracellular Hsp60. The weak PI staining in these speckled cells also led us to question the integrity of the cell membrane and, thus the possibility of mitochondrial Hsp60 staining. Furthermore, a study by Pfister and colleagues (2005) revealed that the number of cells expressing surface Hsp60 was only 1% in unstressed HUVECs and it increased to around 10% in heat-stressed cells. Similarly, only a 'weak staining' was seen in normal aortic ECs as oppose to 'bright staining' in stressed cells (Xu *et al*. 1994). In healthy THP-1 cells, around 20% of the cells had notable speckles which may indicate (1) a higher surface Hsp60 expression in this particular cell type; (2) cells being under an unknown stress, perhaps the additional handling during live cell ICC; (3) better recognition of this antibody to surface Hsp60 epitope than antibodies used by other studies; or (4) cells being partially leaky, as weak PI staining was seen in all cells, potentially allowing mitochondrial Hsp60 staining.

a) PI only

b) Anti-Hsp60 negative

(live cell)

c) Fixed cell ICC

d) Live cell ICC

e) MitoSox red (live cell)

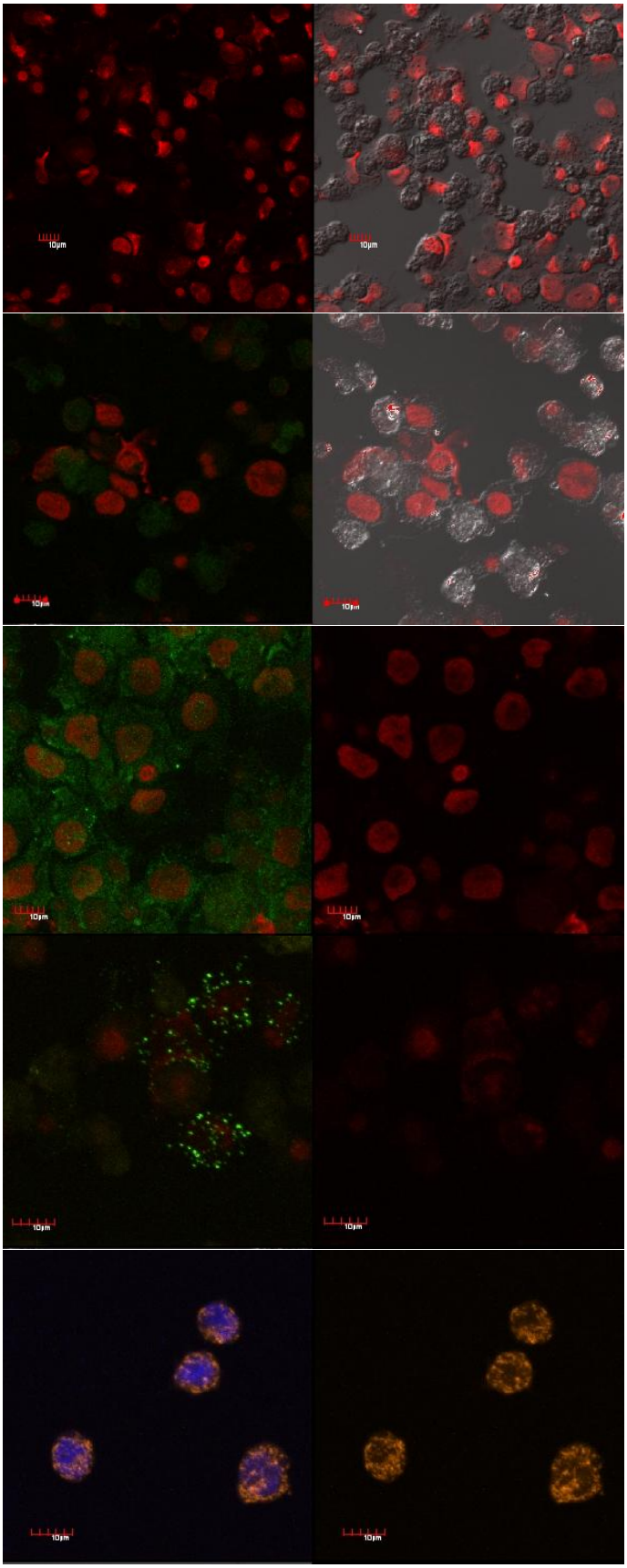

Figure 6.5 – Confocal microscopy of ICC. The description as indicated above. Red = PI; green = FITC; blue = DAPI; and orange = mitoSOX red. The scale bars all show 10 μm.

In summary, this study showed that THP-1 cells have different Hsp60 ICC pattern depending on the sequence of fixation and that ICC in live cells appeared to stain surface Hsp60. There is certainly more work to be done to test the reproducibility of the current staining method and to find a way to reduce non-specific binding of secondary antibody. This could involve adding a blocking agent to the media or employing a more stringent washing step. Also, it should be investigated why healthy cells took up faint PI. Most importantly, experiments which show directly whether metformin treatment has an effect on surface expression of Hsp60 should be carried out. An important consideration here is that increased surface Hsp60 caused by metformin may exacerbate CVD risks in T2D patients who already express elevated levels of adhesion molecules in ECs (Fogelstrand *et al*. 2004; Cipolletta *et al*. 2005; Hartge *et al*. 2007), and monocyte-EC interaction is the one of the key steps in the development of atherosclerosis (Libby 2002; Mestas & Ley 2008).

7 Final Summary and Future Directions

This study looked at several aspects of metformin treatment on human monocytic leukemia THP-1 cells. Chapter 3 showed that metformin at the therapeutic concentrations of metformin (100 μM) had little effects on cell growth rate, cell death and mitochondrial respiration. At a higher concentration (500 μM), however, metformin significantly decreased cell growth rate and mitochondrial dehydrogenase activity. Ten millimolar metformin was cytotoxic to THP-1 cells which raises questions to how valid and relevant it is in those studies that used 10 mM or even higher concentrations.

It is now clear that one of metformin's molecular targets is the complex 1 of the mitochondrial respiratory chain (Owen *et al*. 2000; Guigas *et al*. 2004) and results from MTT assay supported this. Using Hsp60 as a mitochondrial stress marker, it was noted that cells treated with 500 μM metformin had elevated mRNA levels of this marker throughout the 2-week experiment, a relatively long term incubation compared with other studies. At other concentrations the mRNA levels fluctuated but the protein levels increased in a time- and concentration-dependent manner at day 7 and day 14. It is unsure whether the increased expression of Hsp60 represented a mitochondrial-specific response, thus future study should include the expression of other HSPs to rule out general cellular stress response.

The results here also agree with the finding that metformin inhibits cell death (Guigas *et al*. 2004; Detaille *et al*. 2005), which was seen at 500 μM and 1 mM. Interestingly, cytosolic accumulation of Hsp60 has been associated with an anti-apoptosis outcome (Chandra *et al*. 2007). In the diabetic context, metformin may have protective effects against glucotoxicity-induced cell death.

Recently metformin has received much attention for its potential beneficiary effects on CVD outcome in T2D patients. Since monocyte differentiation marks a critical step in atherosclerosis the effects of metformin on THP-1 differentiation was carried out. It was found that 100 μM metformin resulted in significantly higher *cd14* expression in PMA-stimulated monocyte differentiation at 72h. CD14 is a surface receptor for bacterial LPS and it was proposed that through elevated *cd14* cells may respond to an infection better. Future work should confirm the up-regulation of *cd14* at other time points as well as identification of the receptor protein on the cell surface.

Finally, the detection of surface expressed Hsp60 was attempted and it seemed, for THP-1 cells, Hsp60 ICC should be carried out in live cells. In contrary to Pfister *et al*. (2007), the fixatives tried here either did not maintain membrane integrity or changed the antigen structure. ICC in live cells showed 'speckles' of Hsp60 staining which is similar to that described by Xu and colleagues (1994). However, the amount of 'speckles' in healthy cells here appeared to be much higher than other studies. Whether this was due to differences in cell type and antibody used is unclear. Future work should test the reproducibility of this staining procedure and further optimize to reduce non-specific binding and cytospin-induced cell rupture.

Based on the findings in this study, it appeared that THP-1 cells have increased Hsp60 expression under prolonged metformin exposure, even at a therapeutic dosage. THP-1 monocytes also had higher expression of *cd14* at this dosage with accompanying *hsp60* increase. The expression of either protein on the cell surface could have important roles in immunity as (1) both are known to bind PAMP such as LPS and can promote a pro-inflammatory response, and (2) in diabetes, circulatory monocytes

can attach to ECs expressing elevated levels of adhesion molecules and become lipid-laden foam cells, thus fueling an atherosclerotic event. Future studies should focus on these aspects of metformin-induced surface molecules perhaps using a co-culture system containing primary cell cultures and observe their interaction with ECs.

8 References

Aguilar-Zavala H, Garay-Sevilla ME, Malacara JM, Perez-Luque EL. (2008). Stress, inflammatory markers and factors associated in patients with type 2 diabetes mellitus. *Stress and Health* **24**(1): 49-54.

Alard JE, Dueymes M, Mageed RA, Saraux A, Youinou P, Jamin C. (2009). Mitochondrial heat shock protein (HSP) 70 synergizes with HSP60 in transducing endothelial cell apoptosis induced by anti-HSP60 autoantibody. *Faseb Journal* **23**(8): 2772-2779.

Bailey CJ. (2008). Metformin: Effects on micro and macrovascular complications in type 2 diabetes. *Cardiovascular Drugs and Therapy* **22**(3): 215-224.

Bangen JM, Schade FU, Flohe SB. (2007). Diverse regulatory activity of human heat shock proteins 60 and 70 on endotoxin-induced inflammation. Biochemical and Biophysical Research Communications **359**(3): 709-715.

Barazi HO, Zhou L, Templeton NS, Krutsch HC, Roberts D.(2002). Identification of heat shock protein 60 as a molecular mediator of α3β1 integrin activation. *Cancer Research* **62**: 1541-48.

Batandier C, Guigas B, Detaille D, El-Mir MY, Fontaine E, Rigoulet M, Leverve XM. (2006). The ROS production induced by a reverse-electron flux at respiratory-chain complex 1 is hampered by metformin. *Journal of Bioenergetics and Biomembranes* **38**(1): 33-42.

Bausinger H, Lipsker D, Ziylan U, Manie S, Briand JP, Cazenave JP, Muller S, Haeuw JF, Ravanat C, de la Salle H and others. (2002). Endotoxin-free heat-shock protein 70 fails to induce APC activation. *European Journal of Immunology* **32**(12): 3708-3713.

Beisswenger PJ, Howell SK, Touchette AD, Lal S, Szwergold BS. (1999). Metformin reduces systemic methylglyoxal levels in type 2 diabetes. *Diabetes* **48**(1): 198-202.

Bernas T, Dobrucki J. (2002). Mitochondrial and nonmitochondrial reduction of MTT: Interaction of MTT with TMRE, JC-1, and NAO mitochondrial fluorescent probes. *Cytometry* **47**(4): 236-242.

Berridge MV, Herst PM, Tan AS. (2005). Tetrazolium dyes as tools in cell biology: New insights into their cellular reduction. *Biotechnology Annual Review* **11**(11): 127-152.

Binder RJ, Vatner R, Srivastava P. (2004). The heat-shock protein receptors: Some answers and more questions. *Tissue Antigens* **64**(4): 442-451.

Brownlee M. (2001). Biochemistry and molecular cell biology of diabetic complications. *Nature* **414**(6865): 813-820.

Brunmair B, Staniek K, Gras F, Scharf N, Althaym A, Clara R, Roden M, Gnaiger E, Nohl H, Waldhausl W and others. (2004). Thiazolidinediones, like metformin, inhibit respiratory complex I - a common mechanism contributing to their antidiabetic actions? *Diabetes* **53**(4): 1052-1059.

Carvalho C, Correia S, Santos MS, Seica R, Oliveira CR, Moreira PI. (2008). Metformin promotes isolated rat liver mitochondria impairment. *Molecular and Cellular Biochemistry* **308**(1-2): 75-83.

Chandra D, Choy G, Tang DG. (2007). Cytosolic accumulation of Hsp60 during apoptosis with or without apparent mitochondrial release - Evidence that its pro-apoptotic or pro-survival functions involve differential interactions with caspase. *Journal of Biological Chemistry* **282**: 31289-31301.

Chen LL, Sigler PB. (1999). The crystal structure of a GroEL/peptide complex: Plasticity as a basis for substrate diversity. *Cell* **99**(7): 757-768.

Chen M, Yuan JX, Shi YQ, Zhang XS, Hu ZY, Gao F, Liu YX. (2008). Effect of 43 degrees C treatment on expression of heat shock proteins 105, 70 and 60 in cultured monkey Sertoli cells. *Asian Journal of Andrology* **10**(3): 474-485.

Cipolletta C, Ryan KE, Hanna EV, Trimble ER. (2005). Activation of peripheral blood CD14(+) monocytes occurs in diabetes. *Diabetes* **54**(9): 2779-2786.

Davis BJ, Xie ZL, Viollet B, Zou MH. (2006). Activation of the AMP-activated kinase by antidiabetes drug metformin stimulates nitric oxide synthesis in vivo by promoting the association of Heat Shock Protein 90 and endothelial nitric oxide synthase. *Diabetes* **55**(2): 496-505.

de Marco R, Locatelli F, Zoppini G, Verlato G, Bonora E, Muggeo M. (1999). Cause-specific mortality in type 2 diabetes. The Verona diabetes study.

Diabetes Care **22**(5): 756-761.

Detaille D, Guigas B, Chauvin C, Batandier C, Fontaine E, Wiernsperger N, Leverve X. (2005). Metformin prevents high-glucose-induced endothelial cell death through a mitochondrial permeability transition-dependent process. *Diabetes* **54**(7): 2179-2187.

Dykens JA, Jamieson J, Marroquin L, Nadanaciva S, Billis PA, Will Y. (2008). Biguanide-induced mitochondrial dysfunction yields increased lactate production and cytotoxicity of aerobically-poised HepG2 cells and human hepatocytes in vitro. *Toxicology and Applied Pharmacology* **233**(2): 203-210.

Fogelstrand L, Hulthe J, Hulten LM, Wiklund O, Fagerberg B. (2004). Monocytic expression of CD14 and CD18, circulating adhesion molecules and inflammatory markers in women with diabetes mellitus and impaired glucose tolerance. *Diabetologia* **47**(11): 1948-1952.

Gao BC, Tsan MF. (2003). Recombinant human heat shock protein 60 does not induce the release of tumor necrosis factor alpha from murine macrophages. *Journal of Biological Chemistry* **278**(25): 22523-22529.

Ghneim HK, Al-Saleh SS, Al-Shammary FJ, Kordee ZS. (2003). Changes in adenosine deaminase activity in ageing cultured human cells and the role of zinc. *Cell Biochemistry and Function* **21**(3): 275-282.

Goodarzi MO, Bryer-Ash M. (2005). Metformin revisited: Re-evaluation of its properties and role in the pharmacopoeia of modern antidiabetic agents. Diabetes *Obesity & Metabolism* **7**(6): 654-665.

Grant P. (1996). The effect of high- and medium-dose metformin therapy on cardiovascular risk factors in patients with type II diabetes. *Diabetes Care* **19**: 64-66.

Grant P. (2003). Beneficial effects of metformin on haemostasis and vascular function in man. *Diabetes & Metabolism* **29**(6): S44-52.

Guigas B, Detaille D, Chauvin C, Batandier C, De Oliveira F, Fontaine E, Leverve X. (2004). Metformin inhibits mitochondrial permeability transition and cell death: A pharmacological in vitro study. *Biochemical Journal* **382**: 877-884.

Gupta S, Knowlton AA. (2006). Exosome dependent Hsp60 secretion in rat cardiac myocytes. *Journal of Molecular and Cellular Cardiology* **40**(6): 875-876.

Habich C, Baumgart K, Kolb H, Burkart V. (2002). The receptor for heat shock protein 60 on macrophages is saturable, specific, and distinct from receptors for other heat shock proteins. *Journal of Immunology* **168**(2): 569-576.

Habich C, Kempe K, van der Zee R, Burkart V, Kolb H. (2003). Different heat shock protein 60 species share pro-inflammatory activity but not binding sites on macrophages. *FEBS Letters* **533**(1-3): 105-109.

Habich C, Kempe K, van der Zee R, Rumenapf R, Akiyama H, Kolb H, Burkart V. (2005). Heat shock protein 60: Specific binding of lipopolysaccharide. *Journal of Immunology* **174**(3): 1298-1305.

Hardie DG, Hawley SA, Scott J. (2006). AMP-activated protein kinase - development of the energy sensor concept. *Journal of Physiology-London* **574**(1): 7-15.

Hartge MM, Unger T, Kintscher U. (2007). The endothelium and vascular inflammation in diabetes. *Diabetes and Vascular Disease Research* **4**(2): 84-88.

Hattori Y, Suzuki K, Hattori S, Kasai K. (2006). Metformin inhibits cytokine-induced nuclear factor kappa b activation via AMP-activated protein kinase activation in vascular endothelial cells. *Hypertension* **47**(6): 1183-1188.

Hemmingsen B, Lund SS, Wetterslev J, Vaag A. (2009). Oral hypoglycaemic agents, insulin resistance and cardiovascular disease in patients with type2 diabetes. European *Journal of Endocrinology* **161**: 1-9.

Henderson B, Mesher J. (2007). The search for the chaperonin 60 receptors. *Methods* **43**(3): 223-228.

Hochleitner BW, Hochleitner EO, Obrist P, Eberl T, Amberger A, Xu QB, Margreiter R, Wick G. (2000). Fluid shear stress induces heat shock protein 60 expression in endothelial cells in vitro and in vivo. *Arteriosclerosis Thrombosis and Vascular Biology* **20**(3): 617-623.

Hoppichler F, Lechleitner M, Traweger C, Schett G, Dzien A, Sturm W, Xu QB.

(1996). Changes of serum antibodies to heat-shock protein 65 in coronary heart disease and acute myocardial infarction. *Atherosclerosis* **126**(2): 333-338.

Horvath I, Multhoff G, Sonnleitner A, Vigh L. (2008). Membrane-associated stress proteins: More than simply chaperones. *Biochimica Et Biophysica Acta-Biomembranes* **1778**(7-8): 1653-1664.

Isakovic A, Harhaji L, Stevanovic D, Markovic Z, Sumarac-Dumanovic M, Starcevic V, Micic D, Trajkovic V. (2007). Dual antiglioma action of metformin: Cell cycle arrest and mitochondria-dependent apoptosis. *Cellular and Molecular Life Sciences* **64**(10): 1290-1302.

Itoh H, Komatsuda A, Ohtani H, Wakui H, Imai H, Sawada K, Otaka M, Ogura M, Suzuki A, Hamada F. (2002). Mammalian Hsp60 is quickly sorted into the mitochondria under conditions of dehydration. *European Journal of Biochemistry* **269**(23): 5931-5938.

Janeway CA. (1992). The immune-system evolved to discriminate infectious nonself from noninfectious self. *Immunology Today* **13**(1): 11-16.

Kahn SE, Haffner SM, Heise MA, Herman WH, Holman RR, Jones NP, Kravitz BG, Lachin JM, O'Neill MC, Zinman B and others. (2006). Glycemic durability of rosiglitazone, metformin, or glyburide monotherapy. *New England Journal of Medicine* **355**(23): 2427-2443.

Kang JH, Ryu HS, Kim HT, Lee SJ, Choi UK, Park YB, Huh TL, Choi MS, Kang TC, Choi SY and others. (2009). Proteomic analysis of human macrophages exposed to hypochlorite-oxidized low-density lipoprotein. *Biochimica Et Biophysica Acta-Proteins and Proteomics* **1794**(3): 446-458.

Karbowski M, Youle RJ. (2003). Dynamics of mitochondrial morphology in healthy cells and during apoptosis. *Cell Death and Differentiation* **10**(8): 870-880.

Kirpichnikov D, McFarlane SI, Sowers JR. (2002). Metformin: An update. *Annals of Internal Medicine* **137**(1): 25-33.

Kol A, Lichtman AH, Finberg RW, Libby P, Kurt-Jones EA. (2000). Cutting edge: Heat shock protein (HSP) 60 activates the innate immune response: CD14 is an essential receptor for hsp60 activation of mononuclear cells. *Journal of Immunology* **164(**1): 13-17.

Kwong LK, Sohal RS. (1998). Substrate and site specificity of hydrogen peroxide generation in mouse mitochondria. *Archives of Biochemistry and Biophysics* **350**(1): 118-126.

Lee YH, Lee JC, Moon HJ, Jung JE, Sharma M, Park BH, Yi HK, Jhee EC. (2008). Differential effect of oxidative stress on the apoptosis of early and late passage human diploid fibroblasts: Implication of heat shock protein 60. *Cell Biochemistry and Function* **26**(4): 502-508.

Levy-Rimler G, Bell RE, Ben-Tal N, Azem A. (2002). Type I chaperonins: Not all are created equal. *FEBS Letters* **529**(1): 1-5.

Levy-Rimler G, Viitanen P, Weiss C, Sharkia R, Greenberg A, Niv A, Lustig A, Delarea Y, Azem A. (2001). The effect of nucleotides and mitochondrial chaperonin 10 on the structure and chaperone activity of mitochondrial chaperonin 60. *European Journal of Biochemistry* **268**(12): 3465-3472.

Liao DF, Jin ZG, Baas AS, Daum G, Gygi SP, Aebersold R, Berk BC. (2000). Purification and identification of secreted oxidative stress-induced factors from vascular smooth muscle cells. *Journal of Biological Chemistry* **275**(1): 189-196.

Libby P. (2002). Inflammation in atherosclerosis. *Nature* **420**(6917): 868-874.

Llorca O, Martin-Benito J, Ritco-Vonsovici M, Grantham J, Hynes GM, Willison KR, Carrascosa JL, Valpuesta JM. (2000). Eukaryotic chaperonin cct stabilizes actin and tubulin folding intermediates in open quasi-native conformations. *EMBO Journal* **19**(22): 5971-5979.

Lowell BB, Shulmanz GI. (2005). Mitochondrial dysfunction and type 2 diabetes. *Science* **307**(5708): 384-387.

Ludewig B, Laman JD. (2004). The in and out of monocytes in atherosclerotic plaques: Balancing inflammation through migration. *Proceedings of the National Academy of Sciences of the United States of America* **101**(32): 11529-11530.

Lund SS, Tarnow L, Stehouwer CDA, Schalkwijk CG, Teerlink T, Gram J, Winther K, Frandsen M, Smidt UM, Pedersen O and others. (2008). Impact of metformin versus repaglinide on non-glycaemic cardiovascular risk markers related to inflammation and endothelial dysfunction in non-obese patients with type 2 diabetes. *European Journal of Endocrinology* **158**(5):

631-641.

Mamputu JC, Wiernsperger N, Renier G. (2002). Metformin inhibits differentiation of human monocytes into macrophages and foam cell formation. *Diabetologia* **45**: 174.

Marroquin LD, Hynes J, Dykens JA, Jamieson JD, Will Y. (2007). Circumventing the crabtree effect: Replacing media glucose with galactose increases susceptibility of HepG2 cells to mitochondrial toxicants. *Toxicological Sciences* **97**(2): 539-547.

Marshall NJ, Goodwin CJ, Holt SJ. (1995). A critical-assessment of the use of microculture tetrazolium assays to measure cell-growth and function. *Growth Regulation* **5**(2): 69-84.

Martinus RD, Linnane AW, Nagley P. 1(993). Growth of rho 0 human Namalwa cells lacking oxidative phosphorylation can be sustained by redox compounds potassium ferricyanide or coenzyme Q10 putatively acting through the plasma membrane oxidase. *Biochemistry and molecular biology international* **31**(6): 997-1005.

Martinus RD, Garth GP, Webster TL, Cartwright P, Naylor DJ, Hoj PB, Hoogenraad NJ. (1996). Selective induction of mitochondrial chaperones in response to loss of the mitochondrial genome. *European Journal of Biochemistry* **240**(1): 98-103.

Mather KJ, Verma S, Anderson TJ. (2001). Improved endothelial function with metformin in type 2 diabetes mellitus. *Journal of the American College of Cardiology* **37**(5): 1344-1350.

Matzinger P. (1998). An innate sense of danger. *Seminars in Immunology* **10**(5): 399-415.

MedlinePlus. (2008). *Metformin*. Retrieved from http://www.nlm.nih.gov/medlineplus/druginfo/meds/a696005.html

Mellbin LG, Malmberg K, Norhammar A, Wedel H, Ryden L, for the DI. (2008). The impact of glucose lowering treatment on long-term prognosis in patients with type 2 diabetes and myocardial infarction: A report from the DIGAMI2 trial. *Eur Heart J* **29**(2): 166-176.

Mestas J, Ley K. (2008). Monocyte-endothelial cell interactions in the

development of atherosclerosis. *Trends in Cardiovascular Medicine* **18**(6): 228-232.

Ministry of Health. (2002). *Diabetes in New Zealand: Models and forecasts 1996-2011*. Wellington, New Zealand.

Ministry of Health. (2007). *Diabetes surveillance: Population-based estimates and projections for New Zealand, 2001-2011*. Public health intelligence occasional bulletin No. 46. Wellington, New Zealand.

Mulder H, Ling C. (2009). Mitochondrial dysfunction in pancreatic beta-cells in type 2 diabetes. *Molecular and Cellular Endocrinology* **297**(1-2): 34-40.

Nathan DM, Buse JB, Davidson MB, Ferrannini E, Holman RR, Sherwin R, Zinman B. (2009). Medical management of hyperglycemia in type 2 diabetes: A consensus algorithm for the initiation and adjustment of therapy a consensus statement of the american diabetes association and the european association for the study of diabetes. *Diabetes Care* **32**(1): 193-203.

Newman G, Crooke E. (2000). Dnaa, the initiator of *Escherichia coli* chromosomal replication, is located at the cell membrane. *Journal of Bacteriology* **182**(9): 2604-2610.

Nishikawa T, Edelstein D, Du XL, Yamagishi S, Matsumura T, Kaneda Y, Yorek MA, Beebe D, Oates PJ, Hammes HP and others. (2000). Normalizing mitochondrial superoxide production blocks three pathways of hyperglycaemic damage. *Nature* **404**(6779): 787-790.

Osterloh A, Breloer M. (2008). Heat shock proteins: Linking danger and pathogen recognition. *Medical Microbiology and Immunology* **197**(1): 1-8.

Osterloh A, Kalinke U, Weiss S, Fleischer B, Breloer M. (2007). Synergistic and differential modulation of immune responses by hsp60 and lipopolysaccharide. *Journal of Biological Chemistry* **282**(7): 4669-4680.

Osterloh A, Veit A, Gessner A, Fleischer B, Breloer M. (2008). Hsp60-mediated T cell stimulation is independent of TLR4 and IL-12. *International Immunology* **20**(3): 433-443.

Osterloh A, Meier-Stiegen F, Veit A, Fleischer B, von Bonin A, Breloer M. (2004). Lipopolysaccharide-free heat shock protein 60 activates T cells. *Journal of Biological Chemistry* **279**(46): 47906-47911.

Ouslimani N, Peynet J, Bonnefont-Rousselot D, Therond P, Legrand A, Beaudeux JL. (2005). Metformin decreases intracellular production of reactive oxygen species in aortic endothelial cells. *Metabolism-Clinical and Experimental* **54**(6): 829-834.

Owen MR, Doran E, Halestrap AP. (2000). Evidence that metformin exerts its anti-diabetic effects through inhibition of complex 1 of the mitochondrial respiratory chain. *Biochemical Journal* **348**: 607-614.

Passlick B, Flieger D, Zieglerheitbrock HWL. (1989). Identification and characterization of a novel monocyte subpopulation in human peripheral-blood. *Blood* **74**(7): 2527-2534.

Petersen M. (2003). Economic costs of diabetes in the US in 2002. *Diabetes Care* **26**(3): 917-932.

Pfeiffer A, Bottcher A, Orso E, Kapinsky M, Nagy P, Bodnar A, Spreitzer I, Liebisch G, Drobnik W, Gempel K and others. (2001). Lipopolysaccharide and ceramide docking to CD14 provokes ligand-specific receptor clustering in rafts. *European Journal of Immunology* **31**(11): 3153-3164.

Pfister G, Stroh CM, Perschinka H, Kind M, Knoflach M, Hinterdorfer P, Wick G. (2005). Detection of Hsp60 on the membrane surface of stressed human endothelial cells by atomic force and confocal microscopy. *Journal of Cell Science* **118**(8): 1587-1594.

Pirkkala L, Nykanen P, Sistonen L. (2001). Roles of the heat shock transcription factors in regulation of the heat shock response and beyond. *FASEB Journal* **15**(7): 1118-1131.

Pockley AG. (2002). Heat shock proteins, inflammation, and cardiovascular disease. *Circulation* **105**(8): 1012-1017.

Pockley AG. (2003). Heat shock proteins as regulators of the immune response. *Lancet* **362**(9382): 469-476.

Pockley AG, Bulmer J, Hanks BM, Wright BH. (1999). Identification of human heat shock protein 60 (hsp60) and anti-hsp60 antibodies in the peripheral circulation of normal individuals. *Cell Stress & Chaperones* **4**(1): 29-35.

Pockley AG, Wu R, Lemne C, Kiessling R, de Faire U, Frostegard J. (2000). Circulating heat shock protein 60 is associated with early cardiovascular

disease. *Hypertension* **36**(2): 303-307.

Roper NA, Bilous RW, Kelly WF, Unwin NC, Connolly VM. (2002). Cause-specific mortality in a population with diabetes. *Diabetes Care* **25**(1): 43-48.

Scheen AJ. (1996). Clinical pharmacokinetics of metformin. *Clinical Pharmacokinetics* **30**(5): 359-371.

Shamaei-Tousi A, Halcox JP, Henderson B. (2007a). Stressing the obvious? Cell stress and cell stress proteins in cardiovascular disease. *Cardiovascular Research* **74**(1): 19-28.

Shamaei-Tousi A, Stephens JW, Bin R, Cooper JA, Steptoe A, Coates ARM, Henderson B, Humphries SE. (2006). Association between plasma levels of heat shock protein 60 and cardiovascular disease in patients with diabetes mellitus. *European Heart Journal* **27**(13): 1565-1570.

Shamaei-Tousi A, Steptoe A, O'Donnell K, Palmen J, Stephens JW, Hurel SJ, Marmot M, Homer K, D'Aiuto F, Coates ARM and others. (2007b). Plasma heat shock protein 60 and cardiovascular disease risk: The role of psychosocial, genetic, and biological factors. *Cell Stress & Chaperones* **12**(4): 384-392.

Sigler PB, Xu Z, Rye HS, Burston SG, Fenton WA, Horwich AL. (1998). Structure and function in GroEL-mediated protein folding. *Annual Review of Biochemistry* **67**(1): 581-608.

Skrha J, Prazny M, Hilgertova J, Kvasnicka J, Kalousova M, Zima T. (2007). Oxidative stress and endothelium influenced by metformin in type 2 diabetes mellitus. *European Journal of Clinical Pharmacology* **63**(12): 1107-1114.

Sogame Y, Kitamura A, Yabuki M, Komuro S. (2009). A comparison of uptake of metformin and phenformin mediated by hOCT1 in human hepatocytes. *Biopharmaceutics & Drug Disposition* **30**(8): 476-484.

Soltys BJ, Gupta RS. (1996). Immunoelectron microscopic localization of the 60-kda heat shock chaperonin protein (Hsp60) in mammalian cells. *Experimental Cell Research* **222**(1): 16-27.

Soltys BJ, Gupta RS. (1997). Cell surface localization of the 60 KDa heat shock

chaperonin protein (hsp60) in mammalian cells. *Cell Biology International* **21**(5): 315-320.

Takeda K, Akira S. (2004). TLR signaling pathways. *Seminars in Immunology* **16**(1): 3-9.

Teshima S, Rokutan K, Takahashi M, Nikawa T, Kishi K. (1996). Induction of heat shock proteins and their possible roles in macrophages during activation by macrophage colony-stimulating factor. *Biochemical Journal* **315**: 497-504.

Triantafilou M, Triantafilou K. (2002). Lipopolysaccharide recognition: CD14, TLRs and the LPS-activation cluster. *Trends in Immunology* **23**(6): 301-304.

Tsan MF, Gao BC. (2004). Cytokine function of heat shock proteins. *American Journal of Physiology-Cell Physiology* **286**(4): C739-C744.

Tsukamoto K, Knoshita M, Kojima K, Mikuni Y, Kudo M, Mori M, Fujita M, Horie E, Shimaza N, Teramoto T. (2002). Synergically increased expression of CD36, CLA-1 and CD68, but not of SR-a and LOX-1, with the progression to foam cells from macrophages. *Journal of atherosclerosis thrombosis* **9**: 57-64.

Tuomisto TT, Riekkinen MS, Viita H, Levonen AL, Yla-Herttuala S. (2005). Analysis of gene and protein expression during monocyte-macrophage differentiation and cholesterol loading - cDNA and protein array study. *Atherosclerosis* **180**(2): 283-291.

Turner RC, Holman RR, Cull CA, Stratton IM, Matthews DR, Frighi V, Manley SE, Neil A, McElroy K, Wright D and others. (1998). Intensive blood-glucose control with sulphonylureas or insulin compared with conventional treatment and risk of complications in patients with type 2 diabetes (UKPDS 33). *Lancet* **352**(9131): 837-853.

Vabulas RM, Ahmad-Nejad P, da Costa C, Miethke T, Kirschning CJ, Hacker H, Wagner H. (2001). Endocytosed Hsp60s use toll-like receptor 2 (TLR2) and TLR4 to activate the toll/interleukin-1 receptor signaling pathway in innate immune cells. *Journal of Biological Chemistry* **276**(33): 31332-31339.

Wallin RPA, Lundqvist A, More SH, von Bonin A, Kiessling R, Ljunggren HG. (2002). Heat-shock proteins as activators of the innate immune system. *Trends in Immunology* **23**(3): 130-135.

Wang DS, Kusuhara H, Kato Y, Jonker JW, Schinkel AH, Sugiyama Y. (2003). Involvement of organic cation transporter 1 in the lactic acidosis caused by metformin. *Molecular Pharmacology* **63**(4): 844-848.

Wellen KE, Hotamisligil GS. (2005). Inflammation, stress, and diabetes. *Journal of Clinical Investigation* **115**(5): 1111-1119.

Wick G, Knoflach M, Xu QB. (2004). Autoimmune and inflammatory mechanisms in atherosclerosis. *Annual Review of Immunology* **22**: 361-403.

Wiedemann N, Frazier AE, Pfanner N. (2004). The protein import machinery of mitochondria. *Journal of Biological Chemistry* **279**(15): 14473-14476.

Wiernsperger NF. (1999). Membrane physiology as a basis for the cellular effects of metformin in insulin resistance and diabetes. *Diabetes & Metabolism* **25**(2): 110-127.

Wilcock C, Bailey CJ. (1994). Accumulation of metformin by tissues of the normal and diabetic mouse. *Xenobiotica* **24**(1): 49-57.

Williams R, Palmer J. (1975). Farewell to phenformin for treating diabetes mellitus. *Annal International Medicine* **83**: 567-568.

Witters LA. (2001). The blooming of the French lilac. *Journal of Clinical Investigation* **108**(8): 1105-1107.

Wong AKF, Howie J, Petrie JR, Lang CC. (2009). Amp-activated protein kinase pathway: A potential therapeutic target in cardiometabolic disease. *Clinical Science* **116**(7-8): 607-620.

World Health Organization. (2006). Definition and diagnosis of diabetes mellitus and intermediate hyperglycemia: Report of a WHO/IDF consultation.

Wright BH, Corton JM, El-Nahas AM, Wood RFM, Pockley AG. (2000). Elevated levels of circulating heat shock protein 70 (Hsp70) in peripheral and renal vascular disease. *Heart and Vessels* **15**(1): 18-22.

Wulffele MG, Kooy A, Lehert P, Bets D, Ogterop JC, van der Burg BB, Donker AJM, Stehouwer CDA. (2002). Combination of insulin and metformin in the treatment of type 2 diabetes. *Diabetes Care* **25**(12): 2133-2140.

Xu Q, Schett G, Perschinka H, Mayr M, Egger G, Oberhollenzer F, Willeit J, Kiechl S, Wick G. (2000). Serum soluble heat shock protein 60 is elevated

in subjects with atherosclerosis in a general population. *Circulation* **102**: 14-20

Xu QB, Schett G, Seitz CS, Hu Y, Gupta RS, Wick G. (1994). Surface staining and cytotoxic activity of heat-shock protein 60 antibody in stressed aortic endothelial cells. *Circulation research* **75**(6): 1078-85.

Zarich SW. (2009). Potential of glucose-lowering drugs to reduce cardiovascular events. *Current Diabetes Reports* **9**(1): 87-94.

Zhao Q, Wang JH, Levichkin IV, Stasinopoulos S, Ryan MT, Hoogenraad NJ. (2002). A mitochondrial specific stress response in mammalian cells. *EMBO Journal* **21**(17): 4411-4419.

Zheng LM, He M, Long M, Blomgran R, Stendahl O. (2004). Pathogen-induced apoptotic neutrophils express heat shock proteins and elicit activation of human macrophages. *Journal of Immunology* **173**(10): 6319-6326.

Zou MH, Kirkpatrick SS, Davis BJ, Nelson JS, Wiles WG, Schlattner U, Neumann D, Brownlee M, Freeman MB, Goldman MH. (2004). Activation of the amp-activated protein kinase by the anti-diabetic drug metformin in vivo - role of mitochondrial reactive nitrogen species. *Journal of Biological Chemistry* **279**(42): 43940-43951.